Master's thesis

NTNU
Norwegian University of Science and Technology
Faculty of Engineering
Department of Geoscience and Petroleum

Karsten Skrettingland

Mitigating Axial Stick-Slip During Connections on a Floating Vessel

Master's thesis in Petroleumsfag
Supervisor: Sigbjørn Sangesland
June 2020

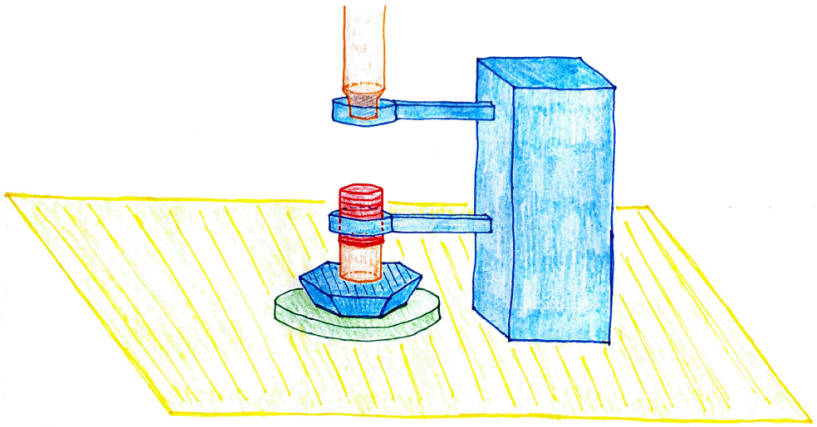

NTNU
Norwegian University of
Science and Technology

Karsten Skrettingland

Mitigating Axial Stick-Slip During Connections on a Floating Vessel

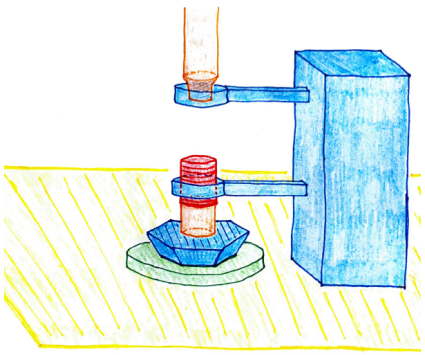

Master's thesis in Petroleumsfag
Supervisor: Sigbjørn Sangesland
June 2020

Norwegian University of Science and Technology
Faculty of Engineering
Department of Geoscience and Petroleum

NTNU
Norwegian University of
Science and Technology

Sammendrag

Det finnes få gode løsninger for å hindre et fluktuerende bunnhullstrykk under koblinger på en flyterigg. MPD-teknologi gjør det mulig å holde et stabilt trykk, men bare dersom borestrengens bevegelse er forutsigbar. Under koblinger settes strengen i slips, hvilket betyr at heave-kompensasjonssystemet kobles fra og strengen følger riggens bevegelse. Strengen vil da være utsatt for ukontrollerte aksielle bevegelser.

Den første delen av denne oppgaven diskuterer sammenhengen mellom rotasjonshastighet og aksiell stick-slip periode. Observasjoner gjort med en forenklet modell viser at en borestreng på 4,000 meter, i en høyavviksbrønn og med bølgehøyde på 3 meter, krever en rotasjons-hastighet på 168 RPM for å sikre at rotasjonen gjenopptas før kompresjonskreftene overkommer den aksielle friksjonen. Grunnet manglende data tar studien utgangspunkt i konsepter og forenklede scenarier, med antagelser der det er nødvendig.

Deretter brukes en annen modell til å forutsi den dynamiske responsen i borestrengen under torsjonale vibrasjoner med demping, og til å bestemme egenfrekvensene til systemet. Resultatene sammenlignes med analytiske tilnærminger. Dempingskoeffisienten påvirker borestrengresponsen sterkt ved egenfrekvensene, og selv om resonans i DP-seksjonen er en trussel og må overvåkes, anses resonans i DC-seksjonen som svært usannsynlig.

Til slutt presenteres tre mulige tiltak for å begrense problemet med aksiell stick-slip. Denne delen inneholder beskrivelser, skisser og sammenligning av tre ulike verktøy. Disse er 1) en nedihulls motor, 2) en swivel-sub som installeres på toppen av hver rørlengde og 3) installasjon av en roterende Iron Rough Neck (IRN) på boredekket. Swivel-suben, i kombinasjon med MPD-teknologi, anbefales som et billigere alternativ til eksisterende løsninger.

For videre arbeid foreslås implementering av reelle brønndata, utvikling av en prototype og innledning av dialog med industrien for å diskutere krav og muligheter for et nytt verktøy.

Summary

There are few good solutions available to mitigate the fluctuating bottom hole pressure during connections on a floating vessel. MPD-technology can maintain a stable bottom hole pressure, but only if the drill pipe movement is predictable. During connections, the heave compensation system is disconnected, and the string is suspended in slips, meaning that the string follows the rig movement. Weight stacking and axial stick-slip is then a threat.

The first part discusses the relationship between top drive velocity and axial stick-slip period. Observations based on a simplified model, show that a drill string with length 4,000 meters, in a highly deviated wellbore and with a wave height of 3 meters, requires a top drive rotation of 168 RPM to ensure that rotation commences before the compressional forces exceed the axial drag. Due to a lack of data, the study is largely based on concepts and hypothetical scenarios, assuming reasonable values where needed.

The second part uses a simplified drill string model to predict the dynamic response of angular drill string vibrations with damping, and to determine the natural frequency modes of the drill string system. The results are compared to analytic approximations. The damping coefficient greatly affects the drills string response at the resonant frequencies and while the occurrence of DP resonance during torsional stick-slip is a threat and must be monitored, DC resonance is deemed highly unlikely.

The final part proposes three measures to mitigate the axial stick-slip problem, with descriptions, sketches and a comparison. The evaluated measures are 1) the installation of a downhole PDM tool, 2) the implementation of a swivel sub on top of each stand and 3) the installation of a rotating Iron Roughneck (IRN) on the drill floor. The swivel sub, in combination with MPD technology, is recommended as a cheaper alternative to existing solutions.

For further work is suggested the implementation of real data, the development of a prototype and the start of a dialogue with the industry to discuss the criteria and possibilities of a new tool.

Preface

This thesis is the culmination of my studies for a masters' degree in Petroleum Technology at the Norwegian University of Science and Technology (NTNU). The thesis was written from January to June 2020.

The topic of this study was formulated together with my supervisor, Professor Sigbjørn Sangesland, after I learned about the issue during my summer internship at ConocoPhillips Norge in 2019.

I would like to accredit Professor Sangesland for the initial idea of a PDM based tool in Chapter 7, and for being helpful throughout the process of writing this report, offering guidance and feedback when needed. I would also like to acknowledge Professor Tor Berge Gjersvik for input on Chapter 6 and for the initial idea of a rotating iron roughneck in Chapter 7. Lastly, I want to thank my fellow classmates for five great years at NTNU, and for a positive and constructive study environment.

Hopefully, this thesis can trigger further research on the topic, leading to the development of a new tool.

Karsten Skrettingland

Trondheim, June 01, 2020

List of Figures

List of Tables

Abbreviations

AHC	Active Heave Compensation
AOT	Axial Oscillation Tool
BHA	Bottom Hole Assembly
BHP	Bottom Hole Pressure
BOT	Breakout Torque
CCS	Continuous Circulation System
DC	Drill Collar
DP	Drill Pipe
ECD	Equivalent Circulating Density
EOB	End of Build
ESD	Equivalent Static Density
ERD	Extended Reach Drilling
GPM	Gallons Per Minute
HCF	Heave Compensated Floor
HSE	Health, Safety and Environment
HWDP	Heavy Weight Drill Pipe
ID	Inner Diameter
IRN	Iron Rough Neck
KOP	Kick Off Point
LCM	Lost Circulation Material
MD	Measured Depth
MODU	Mobile Offshore Drilling Unit
MPD	Managed Pressure Drilling
MUT	Makeup Torque
NOV	National Oilwell Varco
NTNU	Norwegian University of Science and Technology
OD	Outer Diameter
OSHA	Occupational Safety and Health Administration
PDM	Positive Displacement Motor
PSI	Pounds per Square Inch
RPM	Revolutions Per Minute
RSC	Rotary-Shouldered Connections
RSS	Rotary Steerable System
SORP	Self-Oscillating Rotary Percussion
SPM	Strokes Per Minute
SPP	Standpipe Pressure
TD	Total depth
TJOD	Tool Joint Outer Diameter
TOB	Torque on Bit
USD	US Dollar
WOB	Weight on Bit
WOW	Wait on Weather

Nomenclature

Symbol	Description	Units
A	Amplitude	m
A	Cross-sectional area	m^2
b	Complex number	-
B	Complex number	-
c_s	Velocity of shear wave	ft/s
d/dt	Time derivative	-
d/dL	Length derivative	-
d/dx	Length derivative	-
E	Modulus of elasticity (Young's Modulus)	Pa
f	Wave frequency	Hz
$f_{ss,i}$	Stick-slip frequency at natural frequency mode number i	Hz
f_e	Excitation frequency	Hz
f_θ	Angular frequency	Hz
F	Axial Tension	N
G	Modulus of rigidity (Shear Modulus)	Pa
h	Height	m
i	Increment number	-
I_d	Rig mass moment of inertia	kg-m^2
J	Polar moment of inertia	m^4
k	Subscript for BHA or DP	-
k	Spring constant	N/m
k_θ	Rotational stiffness of drill floor	lb-ft/rad
L	Length	m
L_0	Original length	m
m	Mass	kg
m	Element number in wellbore model	-
$m_{DP,i}$	Natural frequency mode number i of drill pipe	-
M	Torque	Nm
M_s	Surface torque	Nm
M_θ	Mass moment of inertia of MODU	lb-ft-sec^2
n	Final increment number	-
N	Normal force	N
r	Radius	m
R	Drag resistance	N
R	Friction vector	N
R_a	Axial friction vector	N
R_t	Tangential friction vector	N
R_{tot}	Total friction vector	N
t	Time	s
t_{as}	Time of axial sticking	s
t_{ts}	Time of torsional sticking	s
T	Wave period	s
T	Torque	Nm
T_1	Shortest sticking time interval	s
T_2	Longest sticking time interval	s
v	Velocity	m/s

Symbol	Description	Units
w	Width	m
w_b	Buoyed string weight	N
x	Distance	m
x_{crit}	Critical displacement length	m

Greek Letters

Symbol	Description	Units
γ_{xy}	Shear strain	-
γ_θ	Torsional damping factor	lb-ft/rad per sec/ft
ε	Material strain	-
η	Complex number	-
θ	Wellbore inclination	degrees
θ	Angular displacement	rad
$\bar{\theta}$	Average wellbore inclination	degrees
$\bar{\theta}$	Complex function	-
λ	Wavelength	m
λ_θ	Wavelength of angular displacement	m
μ	Friction coefficient	-
π	Mathematical constant	-
ρ_θ	Mass polar moment of inertia per unit length of drill string	lb-sec^2
σ	Material stress	Pa
τ_{xy}	Shear stress	Pa
φ	Wellbore azimuth	degrees
ϕ	Phase shift	rad
ω	Angular frequency	rad/s

1 Introduction

One of the most integral factors for the extraction of the remaining oil is the drilling of new wells. Much of the oil worldwide is found in offshore fields, and while it is challenging enough to drill an onshore well, these challenges will multiply when the rig site is floating in the sea. Although the petroleum industry has seen a tremendous progress in technology the past decades, the issue of axial stick-slip during drill pipe connections is yet to be presented with a satisfying solution. Especially in the North Sea and similar harsh environments where the floater is subject to significant heave, this can be a relentless problem, yielding recurring lost time events due to weather conditions or issues related to surge and swab.

Although much effort has been put into controlling heave induced surge and swab, the complexity of this problem is still causing headache. As long as the drill string is hung from the top drive and the behavior is more or less predictable, the utilization of heave compensated systems, managed pressure drilling (MPD) and other technologies will strongly mitigate bottom hole pressure (BHP) fluctuations. The real problem starts when severe axial stick-slip is encountered. The wellbore friction will resist axial movement of the drill string, imposing stick-slip on the drill string system regardless of an active heave compensation. The subsequent and sudden release of axial weight stacking can be very hazardous and highly unpredictable. Another problem is when the drill string is hung off for a connection. This requires the decoupling of heave compensation systems installed on the top drive, which is highly problematic, as the top joint now follows the heave motion of the rig floor, as described by (Daireaux, Dvergsnes, Cayeux, Bergerud, & Kjøsnes, 2019). Some solutions are emerging, like the heave compensated drill floor developed by Huisman or the Continuous Motion Rig developed by West Group. Unfortunately, these solutions are inapplicable to most old-fashioned drilling rigs out there. The industry needs a technology that can be installed to the already existing drilling vessels, and this master thesis is proposing three ways to approach the problem, all based on continuous drill string rotation. Among the evaluated measures are the installation of a positive displacement motor (PDM) tool, the implementation of a swivel sub on top of each stand and the installation of a rotating iron rough neck (IRN) on the drill floor. The three solutions will promote BHP predictability through continuous drill string rotation, and combining either of these with MPD technology might serve as an alternative and cheaper solution to the axial stick-slip problem.

2 Background

Heave induced axial stick-slip is a complex problem. Investigation of drilled wells in the Equinor operated Troll-field in the Norwegian North Sea shows surprisingly high downhole pressure variations caused by surge and swab during connections (Martin Kvernland et al., 2019). The following section will serve as a foundation for his paper. It will discuss the relevance of axial stick-slip to the petroleum industry and look at the motivation to come up with a solution. It will then provide background information necessary to understand the topic of this report. It will also introduce physical concepts that are relevant for the discussion and development of a new axial stick-slip mitigation tool.

2.1 Motivation

While many oil fields have been producing for decades, some fields are yet to be developed because the challenges are currently too big. One such challenge is the operational drilling window that lies between the pore pressure gradient and the fracture pressure gradient. With increasing wellbore length, it becomes harder to control this window due to the pressure loss in the mud flow, and the difference between flowing (ECD) and static (ESD)[1] bottom hole pressure. Also, the deep waters in some areas[2] will lead to a worryingly narrow pressure window, which currently hampers the development. Controlling the axial stick-slip, and hence the issues of surge and swab, might open for development of these fields. Therefore, a solution is expected to be welcome by the operators.

Extended Reach Drilling (ERD) has become an integral part of the petroleum industry, and challenges originating from excessive torque and drag along the drill string are complicating the field development. Control of axial stick-slip will improve weight transfer to bit, directional drilling, hole cleaning, gas influx, etc. and thereby reduce non-productive time (NPT) events and the overall drilling costs.

According to (Noreng, 2016), weather conditions in the North Sea are especially harsh, and drilling here is normally feasible for only 175 days a year. Improved control of axial stick-slip

[1] Equivalent circulating density (ECD) and equivalent static density (ESD).
[2] e.g. Brazil and Gulf of Mexico. Wells in the Gulf of Mexico might require up to 10 casing/liner intervals to reach target depth.

would enable contractors to drill more in rougher weather conditions, saving a lot of time and costs by reducing the time spent waiting on weather (WOW).

2.2 Stick-Slip Phenomenon

2.2.1 Axial Stick-Slip

The weight on bit (WOB) is controlled from the surface, by adjusting the hook load. In some horizontal wells it might even be necessary to push downwards in order to gain enough WOB. This is due to the drag forces that resist axial movement of the drill string. These forces also resist drill string movement when off bottom. As the wellbore length increases, it will be harder to control weight transfer in the string. Due to elasticity, a long drill string will not move as a rigid body, but as a long spring. Some parts may be sliding while other parts are stationary. The friction factor along the drill string varies continuously, depending on casing, open hole, cuttings bed and more. Since there is a difference between static and dynamic friction, weight is sometimes released suddenly. This released weight is transmitted down the string and can eventually yield severe shocks to the BHA. This phenomenon is defined as axial stick-slip, and the problem increases with deeper wells and larger horizontal displacement. Axial stick-slip can be mitigated with the use of rotation, but the introduction of torsional stick-slip is a complicating factor. The relationship between axial and torsional stick-slip is discussed in Chapter 5.

2.2.2 Torsional Stick-Slip

Torsional stick-slip is the phenomenon that occurs when the top drive is rotating the upper end of the drill string continuously, while the bottom of the string alters between a stationary and rotating behavior. When the BHA is stationary, the drill string torsion increases linearly with the angular velocity. Once the torque is sufficiently high to overcome the friction, the stationary part will experience an abrupt change in angular velocity, rotating very fast for a short while. When the drill string torque is too low to maintain rotation, or the friction is too high, rotation ceases and a new cycle of stick-slip starts. Thus, the stick-slip phenomenon is a constantly ongoing fight between torque and friction. Downhole measurements have shown that when the drill string is subject to strong stick-slip conditions, the downhole rotational speed can change from stationary to more than 400 RPM in just a fraction of a second (Cayeux et al., 2020). This pattern repeats itself over and over, causing BHA tool failure and reduced drilling efficiency.

2.3 Heave

The behavior of a floating vessel is mostly dependent on the sea state. Although inertia will heavily dampen the movement compared to the sea surface, the motion of the floating vessel can be significant. The vertical position of the floater with respect to time is determined by the amplitude and frequency of the in situ waves. In deep water, the motion of the sea can appear quite chaotic, and seemingly random. However, this random sea is merely a combination of multiple harmonic waves, propagating in different directions and with different phase velocities (see Figure 1). The significant wave height, a common term in ocean engineering, is the average of the highest one third of the waves in a timespan. The wave height is the vertical distance between the crest and the trough (i.e. two times the amplitude). According to the oil and gas magazine Offshore[3], some typical North Sea weather conditions correspond to a heave of 3.5 meter. Although rig heave should be described by a multivariable equation, this paper will assume it to be a harmonic, sinusoidal wave.

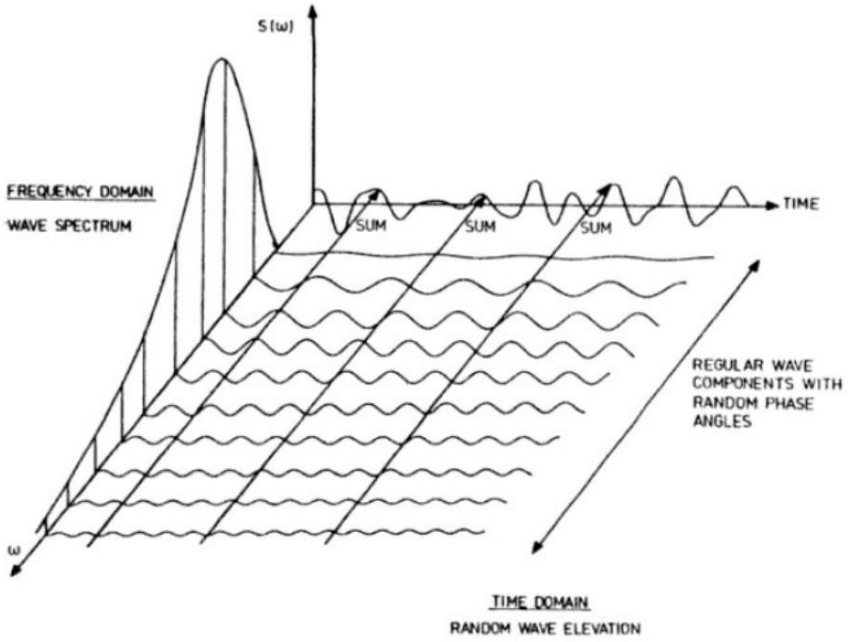

Figure 1: Schematic of the relationship between frequency domain and time domain representation of waves. Random sea can be discretized into a combination of harmonic waves. (Faltinsen, 1991, p. 24)

2.4 Surge and Swab

When the drill string is placed in slips without heave compensation, it will follow the behavior of the drill floor. On a floater experiencing heave, this will inevitably cause trouble with the

[3] Offshore Magazine (1st November 2018)

downhole pressure. The combination of a drill string that can be several kilometers long, the elasticity of the string, the friction along the borehole wall/casing and the heave of the rig, gives a resulting BHA movement that is far from predictable. However, it is fair to assume that a downwards movement of the rig will induce a similar downwards movement of the BHA, with some delay. This is called "surge". Conversely, an upwards movement of the rig will eventually induce an upwards movement of the BHA. This is called "swab". As the mud enclosing the drill string is close to incompressible, the BHP will be greatly affected by the drill string moving up or down, causing changes to the displaced mud volume.

2.4.1 Bottom Hole Pressure

Concerning the BHP, both surge and swab will yield an unstable well if the movement is substantially big. Surge will induce a pressure increase, threatening to fracture the formation if the pressure exceeds the fracture gradient. If the formation fractures, this will lead to mud losses and subsequently a reduced BHP due to the hydrostatic mud column getting smaller. If lost circulation material (LCM) is not added fast enough, this will induce an influx that could develop into a blowout[4]. Swab on the other hand, will induce a pressure reduction as the BHA moves out of the hole. Similarly, this may also induce an influx of pore fluid. If the operational window between the pore pressure gradient and the fracture gradient is narrow, drilling with heave can be extremely challenging, and the well is often considered undrillable.

2.4.2 Managed Pressure Drilling

The utilization of MPD greatly mitigates the effects of surge and swab. By actively adjusting the surface back pressure on the mud return line, it is possible to counteract the fluctuations in downhole pressure. As the well can be very long, and the speed of sound in mud is in the range of 1500 meters per second, the pressure pulses from surface must be sent several seconds in advance. For this technology to be effective, the pressure fluctuations must be predictable. Thus, it is only deployed on fixed installations and floaters in benign water conditions. According to (Wijning, 2019), typical North Sea heave conditions of 3.5 meters can result in downhole pressure fluctuations of up to 30 bar. Areas with harsh weather conditions and waters deeper than the maximum water depth for jackups[5] are therefore very challenging. Wells with narrow pressure windows located in such areas, therefore cannot be economically exploited today.

[4] An uncontrolled flow of hydrocarbons to surface.
[5] About 120 meters.

2.5 Vibrations

There is an intricate relationship between axial and tangential drill string displacement. Displacing an element of the string, either axially or tangentially, will affect the stress situation in the majority of the string. The elements close to the disturbed point will respond instantly, while the elements further away generally have a dampened and delayed response when the disturbance is finally communicated there. Section 6.2.2 discussed the concept of natural frequencies in a material, which is a set of frequencies that inflict resonance and should be avoided. There are three types of vibrations:

- Axial vibrations (e.g. sound moving through air). Travelling with p-wave velocity.
- Lateral vibrations (e.g. guitar string). Travelling with s-wave velocity.
- Torsional vibrations (e.g. wrenching a cloth). Travelling with s-wave velocity.

2.6 Friction

2.6.1 Friction Model

Normal dry friction is subdivided into static and dynamic friction. A normal assumption is that the static friction is valid until the movement commences and the dynamic friction takes over in an instant. After movement commences, the dynamic friction force is independent of the slipping velocity. This is called the Coulomb's law of friction (see Figure 2a). Although Coulomb's model is a fairly accurate approximation, it has some limitations just as the friction coefficient switches from static to dynamic. The Stribeck friction model evaluates this transition zone, suggesting a different friction coefficient just as movement commences (see Figure 2b). The friction coefficient is actually not independent of slipping velocity, and this introduces the viscous friction (see Figure 2c). However, Coulomb's approximation often seems to be an adequate representation of the friction forces and will be applied to the calculations in this paper.

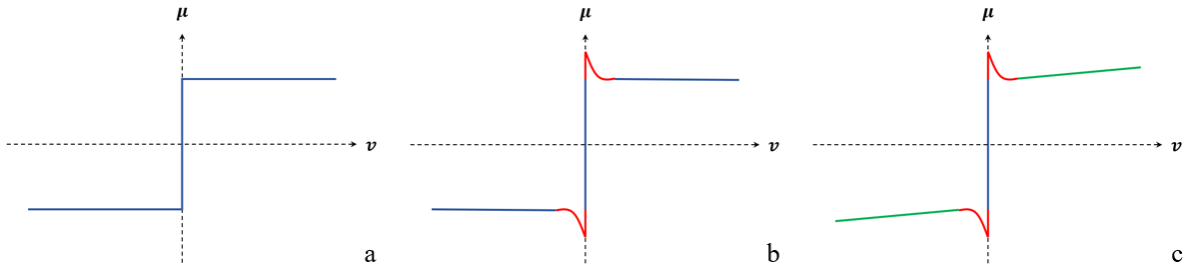

Figure 2: Different models of friction factor as a function of velocity. a) Coulomb friction model. b) Stribeck friction in red. c) Viscous friction in green.

Note that:

- The static friction coefficient is always higher than the dynamic friction coefficient.
- As the drill string is submerged in drilling mud, in might be erroneous not to evaluate the lubricated friction, especially if lubricants are added to the mud. This is neglected.

2.6.2 Friction Vector

Amonton's two laws of friction state that 1) the summed normal force over an element is the same, regardless of contact area, and that 2) the friction force is proportional with the normal force.

$$R = \mu \cdot N \tag{2.1}$$

The friction vector is always pointing in the opposite direction of the relative movement between two acting surfaces. The total friction vector is dependent on the axial and tangential friction vectors (see Figure 3).

$$R_{tot} = \sqrt{(R_a)^2 + (R_t)^2} \tag{2.2}$$

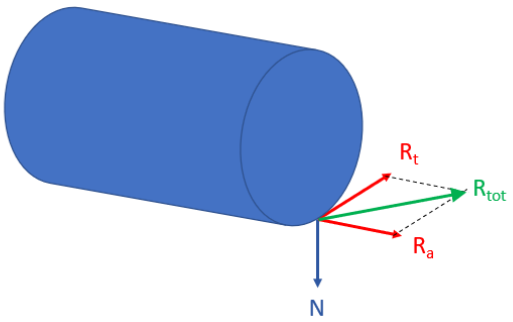

Figure 3: Relationship between axial, tangential and total drag.

If the loss to friction is independent of velocity, an added rotational velocity will decrease the axial drag component of the friction vector (see Figure 4).

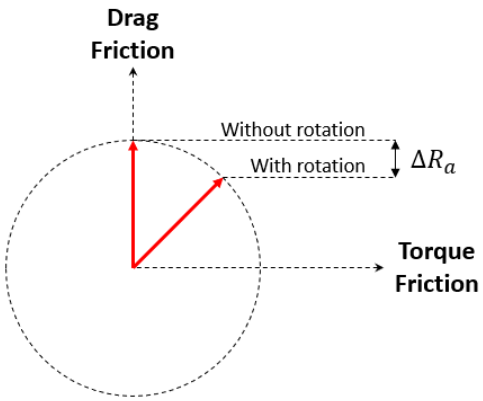

Figure 4: If the loss to friction is independent of velocity, an added rotational velocity will decrease the axial drag component of the friction vector.

Rotation can be used to "rotate out" the axial drag forces. The axial drag forces at top and bottom of the heave movement are minimized when the low axial velocity is combined with high rotational speed. Rotation will help prevent weight stacking when the rig heaves. By rotating the string, the total friction vector will deviate from the axial direction and tend towards a tangential direction. This reduction of axial drag as a function of RPM is plotted in Figure 5. For example, a tangential velocity of 100 RPM will reduce the axial drag by 35%.

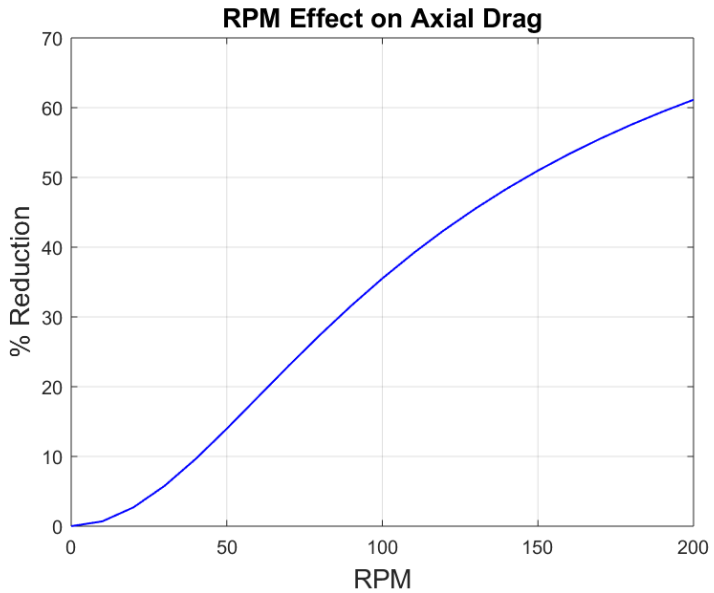

Figure 5: Percentage reduction in axial drag as a function of tangential velocity. The graph is valid for the drill string illustrated in Figure 8 in combination with the maximum heave velocity of the wave in Figure 11. The drill string is assumed to be a rigid body.

2.7 Drill String Dynamics

A normal approach to drill string dynamics is the soft string assumption which basically assumes that the drill string is resting on the low side of the wellbore, like a rope or a chain. It neglects the bending stiffness of the drill string, even in tension, and neglects the effect of localized contact points. Despite being far from the truth, this model has proven to be a surprisingly good approximation. A stiff string model has recently been developed to account for the bending stiffness of the string, but this has not been applied here.

3 State of the Art

The early 1980's saw the introduction of passive and active heave compensation systems, and by the mid- to late 1990's, Active Heave Compensation (AHC) systems was installed on many of the semisubmersible rigs working in the North Sea. Likewise, the MPD has turned out to be very useful, and has been widely deployed on fixed installations. However, the heave experienced on semisubmersible rigs is restricting the use of this technology on vessels subject to heave, due to the downhole pressure fluctuations. Following are some of the latest inventions that will boost the downhole pressure control.

3.1 Technology & Innovations

3.1.1 Continuous Circulation System

A continuous circulation system (CCS) allows for continuous circulation during drill pipe connections by redirecting the flow on the rig floor. The technology is described by (Badran, Gooneratne, Ahsalan, & Shaarawi, 2019) and has already been developed by several companies. The technology can be implemented with some modifications to the rig, requiring a special sub on top of each stand[6] and the installation of a remote manifold on the rig floor. The system is a good idea regardless of the axial stick-slip problem, as it prevents several issues that occur during connections. Among these are the thermal heating of mud and subsequent influx to the well, the accumulation of cuttings and the difference in BHP when circulation ceases.

3.1.2 Automated Downhole Choking

Mitigating axial stick-slip will not eliminate the downhole pressure fluctuations due to surge and swab, it will merely make the downhole pressure fluctuations more predictable by eliminating the sudden weight releases. In order to control the pressure fluctuations when the drill string is in slips, it will therefore be necessary to combine it with a pressure controlling technology, for instance the autonomous downhole choke described by (M. Kvernland et al., 2018). This is a fully autonomous choke, regulated by signals from a downhole accelerometer. It is installed in the bottom hole assembly (BHA) to avoid the challenge of time delay. The tool will use the drill string itself as an accumulator for pressure, and the system has been tested in laboratories, indicating significant dampening of the pressure fluctuations (see Appendix A).

[6] The drill pipe is stored vertically on the drill floor in 30 ft intervals (stands). One stand consists of three joints, approximately 10 ft each.

Full-scale computer simulations show that the heave-induced pressure fluctuations can be reduced by up to 80 % by utilizing the downhole choke, but for this to work, the downhole pressure needs to be predictable.

3.1.3 Heave Compensated Floor

The Heave Compensated Floor (HCF) by Huisman Equipment BV is a solution to the lack of heave compensation during connections. Until now, the heave compensation system on the top drive has been decoupled to place the drill string in slips and connect a new stand. Consequently, the drill pipe will heave in the wellbore during connections, resulting in surge and swab issues. With the HCF, the entire drill floor is moved onto a heave compensating hydraulic system, and this results in a harsh-environment semisubmersible rig that is designed to promote floor stability equal to that of a jackup rig. This concept is expected to be a game changer in harsh environment drilling operations, for instance in the North Sea, as it will allow the contractors to utilize MPD for downhole pressure control. However, it is an expensive solution that requires comprehensive modifications of today's Mobile Offshore Drilling Units (MODU). A cheaper and more adaptive solution would be preferable.

3.1.4 Continuous Motion Rig

The Continuous Motion Rig by (WestGroup, 2020) is a derrick system that enables continuous tripping and rotation of the drill string without having to place the drill string in slips. The system uses a fully automated drill floor with two lift systems working in tandem. Break out and spinning is done by a tong mounted in the travelling assembly, while two pipe handlers move pipe between the center line and the rack back position. The system allows for continuous circulation. A constant tripping speed eliminates pressure fluctuations caused by a start/stop motion, and continuous circulation eliminates the pressure fluctuations in ECD. The Continuous Motion Rig system can be installed onshore and offshore, on jack-ups, semi submersibles and drill ships, and basically provides a solution for maintaining continuous rotation during connections. However, it does not seem to offer heave compensation during hoisting, and the installation process comes with significant rig modifications and expenses.

3.2 Surface RPM & Downhole Torsional Stick-Slip

3.2.1 High-Frequency Measurements

(Cayeux et al., 2020) used high-frequency magnetometers to measure the downhole rotational speed in two wells in the Greater Ekofisk Area, referred to as well A and B. Measurements were done both on bottom and off bottom, but only the latter is relevant during drill pipe connections. The evaluated wells are drilled with geo-steering, having complex trajectories and a horizontal section at the bottom, yielding significant wellbore friction. Total depth (TD) is approximately 6 km MD for Well A and 5 km MD for well B. Both wells have tapered drill strings which include approximately 100 m BHA and 120 m HWDP.

Figure 6 shows the distribution of downhole RPM as a function of surface RPM. Below a surface RPM of 120, the downhole RPM was very fluctuating, ranging from zero in the stick phase to 300 in the slip phase. The average peak downhole RPM during a slip phase reached up to 2.5 times the surface RPM. Put into perspective, traditional vibration sensors often record samples at 0.1 - 0.2 Hz, which at 300 RPM corresponds to 25-50 rotations between each measurement. This greatly limits the possibility to understand downhole drill string dynamics and substantiates the importance of high-frequency measurements. A short discussion of vibration sampling rate is found in Appendix B. Figure 7 shows the off bottom stick time percentage for a range of surface rotational speeds. For low surface RPMs the bit is stationary more than 80% of the time, while for high surface RPMs the bit is rotating more than 95% of the time.

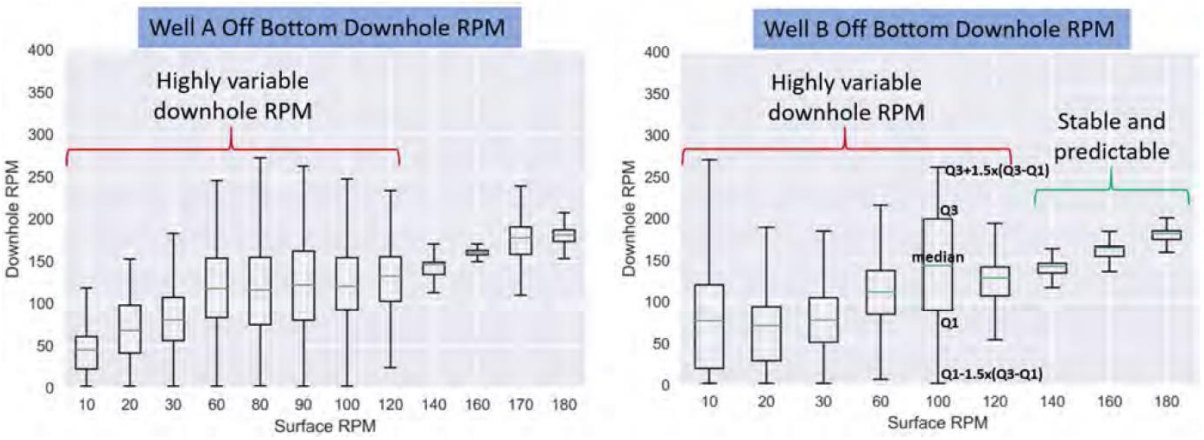

Figure 6: Off bottom downhole RPM vs surface RPM for two separate wells (left and right). Each box spans from the first quartile (Q1) to the third quartile (Q3) while the whiskers represent the box edges ±1.5 times the interquartile range (Q3-Q1). (Cayeux et al., 2020).

The target zone is defined as a small interval of ideal downhole RPM. The percentage of downhole RPM inside the target zone was close to zero for surface RPMs up to around 100, but above this it followed an increasing trend. Generally, a surface rotational speed below 120-140 RPM will lead to severe downhole torsional oscillations. This is valid both for drilling and off-bottom operations. Thus, for these wells 140 RPM is arguably the minimum surface RPM where the periodic stick-slip pattern is eliminated.

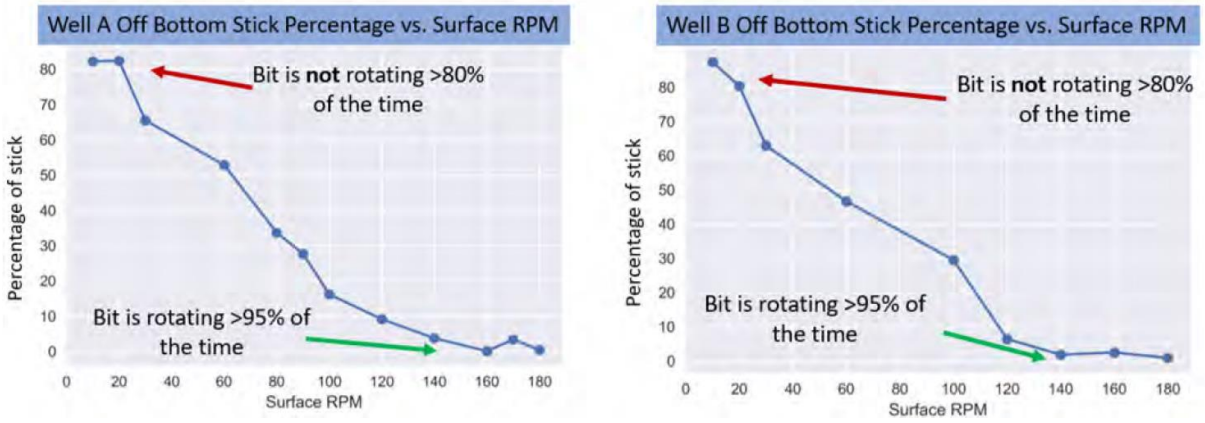

Figure 7: Off bottom stick percentage vs surface RPM for two separate wells (left and right). (Cayeux et al., 2020).

These findings suggest that a low surface RPM during connections will generate severe torsional stick-slip at the bit. However, it is important to notice the difference in boundary conditions between the case above and the topic of this paper. The findings above are valid if there is no axial movement, i.e. on a fixed installation or with an active heave compensation system. This paper assumes that the drill string is in slips on a heaving drill floor, detached from heave compensation. The result is an oscillating axial movement of the drill string, at least in the upper parts of the well. The axial movement will help transport the torque down the string. Therefore, the required minimum surface RPM is likely lower than 140 RPM.

3.2.2 Redefining best practice

Most of the big service companies are currently using slow rotation as best practice, to avoid shocks and damage to downhole equipment. When starting up after a drilling break, slow rotation is normally established before the top drive speed is increased through several stages up to the desired RPM. This has been done to break the gel[7] before pumping commences. New

[7] Breaking the gel will lower the mud viscosity and thereby reduce the flowing friction loss.

research shows that this method might have detrimental effects on shock mitigation. (Cayeux et al., 2020) has done research on torsional stick-slip based on high-frequency downhole measurements of 200-300 Hz along with results obtained with a transient torque and drag model. Apparently, slow rotation in long wells are very hard to establish because of the large wellbore friction, and despite a constant top drive rotation, the bit experiences huge accelerations and variations in RPM. The paper suggests that for a long and elastic drill string, it seems better to initiate top drive rotation directly to a value above a minimum threshold. This limits the duration of torsional stick-slip oscillations, and the associated risk for intense drill string whirl above the BHA. The research showed that an initial top drive speed of 30 RPM led to downhole stick-slip with peaks reaching 200 RPM. Commencement of the downhole rotation, relative to surface rotation, was delayed by about 10 seconds for a drill string of approximately 3400 m. Slow rotation is currently the standard approach when starting up, and a change should be considered. The paper states that a direct start up to 160 RPM on the top drive made the torsional oscillations at the bit dampen out.

There are several reasons why the above is not applicable to the situation in this paper; connections on a floating vessel. The 10 seconds of torque transport imply that the torque is initially worked out of the string, which is not the case during constant rotation. Also, the wells are drilled from fixed installations on the Ekofisk field, so the findings do not consider axial drill string motion caused by heave. This would likely result in a lower threshold RPM because of the moving drill string meaning that 1) static friction is replaced with dynamic friction and 2) the friction vector has an axial component and is not purely tangential.

4 The Wellbore & Drill String

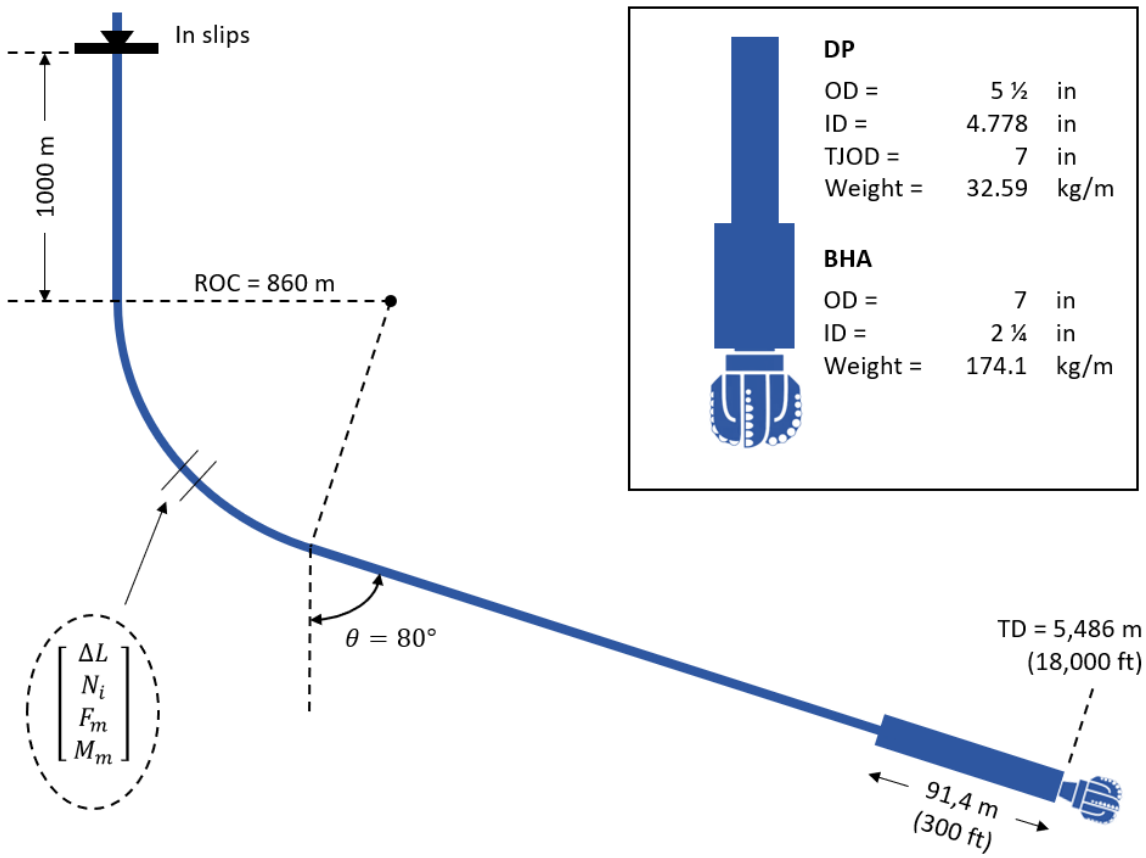

Figure 8: A conceptual sketch of the wellbore trajectory and the drill string dimension that will be used in this paper. The figure is not to scale.

4.1 Theory

4.1.1 Summary

- The wellbore comprises a vertical section, a curve with constant build-up rate and a tangent section (see Figure 8). The wellbore has a total depth of 18,000 ft MD (=5,486 m).
- For simplicity, the drill string is divided into two sections; a BHA element at the bottom, and a continuous drill pipe element above that stretches from BHA to the drill floor where the string is hanging in slips. The string is discretized into *n* elements.
- The calculations start at the bottom of the hole with WOB and torque on bit (TOB) and works its way up the drill string by computing the axial tension (F), the normal

force (N) and the torque (M) at each differential element. The bit is just off bottom, so $\mathrm{WOB} = \mathrm{TOB} = 0$.

- Two approaches often used for calculating the axial stresses are the principle of buoyancy factor and the principle of pressure-forces on cross-sectional changes. These calculations will apply the first method, with a buoyancy factor of 0.82.
- The discrete method is applied on the curved section. The result is three separate profiles, one for each parameter, plotted as a function of measured depth. Eventually, this yields a surface axial tension and a surface torque required to pull or twist the bit, respectively.

4.1.2 Assumptions

In order to simplify the calculations, the following assumptions are made:

- No normal forces (i.e. no contact) exist between the drill string and the casing in the vertical section of the well (good assumption).
- No weight is applied to the bit during tripping (good assumption).
- There is a constant friction factor and hole diameter throughout the entire wellbore. Neglecting difference between static and dynamic friction factor (poor assumption).
- The wellbore is J-shaped with a vertical section, a constant build section and a straight tangent (poor assumption).
- No restoring forces are present in the string due to compression/elongation. The drill string is stationary (poor assumption).
- Axial tension from drill string acceleration is neglected (poor assumption).
- The drill string has no bending stiffness, even in tension. It acts like a rope. This is called the “soft string model” (surprisingly good/fair assumption).
- The weight is evenly distributed on the contact surface. Neglecting the effect of localized contact points (poor assumption).

4.1.3 The Discrete Model

The discrete model is used in the curved section to calculate axial tension (F), torque (M) and normal force (N) on a differential drill string element. The elements are separated by a constant interval length (ΔL) with elements numbered $m = (1,2,3 \dots n)$. The subscript m denotes the current element while *m-1* denotes the previous element (closer to the bit). The subscripts 1

and n represent the bit and surface, respectively. The discrete model utilizes the following equations

$$F_m = F_{m-1} + w_b \cdot \cos\bar{\theta} \pm \mu \cdot N \tag{4.3}$$

$$M_m = M_{m-1} + \mu \cdot r \cdot N \tag{4.4}$$

where "plus" means pulling the drill string (upwards heave) and "minus" means lowering the drill string (downwards heave). The buoyed weight, average inclination and friction factor is denoted w_b, $\bar{\theta}$ and μ, respectively. The radius (r) is defined as half the outer diameter for the collar section and half the tool joint outer diameter (TJOD) for the drill pipe section. The normal force on a differential element depends on the buoyed weight of the element, the wellbore inclination and the dog leg severity (DLS) which is the combined change in inclination and azimuth (φ). It can be written as

$$N = \sqrt{(F_{m-1} \cdot \Delta\varphi \cdot \sin\bar{\theta})^2 + (w_b \cdot \sin\bar{\theta} + F_{m-1}\Delta\theta)^2} \tag{4.5}$$

If the azimuth is constant, the first term inside the square root becomes zero because $\Delta\varphi = 0$ and the equation is reduced to

$$N = w_b \cdot \sin\bar{\theta} + F_{m-1}\Delta\theta \tag{4.6}$$

For the straight sections, equation (4.3-4.5) is simply reduced to

$$F_m = F_{m-1} + w_b \cdot \cos\theta \pm \mu \cdot N \tag{4.7}$$

$$M_m = M_{m-1} + \mu \cdot r \cdot N \tag{4.8}$$

$$N = w_b \cdot \sin\theta \tag{4.9}$$

4.2 Results

Table 1: Drill string properties and wellbore trajectory data. All lengths are given as measured depths (MD).

Category	Property	Value	Units
Drill Collars	Length	300	ft
	Weight	174.11	kg/m
	OD	7	in
	ID	2 ¼	in
Drill Pipe	Weight	32.59	kg/m
	OD	5 ½	in
	ID	4.778	in
	TJOD	7	in
Steel Properties	Modulus of elasticity E (Young's Modulus)[8]	200	GPa
	Modulus of rigidity G (Shear Modulus)	79.3	GPa
Wellbore Trajectory	Total depth (TD)	5486	m
	Tangent length	3286	m
	Vertical section	1000	m
	Radius of curvature (ROC)	860	m
	Build up rate (BUR)	2	deg/30m
	Sail angle	80	deg
Other	Friction coefficient (static)	0.18	-
	Buoyancy factor	0.82	-
	Gravitational acceleration	9.81	m/s^2
	WOB	0	N
	TOB	0	Nm
	Incremental length (ΔL)	1	m

[8] Youngs modulus of elasticity for stainless steel ranges from 193-204 GPa (ASM, 1990), so it will be set to 200 GPa

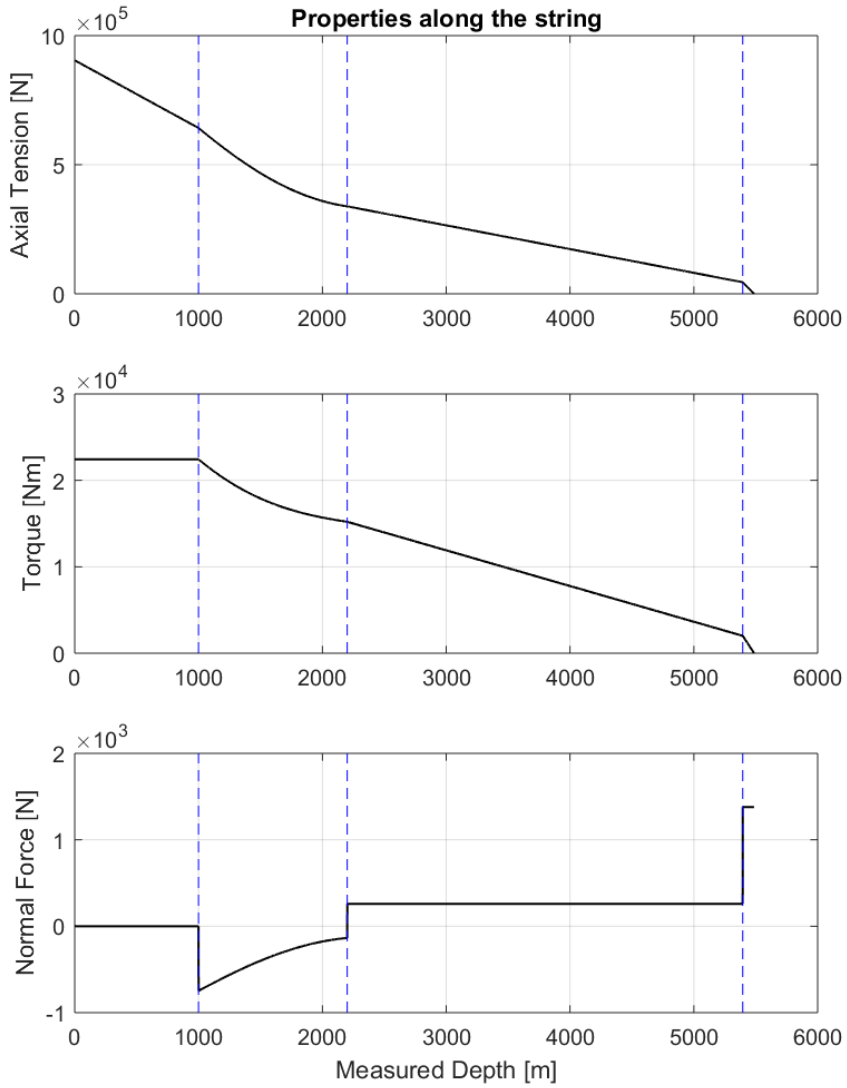

Figure 9: Profiles of axial tension (F), drill string torque (M) and normal force (N) along the string for the situation illustrated in Figure 8. All data is listed in Table 1. TD=18,000 ft =5486 m. The three vertical lines mark the KOP, EOB and Top of BHA from left to right. The measured depths at these points are 1000m, 2201m and 5395 m, respectively.

Table 2: Numeric values for a chosen set of points in the well.

Label	Measured Depth [m]	Axial Tension [kN] (cumulative)	Torque [kNm] (cumulative)	Normal Force [N] (per meter)
Surface	0	904.1	22.4	0
KOP	1000	642.3	22.4	0 / -747
EOB	2201	338.6	15.2	-136 / 258
Top of BHA	5395	44.8	2.0	258 / 1 379
TD	5486	0	0	1 379

Axial Tension: A heavy BHA gives a rapid increase in tension from the bottom. From the top of BHA to the EOB the tension increases more slowly, due to the lighter DP. Inclination is unchanged. From EOB the slope increases due to $\cos\theta$ getting bigger and a continuously growing normal force. At the KOP there is a reduction in slope, caused by the elimination of normal forces in the vertical section.

Torque: The heavy BHA also induces a rapid increasing torque along the BHA. The slope reduces at the top of BHA as the heavy collars are changed with lighter drill pipe joints. A change in outer diameter would also affect the torque, but in this case the TJOD equals the BHA-OD at 7 inches. The slope of the torque is always mirroring the absolute value of the normal force. This is also true for the curve. No normal force in the vertical section yields a constant torque from the KOP to surface.

Normal Force: A heavy BHA resting on the low side results in high values at the bottom. Where the DP starts at top of BHA, the normal force is significantly lower. It remains constant along the tangent section. At the EOB, the pipe is forced against the top side, yielding negative values. These are increasing in magnitude as the inclination tends towards vertical and the fulcrum point just below the KOP. In the vertical section there is no normal force due to $\sin\theta = 0$.

4.3 Discussion

Drag Resistance: The tension at the drill floor will be equal to the supported weight of the drill string, and it will depend on whether the rig is heaving upwards or downwards. The difference between surface tension during upwards heave and surface tension during downwards heave, will be equal to two times the drag resistance in the well. Importantly, this requires the establishment of a constant heaving velocity in both situations, i.e. no mass forces due to acceleration are present. The total drag resistance can also be found by multiplying the summed normal force along the drill string with the friction factor.

Surface Values: The accumulated tension from bit to drill floor corresponds to the force that needs to be applied on the top joint in order to pull the bit. Likewise, the accumulated torque corresponds to the torque that needs to be applied on the top joint to initiate bit rotation.

Discretization: Increasing or decreasing the length of a differential drill string element will only affect the values in the curved section. This is the only section where the inclination changes continuously. The smaller discretization, the better results.

Mass Forces: Changing from a stationary drill string to a heaving drill string (i.e. including the forces due to heave acceleration) will affect the surface values. The axial tension will increase over the entire drill string, while the normal force and torque values are only affected in the build-section.

Tool Joint Radius: A higher radius on the tool joints yields a higher tangential velocity compared to the pipe body, so the use of TJOD is not a conservative approach. It implies a hard formation as opposed to a soft formation where the tool joints may dig into the formation. For the entire weight to be supported on the tool joints, it would also require a relatively clean hole.

Rigid Body: The assumptions listed in section 4.1.2 make the drill string a rigid body with no elasticity, meaning that there can be no axial compression or elongation. This implies that any force acting on top of the drill string, is simultaneously affecting the drill bit. Further, it means that the drill floor and drill bit are always moving with identical velocity and acceleration. This is of course a poor and erroneous assumption.

5 Axial Stick-Slip & Minimum RPM

5.1 Approach

The overall objective is to mitigate or prevent axial stick-slip to avoid tool damage caused by axial shocks. The string will slip in the axial direction once it is compressed by a length that is greater than a *critical displacement*, defined below. How long is this critical displacement? How much time is available before an axial shock is initiated? How is this time affected by changes in drill string or wave parameters? What drill string length is required to eliminate axial stick-slip? What values for top drive RPM will mitigate axial stick-slip? In short, the following chapter discusses the torsional stick-slip behavior of the drill string, and its consequences on axial shock mitigation. The approach can be described as follows:

1. Drill string dimensions and wellbore properties are used to determine the critical displacement length, i.e. the vertical heave distance before an axial shock occurs.
2. The rig's heave motion is used to couple the critical displacement length to a certain time interval. This is called the critical time interval.
3. Drill string parameters and surface torque is used to determine the angular deflection just before rotation commences.
4. The angular deflection is coupled with the critical time interval to determine a minimum rotational velocity.

5.2 Theory

5.2.1 Critical Displacement Length

This section evaluates the axial drag forces along the wellbore. What length (x) must the drill string be compressed to generate a restoring force (F) that is large enough to overcome the sum of axial drag forces (ΣR)? See illustration in Figure 10. The figure is only conceptual and not to scale. The evaluated wellbore trajectory is still the one illustrated in Figure 1.

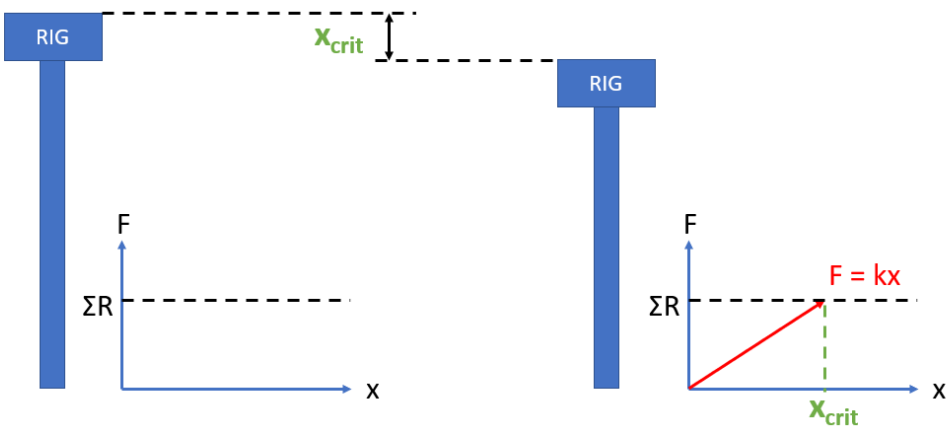

Figure 10: Hooke's law. The restoring force is proportional to the change in length. At what displacement does this force exceed the static friction?

The calculations below assume uniform compression along the drill string, which means that the entire drill string consist of the same material, has a uniform cross-sectional area and is compressed evenly from the rig floor to the bit. The calculations also presuppose that only static friction, and no dynamic friction, is seen over the drill string length during compression. Practically, this means that all axial movement during drill string compression is neglected, which is a bold assumption. Temperature effects are neglected, although higher temperatures result in a lower steel stiffness. This stiffness reduction is only moderate for typical drilling temperatures, but at very high temperatures the value of the elastic modulus decreases rapidly (ASM, 1990). Assuming a linear stress–strain curve, the axial stress (σ) is proportional to the axial strain (ε) and the relationship between the two variables is described by Hooke's law.

$$\sigma = E\,\varepsilon \tag{5.10}$$

This is called elastic deformation, and the coefficient of proportionality is Young's modulus (E). An increasing value for E means a stiffer material, and an idealized rigid body would have an infinite Young's modulus. The Young's modulus of a material can be used to calculate the force it exerts under specific strain. The stress can be written as $\sigma = F/A$ and the strain can be written as $\varepsilon = \Delta L/L_0$. Evaluating the entire drill string as one single and continuous spring that is evenly compressed from top to bottom, the axial restoring force in the string can be written as

$$F = \frac{E\,A\,\Delta L}{L_0} \tag{5.11}$$

where F is the force exerted by the material when contracted or elongated by ΔL, A is the cross-sectional area of the drill string and L_0 is the original length of the string. Hooke's law for a stretched wire can be derived from this relationship

$$F = kx \tag{5.12}$$

where

$$k = \frac{E\,A}{L_0} = \frac{E\,\pi\,\frac{(OD^2 - ID^2)}{4}}{L_0} \tag{5.13}$$

and

$$x = \Delta L \tag{5.14}$$

Evidently, F is proportional with k as showcased in Figure 10. As the normal force on each differential element is already calculated in section 4.1.3, the total drag force is found by multiplying the summed normal force along the string with a friction factor. The total drag force can be written as

$$\sum_{i=1}^{n} R_i = R_1 + R_2 + R_3 + \cdots + R_{n-1} + R_n \tag{5.15}$$

where n is the number of increments between the bit (R_1) and the surface (R_n) and

$$R_i = \mu_{static}\,|N_i| \tag{5.16}$$

Equation (5.15) can also be regarded as the "axial slip tolerance". This can be used to determine the ΔL where the restoring force equals the summed static friction force over the length of the drill string. This is the ΔL where the bottom of the string slips and an axial shock is initiated on the BHA.

$$\mathrm{x_{crit}} = \Delta L = \frac{\sum_{i=1}^{n} R_i}{k} \tag{5.17}$$

Example: A string length of 18,000 ft and the previously given parameters will yield a critical displacement equal to

$$\mathrm{x_{crit}} = \frac{\sum_{i=1}^{n} R_i}{k} = \frac{\mu_{static} \cdot \sum_{i=1}^{n} |N_i|}{\frac{E \cdot A}{L_0}}$$

$$= \frac{0.18 \cdot \sum_{i=1}^{n} |N_i|}{\frac{200\ GPa \cdot \frac{\pi}{4}((5.5 \cdot 0.0254\ m)^2 - (4.778 \cdot 0.0254\ m)^2)}{18 \cdot 10^3 \cdot 0.3048\ m}}$$

$$= \frac{252{,}580\ N}{137{,}070\ N/m} = 1.84\ m$$

5.2.1.1 Alternative Approach

An alternative approach to determine x_{crit} is to use the torque directly. Since both the critical displacement

$$x_{crit} = \frac{\sum_{i=1}^{n} R_i}{k} = \frac{\sum_{i=1}^{n} \mu \cdot |N_i|}{k} = \frac{\mu}{k} \cdot \sum_{i=1}^{n} |N_i| \tag{5.18}$$

and the surface torque (see section 4.1.3)

$$M_s = \sum_{i=1}^{n} M_i = \sum_{i=1}^{n} \mu \cdot r \cdot |N_i| = \mu \cdot r \cdot \sum_{i=1}^{n} |N_i| \tag{5.19}$$

is proportional with the summed normal forces, these can be set equal to each other, yielding

$$\frac{k}{\mu} \cdot x_{crit} = \frac{M_s}{\mu \cdot r} \tag{5.20}$$

and

$$x_{crit} = \frac{M_s}{k \cdot r} = \frac{M_s \cdot L_0}{E \cdot A \cdot r} \tag{5.21}$$

Thus, the critical displacement can be found directly from the surface torque. The radius (r) is discussed in the surface torque derivation.

Example: A string length of 18,000 ft and the previously given parameters will yield a critical displacement equal to

$$x_{crit} = \frac{22{,}432\ Nm \cdot 18 \cdot 10^3 \cdot 0.3048\ m}{200\ GPa \cdot \frac{\pi}{4}((5.5 \cdot 0.0254\ m)^2 - (4.778 \cdot 0.0254\ m)^2) \cdot \frac{7 \cdot 0.0254}{2} m} = 1.84\ m$$

Note that x_{crit} is only dependent on string dimensions and wellbore properties, not on heave conditions. Still, rougher sea states will induce higher axial velocities. The next section tries to couple the critical length with a critical time interval.

5.2.2 Critical Time Intervals

A typical North Sea wave is described by the data in Table 3. For simplicity, the rig heave is assumed to be a simple, sinusoidal wave with constant amplitude and period (fair assumption). The critical axial displacement[9] is constant and given, but the corresponding time interval varies and depends solely on the heave conditions. What is the shortest/longest time interval for the rig to heave a vertical distance of x_{crit}, with the wave data listed below?

Table 3: A typical North Sea wave.

Wave Height	3 m
Amplitude	1.5 m
Period	12 sec

Neglecting the inertia effects of a MODU, its heave behavior can be described with standard oscillation equations. The vessel's position in time, as well as its first and second derivative, can be written as a function of amplitude (A), time (t), angular frequency (ω) and phase shift (ϕ), where $\omega = 2\pi f = 2\pi/T$, f is the wave frequency in oscillations per second and T is the wave period in seconds per oscillation.

The vertical displacement, velocity and acceleration is described by the following three equations, respectively:

$$Y(t) = A \cdot sin\ (\omega t + \phi) \tag{5.22}$$

[9] Where the restoring force exceeds the static friction.

$$Y'(t) = A \cdot \omega \cdot cos\,(\omega t + \phi) \tag{5.23}$$

$$Y''(t) = -A \cdot \omega^2 \cdot sin\,(\omega t + \phi) \tag{5.24}$$

Figure 11 shows these graphs on top of each other. Evidently, the velocity is greatest when the rig floor is in its equilibrium position (i.e. no displacement), while it is zero at the extreme positions (maximum displacement) where the movement changes direction. Consequently, the acceleration is zero at the equilibrium position and greatest at the extreme positions.

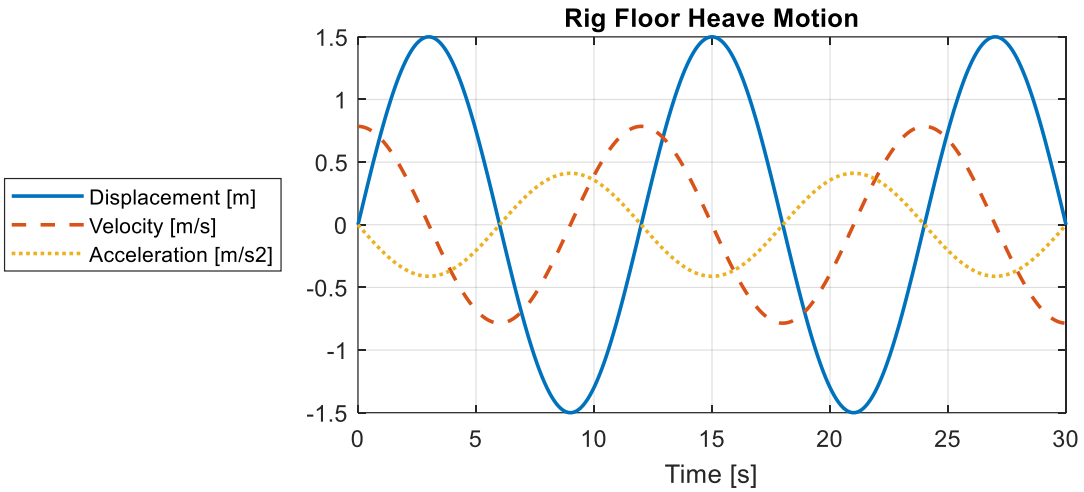

Figure 11: Vertical displacement, velocity and acceleration for a wave with height 3 m and period 12 seconds.

The worst timing of an axial stick event is when the rig offset (relative to MSL) equals half the critical displacement and the velocity is increasing, i.e. the rig is closing in on the MSL with increasing velocity (see Figure 12). The next meters are where x_{crit} is reached in the shortest amount of time. The elapsed time is denoted T_1 and takes place across the MSL, either upwards or downwards. The starting and ending points are determined by

$$\text{Start:} \quad |Y(t)| = 0.5\,x_{crit} \quad \wedge \quad \frac{d}{dt}(|Y'(t)|) > 0$$

$$\text{End:} \quad |Y(t)| = 0.5\,x_{crit} \quad \wedge \quad \frac{d}{dt}(|Y'(t)|) < 0$$

The best timing of an axial stick event is when the rig offset (relative to MSL) is on its way to a maximum, but is exactly one critical displacement away from the crest or trough (see Figure 12). Then the rig will heave to its extreme offset, just avoiding a slip, before heaving back past the initial offset, then an equal displacement in the opposite direction where the restoring force

will finally overcome the static friction and the string slips. This is the longest possible time that the rig can heave without exceeding x_{crit}. The time elapsed is denoted T_2 and can happen either past a crest

$$\text{Start:} \quad Y(t) = A \cdot \sin\left(\left(\frac{1}{2} + 2n\right)\pi\right) - x_{crit} \quad \wedge \quad Y'(t) > 0$$

$$\text{End:} \quad Y(t) = A \cdot \sin\left(\left(\frac{1}{2} + 2n\right)\pi\right) - 2 \cdot x_{crit} \quad \wedge \quad Y'(t) < 0$$

or past a trough

$$\text{Start:} \quad Y(t) = A \cdot \sin\left(\left(\frac{3}{2} + 2n\right)\pi\right) + x_{crit} \quad \wedge \quad Y'(t) < 0$$

$$\text{End:} \quad Y(t) = A \cdot \sin\left(\left(\frac{3}{2} + 2n\right)\pi\right) + 2 \cdot x_{crit} \quad \wedge \quad Y'(t) > 0$$

where n is any positive integer ($n = 1, 2, 3, ...$). An important observation is that once $x_{crit} > A$, it is possible to eliminate axial stick-slip events if the string sticks close to the MSL. This is not very likely as the MSL is where the string sees its maximum velocity, but the window where elimination is possible will expand with drill string length. When $x_{crit} > 2A$ (i.e. the wave height) all axial stick-slip is eliminated. It is no longer relevant where in the heave motion the string sticks as the rig will no longer be able to heave the distance required to generate enough restoring forces. Thus, the BHA will be stationary. As stated above, this presupposes a uniformly distributed restoring force in the string, no drill string rotation during compression, and the unrealistic case with the summed static friction located at the bit. The last assumption means that any axial movement during compression is neglected, allowing the use of a static friction coefficient. Once rotation commences, any restoring forces in the string will be released, but the restoring forces alone will not be large enough to overcome the static friction. To fully remove the shock from an axial sticking it would require a reduced axial velocity (i.e. calmer sea state) or an increased RPM.

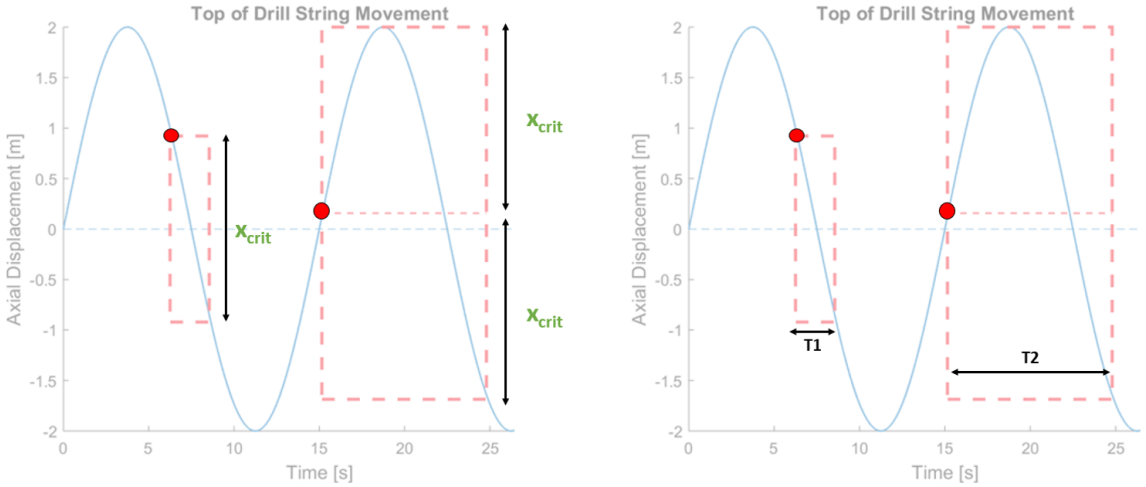

Figure 12: Left: critical displacement, right: critical time intervals. The dashed boxes represent the two scenarios where it takes shortest and longest time for the rig to heave a distance equal to the critical displacement. The red marker represents the point where the string sticks in both cases.

5.2.3 Minimum Required RPM

Knowing the critical displacement length and the time it takes for the rig to heave this distance, this can now be used to estimate a suggested minimum RPM to avoid axial shocks. Ideally, constant rotation should be maintained, but for now, short stops in rotation are allowed[10]. Basically, the maximum time of torsional sticking (t_{ts}) should be less than the minimum time of axial sticking (t_{as}) to mitigate much of the axial shocks.

$$t_{ts,max} < t_{as,min}$$

This means that the sticking interval is terminated with rotation instead of axial overload ($F > \Sigma R$). When rotation commences, there might still be an axial shock as a result of the axial compression during the sticking time, but this shock will be smaller than in the case with no rotation. The following calculations assume an ideal distribution of angular displacement. This means that the distance between each rotation is constant. In reality, this distance is not constant, and the angle of twist in each differential element depends on several parameters, for instance local differences in cross-sectional area or torsional rigidity. The difference between an ideal and a real distribution is illustrated in Figure 13.

[10] The effect can be minimized by timing these across the heave equilibrium point (i.e. the MSL).

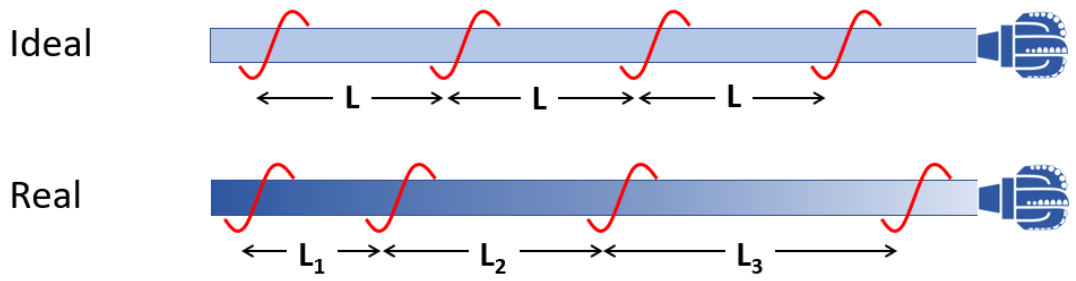

Figure 13: Ideal vs real distribution of angular deflection in a drill string. The difference is caused by wellbore friction and local variations in string properties. Both strings are rotated four times, but while L is constant for the ideal case, $L_1 < L_2 < L_3$ for the real case.

When a uniform shaft is subjected to torque it will twist with an angle that depends on the torsional rigidity of the material and the magnitude of the applied torque. If the torque (T) is evenly distributed in a drill string element with length (ΔL), the angular deflection in radians (θ) can be written as

$$\theta = \frac{\Delta L \cdot T}{J_k \cdot G} \tag{5.25}$$

where the modulus of rigidity (G) is constant and defined as the ratio of shear stress to shear strain

$$G = \frac{\tau_{xy}}{\gamma_{xy}} \tag{5.26}$$

and J_k is the polar moment of inertia defined as

$$J_k = \frac{\pi(OD^4 - ID^4)}{32} \tag{5.27}$$

for a hollow cylinder shaft with outer diameter (OD) and inner diameter (ID). The subscript $k = (1, 2)$ for elements in the BHA and DP section, respectively. As the string is discretized into n steps, equation (5.25) is used to calculate the angular displacement on every differential element. The total angular displacement will then become the summed displacement from the surface and down to the bit. The internal torque is calculated backwards for every incremental step from the surface (n) to the bit (1). See the illustration in Figure 14. The internal torque calculated in one step (i) is assumed valid down to the adjacent step $(i - 1)$. Basically, the torque in every point along the string is assumed equal to the summed friction resistance

between the evaluated depth and the bit. Despite applying significant torque (M_s) on the top joint, the TOB will be equal to zero. The slightest increase in torque will initiate string rotation.

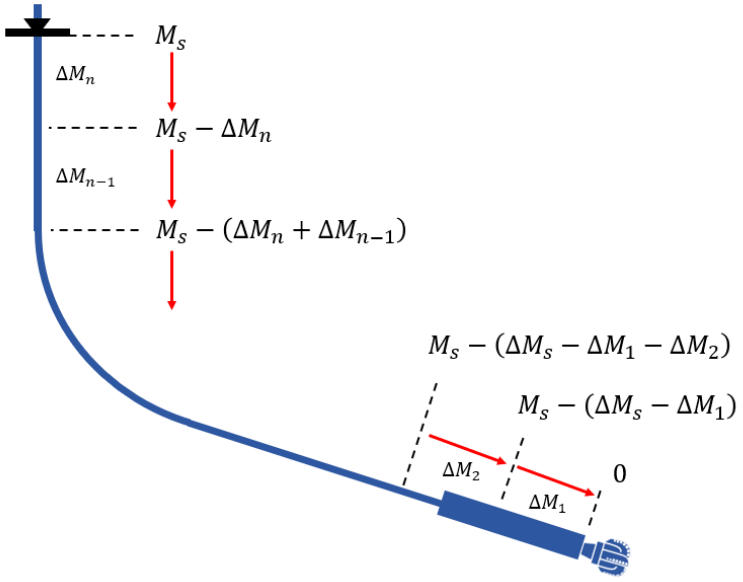

Figure 14: The internal torque is calculated backwards from the surface ($i = n$) *to the bit* ($i = 1$).

Summing up the angular displacement in all elements, the total twist of the drill string is given as

$$\theta = \int_0^{TD} \frac{T(x)}{J(x)G(x)} dx = \sum_{i=1}^{n} \frac{\Delta L \cdot T_i}{J_k \cdot G} \tag{5.28}$$

where $T_n = M_s$, given by equation (5.19). The derivation of the surface torque is outlined in section 4.1.3. Knowing the number of radians that corresponds to the slipping torque, a minimum rotational velocity can easily be deduced from the minimum time of axial sticking. To rotate θ radians in less than $t_{as,min}$ seconds will require a rotation

$$RPM > \frac{\theta}{2\,\pi} \cdot \frac{60}{t_{as,min}} \tag{5.29}$$

Applying the newfound θ in the calculations would imply that the surface torque values are constantly fluctuating between zero and the threshold where rotation commences, with an instantaneous removal of the built up torque once it reaches this threshold. This is obviously incorrect. Friction will prevent the string from unwinding completely and the rotation will stop

long before the string reaches zero torque[11]. The top joint will also continue to rotate throughout the slip period, further sustaining the time of rotation. The following rough estimations are suggested to ensure a more physically correct approach. See illustration in Figure 15.

- The rotation will stop when the angular deflection equals 1/3 of the threshold deflection θ caused by the surface torque.
- One top drive rotation is performed during this slipping phase.
- Thereby the angular deflection is restored to θ radians where rotation commences again.
- This stick-slip cycle repeats itself, effectively every fifth top joint rotation.

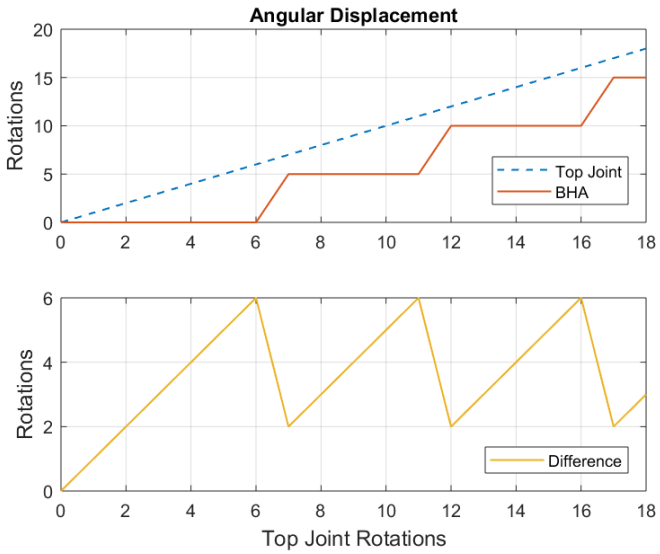

Figure 15: Conceptual illustration of the assumed relationship between the angular displacement in top joint and BHA after starting rotation of a torque free string. Only 2/3 of the rotations needs to be restored in each stick-slip cycle.

When only needing to restore two thirds of the initial drill string torque in every stick-slip cycle, equation (5.29) now becomes

$$RPM > \frac{2}{3} \cdot \left(\frac{\theta}{2\,\pi}\right) \cdot \frac{60}{t_{as,min}} \tag{5.30}$$

[11] It has been observed that a longer and heavier BHA usually promotes a more stable rotational behavior due to the flywheel effect where momentum is stored as kinetic energy. A bigger mass yields bigger moment of inertia.

5.3 Results & Discussion

5.3.1 Critical Displacement & Time

Table 4: Some relevant drill string data, with the rest found in Table 1. Only the length is new.

Parameter	Value	Units	Description
E	200	GPa	Young's modulus for steel
OD	5.5	in	Outer diameter of string (constant)
ID	4.778	in	Inner diameter of string (constant)
L_0	18,000	ft	String length
μ_{static}	0.18	-	Static friction factor

Applying the data in Table 4 to the theory above, k was found to be roughly 137 kN/m. The total drag force on the string was found to be 253 kN. Dividing the required restoring force with the axial drill pipe stiffness yields the corresponding displacement, $x_{crit} = 1.84\ m$. This length is valid for the given string data, and is independent of heave conditions. Figure 16 shows three cases where the critical displacement length (dashed) is plotted over the heaving rig floor displacement (solid) as discussed above. The first box represents the most rapid covering of the critical displacement. This has height x_{crit} and width T_1. The second box represents the longest time interval possible without exceeding x_{crit}. This will always be located on a crest or trough, with height $2 \cdot x_{crit}$ and width T_2.

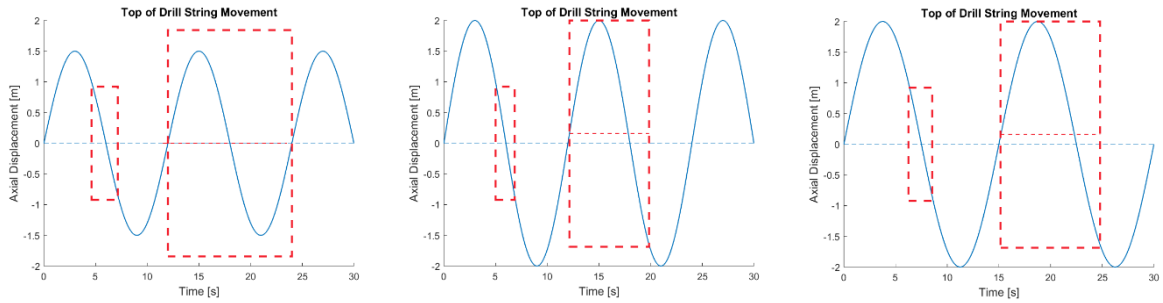

Figure 16: The same drill string is subjected to three different heave conditions, with wave height and wave period equal to: left (3m, 12 sec), middle (4m, 12 sec) and right (4m, 15 sec).

The problem of axial stick-slip is not always relevant in a wellbore and the drill string length has a large impact on x_{crit}. The drill bit of a short drill string (e.g. 500 m) is likely to experience the undamped movement of a heaving rig, only delayed by the time of acoustic travelling in the pipe material. This time is determined by the shear wave velocity for torsion and pressure wave velocity for compression and tension. A very long drill string (e.g. 10 000 m) might

experience significant heave on the rig, but no movement at the bit. This is due to the drill string elasticity and wellbore friction absorbing the energy from rig heaving. As a result, the lower parts of the string can be stationary while the upper parts are heaving. Practically, this can be evaluated by comparing the critical displacement (x_{crit}) to the heave amplitude (A) as discussed in the previous section. A longer drill string will require more compression (increased heave amplitude) to break loose, as the increasing total drag force requires a higher restoring force. The increased drag is not only the result of added length, but also the higher normal forces induced in the curved section. Figure 17 shows the critical displacement for three different string lengths, with numerical data accessible in Table 5. Figure 18 is a visualization of the data in this table, showing critical displacement and sticking times for well lengths between 8-22 000 ft MD. Bear in mind that the total drag force is not only dependent on length, but is much more sophisticated than this model suggests. For instance, the friction coefficient and damping factor could change because of a different roughness, cuttings distribution or wellbore tortuosity.

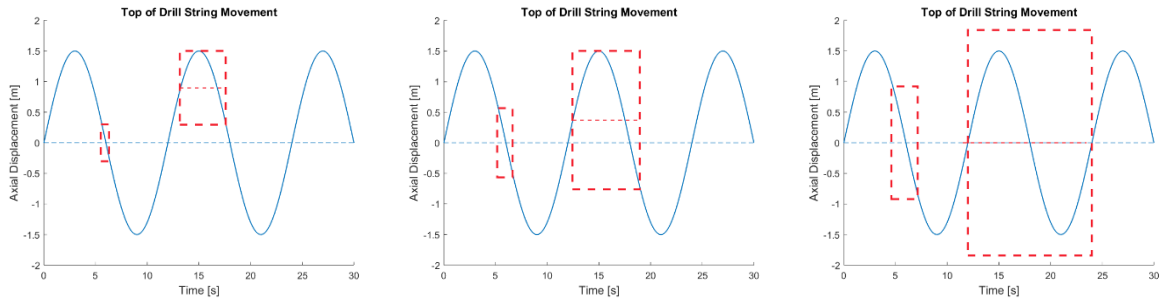

Figure 17: Critical displacement with a string length of 12 000, 15 000 and 18 000 ft, from left to right. The wave is identical with height 3m and period 12 sec. Time intervals are listed in Table 5.

Table 5: Critical displacement and sticking times for a range of drill string lengths. Wave height is 3 m, the period is 12 seconds. The data is plotted in Figure 18.

Drill String Length [ft]	x_{crit} [m]	T_1 [s]	T_2 [s]
8 000	0.19	0.30	2.45
10 000	0.37	0.50	3.35
12 000	0.60	0.80	4.45
14 000	0.93	1.20	5.70
15 000	1.13	1.50	6.50
16 000	1.35	1.80	7.55
18 000	1.84	2.55	No upper limit
20 000	2.41	3.60	No upper limit
22 000	3.04	No upper limit	No upper limit

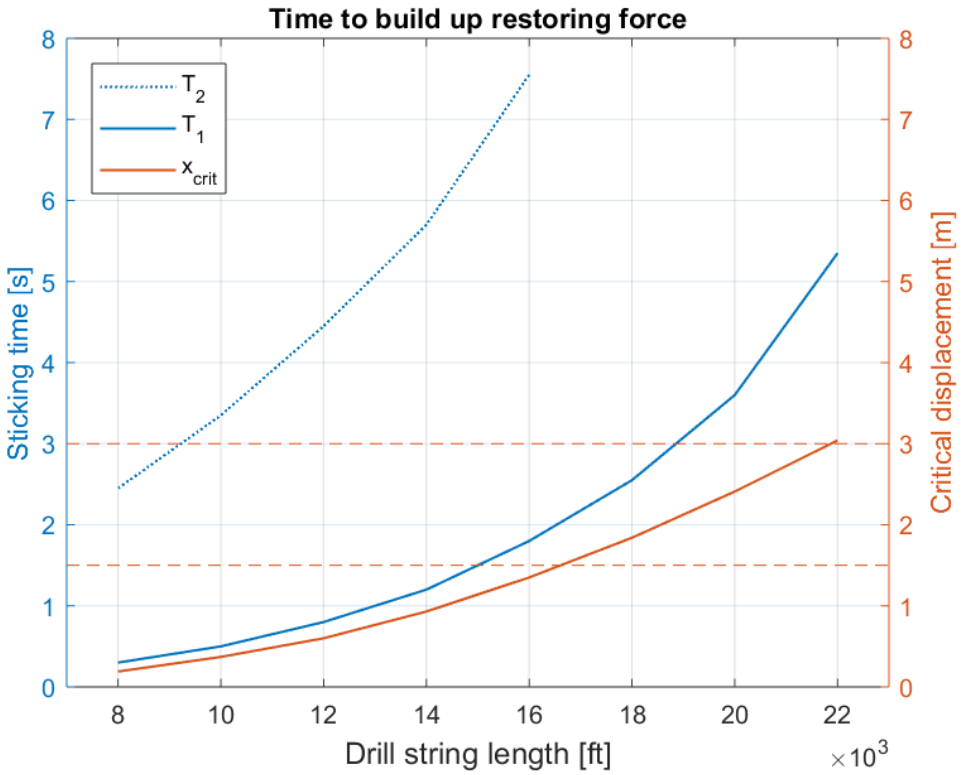

Figure 18: Critical displacement (x_{crit}) and sticking times (T_1, T_2) as a function of drill string length for a wave with height 3 meters and period 12 seconds. The dashed horizontal lines represent the heave amplitude and wave height of 1.5 and 3.0 meters, respectively.

With the given string data, a length of minimum 17,000 ft would open up for the possibility of having a continuously stuck bit, despite a 1.5 meter heave amplitude on the top joint. Obviously, a long string is not favorable if the goal is to maintain drill string movement at all times, but it

can serve to eliminate the axial shocks; which is the very source of the problem. At approximately 22,000 ft, the axial stick-slip is no longer a problem as the critical displacement exceeds the wave height. The issue of axial stick-slip is gradually eliminated between the wave amplitude and the wave height, displayed as horizontal, dashed lines in Figure 18 at 1.5 meters and 3 meters, respectively.

5.3.2 Minimum Required RPM

The time intervals of BHA axial stick-slip have now been determined. The goal is to have a maximum torsional sticking time that is less than the minimum axial sticking time. What RPM must be maintained on the top joint to ensure this? The following results assume a drill string with length 13,000 ft. This length is chosen to be well within the stick-slip area, with a critical displacement small enough to be triggered by the rig heave. All other parameters and assumptions are unchanged and listed in Table 1.

Table 6: Relevant drill string data

Parameter	Value	Units	Description
L	13,000	ft	String length (= 3962 m)
M_s	12,674	Nm	Surface torque
G	79.3	GPa	Modulus of rigidity
BHA_ID	2.25	in	BHA inner diameter
BHA_OD	7	in	BHA outer diameter
DP_ID	4.778	in	DP inner diameter
DP_OD	5.5	in	DP outer diameter

The vertical section and the build section are kept constant, so the difference in string length will only result in a shorter tangent section. The new string forces are displayed in Figure 19.

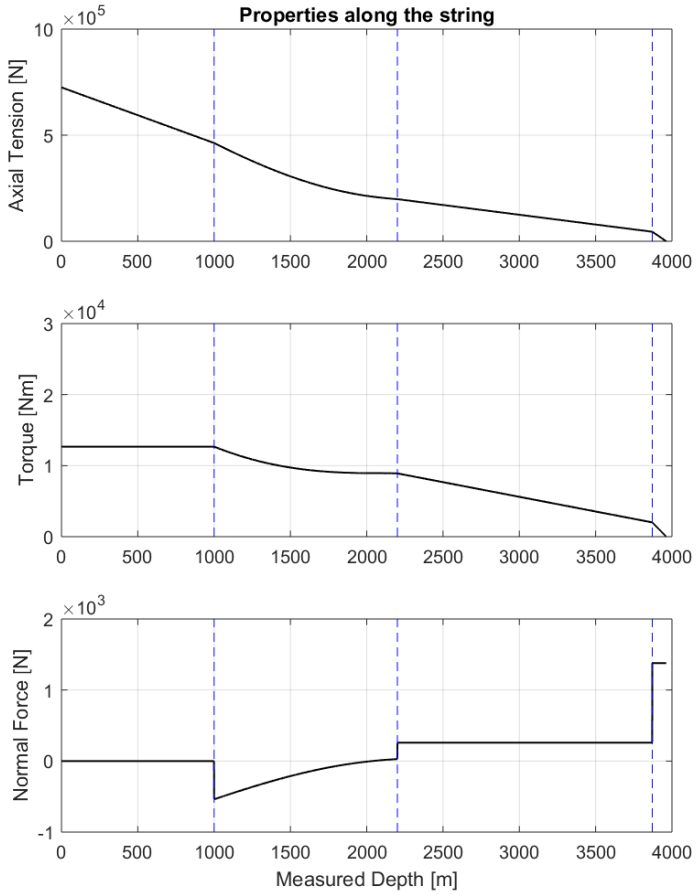

Figure 19: Profiles of axial tension (F), drill string torque (M) and normal force (N) along the string. Data is listed in Table 1 and Table 6. The three vertical lines mark the KOP, EOB and Top of BHA from left to right. The measured depths at these points are 1000m, 2201m and 3871m, respectively.

The new surface torque is 12,674 Nm. The drill string is assumed to be axially stuck during the buildup of surface torque. This assumption neglects the axial drill string compression when the rig heaves and also the shortening of the string when torque is applied. The BHA is assumed to be stationary until the surface torque is reached. When rotation commences at 12,674 Nm, there is an angular displacement between the bit and surface that is equal to

$$\theta = \int_0^{TD} \frac{T(x)}{J(x)G(x)} dx = \sum_{i=1}^{n} \frac{\Delta L \cdot T_i}{J_k \cdot G} = 26.4\, rad = 4.2\, rotations \qquad (5.31)$$

where $\Delta L = 1\,m$, $J_1 = 9.71 \cdot 10^{-5}\,m^4$ and $J_2 = 1.61 \cdot 10^{-5}\,m^4$. The given string data, coupled with rig heave[12] and previously stated assumptions yields $x_{crit} = 0.75\,m$, $T_1 = 1.00\,s$ and $T_2 = 5.00\,s$. Applying the relationship in equation (5.30), this requires a minimum rotational velocity of

$$RPM_1 > \frac{2}{3} \cdot \left(\frac{\theta}{2\,\pi}\right) \cdot \frac{60}{T_1} = \frac{2}{3} \cdot \left(\frac{26.4\,rad}{2\,\pi \dfrac{rad}{rotation}}\right) \cdot \frac{60\,sec/min}{1.00\,sec} = 168 \qquad (5.32)$$

168 RPM to reestablish drill string rotation before the rig can possibly heave more than the critical displacement. Using T_1 means that the rig is heaving past the MSL and that this is the tightest possible window to reestablish rotation. The sticking times can vary between T_1 and T_2, but T_1 is the limiting factor. For perspective, T_2 will yield

$$RPM_2 > \frac{2}{3} \cdot \left(\frac{\theta}{2\,\pi}\right) \cdot \frac{60}{T_1} = \frac{2}{3} \cdot \left(\frac{26.4\,rad}{2\,\pi \dfrac{rad}{rotation}}\right) \cdot \frac{60\,sec/min}{5.00\,sec} = 34 \qquad (5.33)$$

34 RPM, which is the minimum rotational velocity required to reestablish drill string rotation before the rig heaves more than the critical displacement over a crest or trough. Running these calculations for all lengths in Table 5 will give the results plotted in Figure 20. Notice that the required RPM is decreasing with an increasing string length. For example, a string with length 6,000 meters requires a top drive velocity of 125 RPM. This is because the drill string compression (ΔL) is absorbed by a longer drill string (L_0), yielding a lower compressional force when heaving the same distance. Also, the axial drag will increase when the string length increases.

[12] Wave height 3 meters and period 12 seconds. See Figure 11.

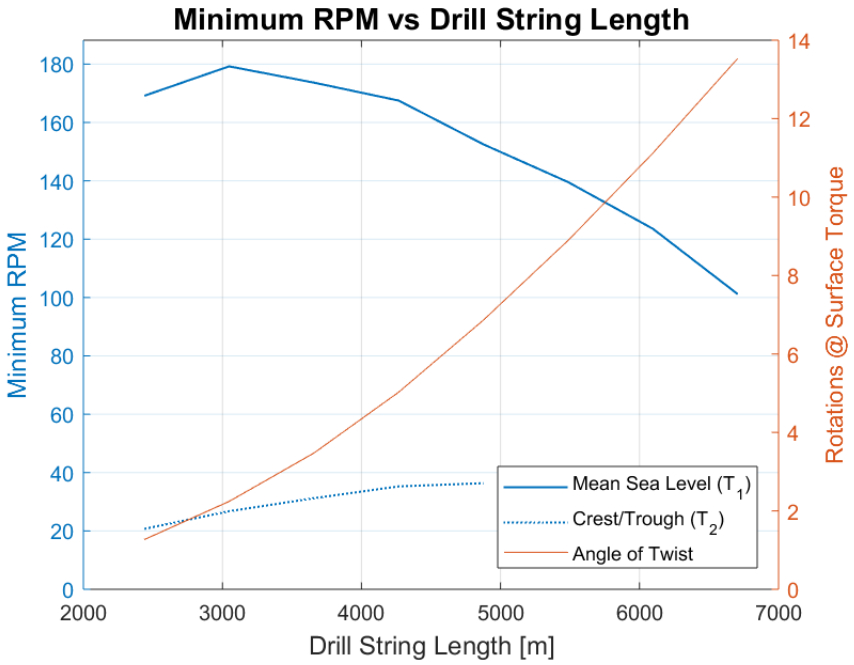

Figure 20: Illustrating the required RPM to ensure that torsional slip happens before axial slip for different drill string lengths. The upper graph shows the required RPM to escape the shortest axial sticking interval (i.e. past MSL). The graph is valid for a wave with height 3 m and period 12 s.

Naturally, the required RPM for the long time intervals (T_2) over a crest or trough is lower than the required RPM for the short time intervals (T_1) across the MSL. The actual RPM lies somewhere between these two curves. The absence of values on the T_2-curve means that there is no upper limit to the sticking time, i.e. a possibility of a stationary BHA. If there are no values on the T_2-curve, the actual RPM lies between the T_1-curve and zero, as is the case above 5000 meters in the case above.

The above approach was applied on the four different waves listed in Table 7. The critical time interval (T_1) for each heave situation is plotted on top of each other in Figure 21, while the corresponding minimum RPM curves are plotted in Figure 22. The graphs stop where the axial stick-slip is no longer a problem (i.e. where x_{crit} exceeds the wave height).

Table 7: Four different waves

	Wave Height [m]	**Wave Period [s]**
Wave 1	2	8
Wave 2	2.5	10
Wave 3	3	12
Wave 4	3.5	14

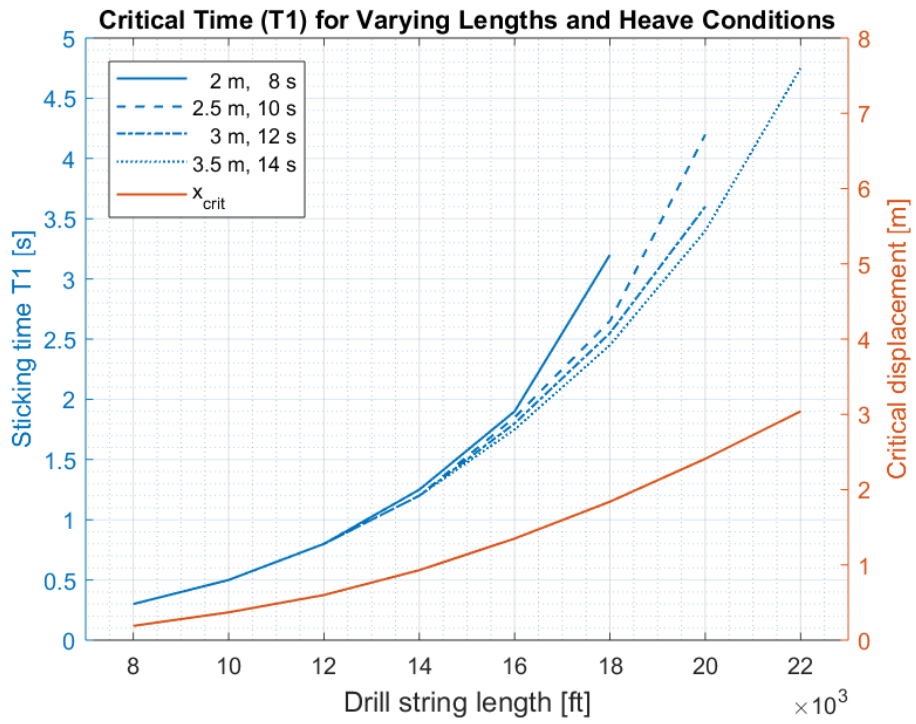

Figure 21: Available time to restart rotation (T_1). String length is on the horizontal axis. Each blue line is the result of a specific wave. Wava data is given in the legend as (wave height, wave period).

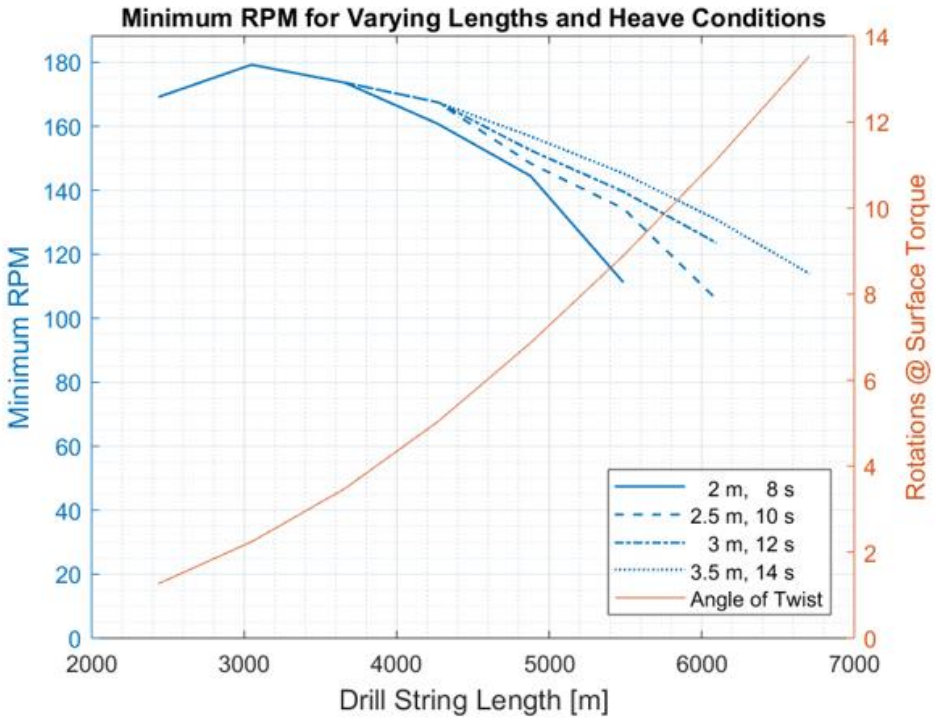

Figure 22: Rotational velocities required to start rotation within T_1. String length is on the horizontal axis. Each blue line is the result of a specific wave. Wava data is given in the legend as (wave height, wave period).

Evaluating the four different T_1-curves in Figure 21, these graphs suggest that T_1 decreases with an increasing wave height, which makes physically sense. However, remember that the heave velocity, which is the basis for the T_1-calculations, is heavily dependent on the chosen wave period. A decrease in T_1 yields an increase in the corresponding RPM, as showcased in Figure 22. In both plots, the effect of wave height seems to increase with drill string length. The observations are only valid for the evaluated range, and may not apply elsewhere. Based on the above graphs, it seems fair to conclude that the minimum required RPM increases with wave height for the evaluated range. Above 3000 m MD, increasing the drill string length will reduce the required RPM. Also, the effect of an increasing wave height seems to be greater for long drill strings than for short.

5.3.3 Comments

MODU: Remember that the rig is not fixed, it's floating. The axial heave movement is the very cause of the problem, so it is fair to assume significant heave movement. This would help transfer torque down the drill string, meaning that the required RPM is likely to be lower than that determined above. In any case, maintaining a constant RPM on the top drive is beneficial in terms of mitigating axial stick-slip.

Surface torque & string length: In the ideal case, the angle of twist would be proportional to the drill string length. In reality, this is not true. Evaluating the line plotted against the right vertical axis in Figure 22, i.e. the total angle of twist, it is clearly curved upwards. Knowing that ΔL, G, J_1 and J_2 are constant, and that the ideal twist is proportional with the total length, the answer obviously lies in the increasing torque values. There are two effects that work to raise the torque. One is simply the torque contribution added by the extra drill string length. The other, which is less obvious, is the increasing normal forces in the bend section (fulcrum point). More weight below the EOB means increased contact forces in the build section. The torque is then proportional with the normal force as seen in equation (5.19). The result is a positive second derivative.

$$\frac{d^2\theta}{dL^2} > 0 \tag{5.34}$$

An interesting takeaway from Figure 22 is that the required RPM has a maximum located around 10,000 ft (i.e. 3048 m). The reason for this is not yet understood. Increasing the drill

string length will have both beneficial and detrimental effects on the required RPM, as explained by Figure 23.

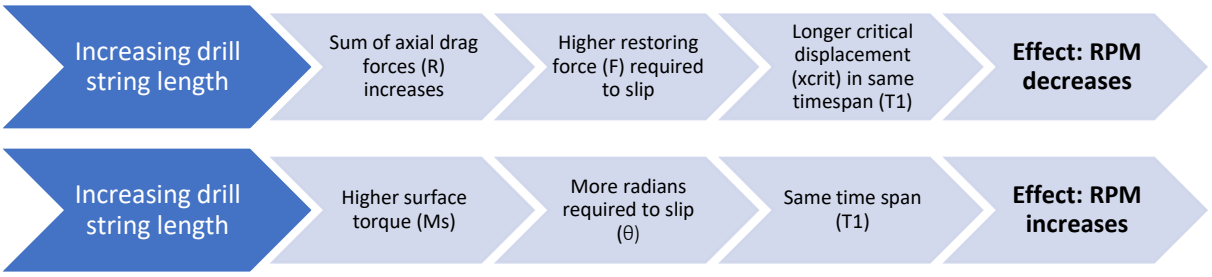

Figure 23: Beneficial and detrimental effects of increasing the drill string length.

6 Angular Drill String Vibrations with Damping

The previous section found a suggested range of RPM to avoid axial stick-slip. As the well is a very complex system, this range of velocities might solve one problem while causing another problem. One such issue is drill string resonance. The drill string system will have certain natural frequencies that cause large angular displacements if sustained for a longer period of time. Such displacements will have adverse effects on equipment lifetime and should therefore be avoided. The content of this chapter can be described by the following two bullet points:

- The angular displacement along the drill string is found for a variation of dampening factors and rotational velocities.
- The natural frequencies for DP and DC are estimated, and the results of a simplified numerical model is compared to that of an analytic approximation.

6.1 Theory

(Dareing & Livesay, 1968) modelled a system with two continuous pipes vibrating in a linearly damped environment. The model showed the vibration response caused by boundary displacements and was written out for the case of axial vibrations. With some modifications, the model should also be applicable to torsional vibrations. The following chapter will present the derivation and discussion of this model; the torsional version of the D&L model. Among important subjects that will be discussed are different boundary conditions, the damping constant and the superposition of drill string movement. The appended script for this section is inspired by previous work done by co-student (Berntsen, 2019) on reproducing this vibration model for the case with axial vibrations.

An illustration of the drill string system with most of the basic components is shown in Figure 24, along with the coordinate system used in the analysis. The function $\theta(x,t)$ represents the angular displacement of a point along the string at any given time. θ_1 refers to the displacement in the collar section, while θ_2 refers to the displacement in the drill pipe section. The general solution derived below is valid for both drill pipe and drill collar. The following model can easily be modified to include any given number of sections, as outlined in the original paper. For simplicity, this analysis treats only the two sections mentioned above.

Summing all forces that act on a differential element and equating them to the inertia term gives the equation below. J is the polar moment of inertia, G is the shear modulus, γ_θ is the torsional damping factor and ρ_θ is the mass polar moment of inertia per unit length of drill string.

$$JG\frac{\partial^2\theta}{\partial x^2} = \gamma_\theta\frac{\partial\theta}{\partial t} + \rho_\theta\frac{\partial^2\theta}{\partial t^2} \tag{6.35}$$

The friction term in equation (6.35) is the primary difference between this and previous mathematical analyses of the same problem; (Bailey & Finnie, 1960) and (Paslay & Bogy, 1963). This term implies that the local friction is proportional to the local linear velocity and it requires the assumption that viscous friction can be substituted for rubbing, fluid and material friction with reasonable accuracy. This is true if the decay per vibration cycle is somewhat similar in both cases, as shown by (Den Hartog, 1956).

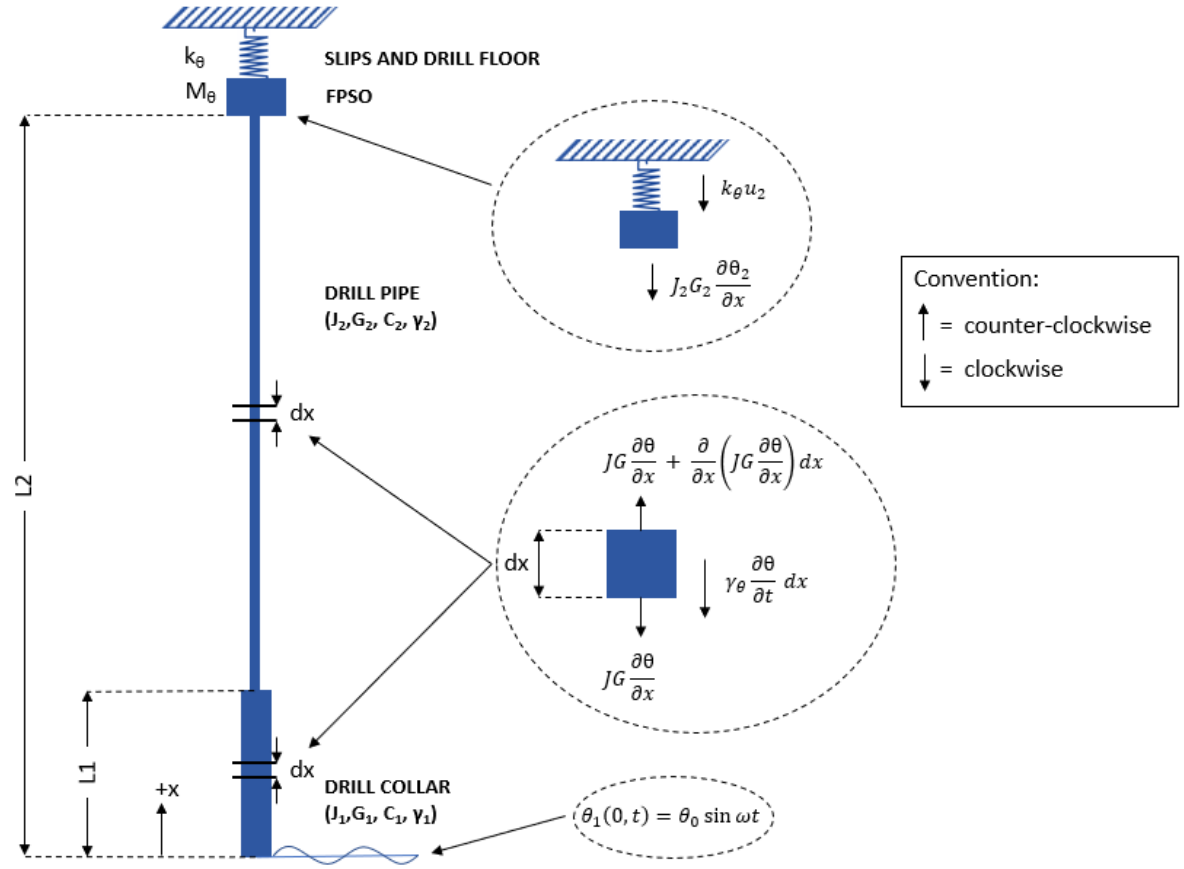

Figure 24: This is the system used to evaluate the natural frequencies in a drill string. The string consists of two sections. The encircled equations of motion are derived in the following section. The figure is not to scale.

6.1.1 Boundary Conditions

By summing all the forces that act on the uppermost joint, it will yield the equilibrium equation that can be used as a boundary condition on the top joint. M_θ is the mass moment of inertia of the entire MODU and k_θ is the torsional stiffness of the slips and the drill floor. Both parameters are discussed further in section 6.3.

$$M_\theta \frac{\partial^2 \theta_2}{\partial t^2} + J_2 G_2 \frac{\partial \theta_2}{\partial x} + k_\theta \theta_2 = 0 \tag{6.36}$$

The system consists of two sections, a drill pipe section and a drill collar section, and these are connected rigidly at a distance $x = L_1$ from the bit (see Figure 24). This will mean that both the drill pipe and the drill collar experience the same movement at the connection, resulting in a new pair of boundary conditions. These can be formulated as one for the angular displacement (6.37) and one for the section material stress (6.38)

$$\theta_1(L_1, t) = \theta_2(L_1, t) \tag{6.37}$$

$$J_1 G_1 \frac{\partial \theta_1(L_1, t)}{\partial x} = J_2 G_2 \frac{\partial \theta_2(L_1, t)}{\partial x} \tag{6.38}$$

The bit angular displacement is periodic and can be written as

$$\theta_1(0, t) = \theta_0 \sin \omega t \tag{6.39}$$

where ω is the angular frequency in radians per second. With a velocity of N rotations per minute and an excitation frequency of once every 4$^{\text{th}}$ rotation ($f_e = 0.25$), this is defined as

$$\omega = 2\pi f = 2\pi \cdot \frac{f_e \, N}{60} \tag{6.40}$$

6.1.2 Equation of motion

The next step will be to define an equation that includes all forces acting on a single, differential element in the string (6.41). The left side represents the force from internal material stress, determined by the material stiffness. The first term on the right side is a damping force that includes all of wellbore friction, material friction and viscous effects. The last term is the inertial force caused by the angular momentum.

$$JG \frac{\partial^2 \theta}{\partial x^2} = \gamma_\theta \frac{\partial \theta}{\partial t} + \rho_\theta \frac{\partial^2 \theta}{\partial t^2} \tag{6.41}$$

The same equation can be written as

$$JG\theta_{xx} = \gamma_\theta \theta_t + \rho_\theta \theta_{tt} \tag{6.42}$$

This differential equation describes the movement of any differential element in the drill string model. It is applicable to both the drill pipe and the drill collar section. This equation, together with the boundary conditions above, must be satisfied to determine the function $\theta(x,t)$ that describes the drill string response when subjected to the excitation pattern in (6.40). The angular displacement (θ) is a function of time (t) and distance from the bit (x).
The following complex function describes the angular displacement. It satisfies the above and has both real and imaginary components.

$$\theta(x,t) = \bar{\theta}(x)e^{i\omega t} + static\ terms \tag{6.43}$$

Only the terms of dynamic displacement are relevant, so the static terms are neglected, and the equation is reduced to

$$\theta(x,t) = \bar{\theta}(x)e^{i\omega t} \tag{6.44}$$

Substituting (6.44) into (6.41) gives

$$JG\frac{\partial^2 \bar{\theta}}{\partial x^2}e^{i\omega t} = \gamma_\theta \bar{\theta} i\omega e^{i\omega t} + \rho_\theta \bar{\theta}(-\omega^2)e^{i\omega t} \tag{6.45}$$

The unknown complex function $\bar{\theta}$ is the one which satisfies

$$\frac{d^2\bar{\theta}}{dx^2} + \eta^2\bar{\theta} = 0 \tag{6.46}$$

where

$$\eta^2 = \frac{\omega^2}{{c_s}^2} - i\frac{\gamma_\theta \omega}{JG} \tag{6.47}$$

and c_s is the shear wave velocity in stainless steel. Solving this complex differential equation (6.47) yields a solution on the form

$$\bar{\theta}(x) = B\sin(\eta x + b) \tag{6.48}$$

where B, η and b are complex numbers. B and b depend on the boundary conditions in (6.36) and (6.39). Substituting (6.48) into (6.44) yields

$$\theta(x,t) = B\sin(\eta x + b)e^{i\omega t} \tag{6.49}$$

which describes the dynamic angular displacement in a drill string element. The complex equation has both real and imaginary components and is a solution to two separate problems. The real part solves one problem and the imaginary part solves another. Which part to choose depends on the mathematical formulation of the boundary conditions. The boundary conditions at the bit can be written as

$$\theta_0 \sin \omega t = Re[-i\theta_0 e^{i\omega t}] \tag{6.50}$$

And thus, the real part of equation (6.49) is the desired solution if $[-i\theta_0 e^{i\omega t}]$ is satisfied at $x = 0$. The angular displacement of the damped drill string is then described by the real parts of

$$\theta_1(x,t) = B_1 \sin(\eta_1 x + b_1) e^{i\omega t} \ , \qquad 0 \le x \le L_1 \tag{6.51}$$

$$\theta_2(x,t) = B_2 \sin(\eta_2 x + b_2) e^{i\omega t} \ , \qquad L_1 \le x \le L_2 \tag{6.52}$$

Both $\theta_1(x,t)$ and $\theta_2(x,t)$ have two unknowns, which amounts to a total of four unknowns, labelled B_1, B_2, b_1 and b_2. These can be determined by the four boundary conditions. Starting at the bit, (6.39) is used to find

$$B_1 = -\frac{i\theta_0}{\sin b_1} \tag{6.53}$$

The boundary conditions at the top of the drill collars ($x = L_1$), represented by (6.37) and (6.38), yield

$$B_2 = -\frac{i\theta_0}{\sin b_1} \frac{\sin(\eta_1 L_1 + b_1)}{\sin(\eta_2 L_1 + b_2)} \tag{6.54}$$

and

$$b_1 = \tan^{-1}\left[\frac{J_1 G_1 \eta_1}{J_2 G_2 \eta_2} \tan(\eta_2 L_1 + b_2)\right] - \eta_1 L_1 \tag{6.55}$$

while the last boundary condition at the top of the drill pipe is represented by (6.36) and yield

$$b_2 = \tan^{-1}\left(\frac{J_2 G_2 \eta_2}{M_\theta \omega^2 - k_\theta}\right) - \eta_2 L_2 \tag{6.56}$$

6.1.3 Purpose of simulation

When applying the above theory, it is possible to simulate the dynamic effects of a periodic excitation that obstructs the bit rotation. Due to superposition, all static terms can be left out, focusing solely on the dynamic angular displacement. Practically, this means that we exclude the constant rotation exerted on the top joint and only evaluate what is assumed to be a periodic disturbance on the bit. The purpose of the following simulations is to determine the natural frequencies of the drill string, i.e. specific excitation frequencies that lead to resonance in the string. After determining the natural frequencies, the RPM can be adjusted to circumvent the resonance problem.

6.1.4 Quality Checking Results

To check that the results are sound, the derivation below is used to approximate the natural frequencies of standing waves in a string. Note that this approach will assume a uniform cross-section, neglecting the 300 ft of DC at the bottom.

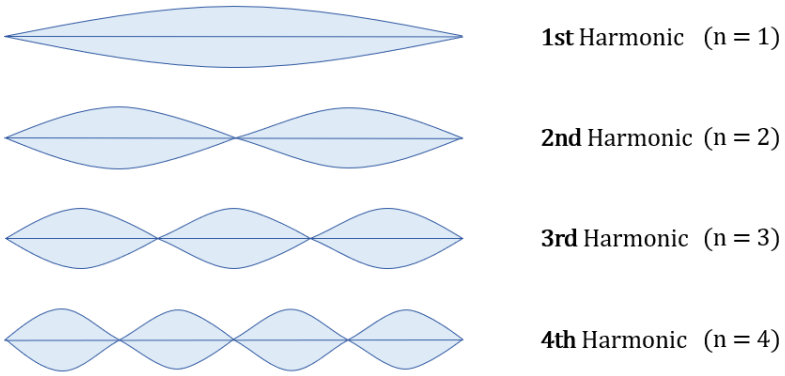

Figure 25: The four lowest natural frequencies for a string. This conceptual illustration shows lateral displacement, but it is transferrable to angular displacement.

The first three harmonic modes of vibration in a string with length L_2 can be written as

1. $L_2 = \frac{1}{2}\lambda$
2. $L_2 = \frac{2}{2}\lambda$
3. $L_2 = \frac{3}{2}\lambda$

Thus, any harmonic mode can be written on the form $L_2 = n\lambda/2$, meaning that the wavelength (λ) of any natural frequency mode is given by

$$\lambda_n = \frac{2}{n} L_2 \tag{6.57}$$

where $n = (1, 2, 3, \dots)$ is the mode number. The wavelength of a sinusoidal waveform traveling at constant speed (v) in a linear media is given by

$$\lambda = \frac{v}{f} \tag{6.58}$$

where f is the frequency. The wavelength of the angular displacement (λ_θ) can then be expressed in terms of shear velocity (c_s) and angular frequency (f_θ) as

$$\lambda_\theta = \frac{c_s}{f_\theta} \tag{6.59}$$

meaning that the angular frequency is

$$f_\theta = \frac{c_s}{\lambda_\theta} = \frac{c_s}{2L_2/n} \tag{6.60}$$

and the corresponding RPM is given by

$$RPM = \frac{f_\theta}{f_e} \cdot 60\ s/min = \frac{c_s}{2L_2/n} \cdot \frac{1}{f_e} \cdot 60 \tag{6.61}$$

where f_e is the number of excitations per rotation (e.g. 0.25 for once every fourth round) and the answer is multiplied with a factor of 60 to go from seconds to minutes.

6.2 Results

Table 8: Drill string data. See Figure 24.

Category	Description	Parameter	Value	Units
Drill Collars	DC length	L_1	300	ft
	DC outer diameter	OD_1	7	in
	DC inner diameter	ID_1	2 ¼	in
	DC polar moment of inertia	J_1	233	in^4
Drill Pipe	Total string length	L_2	10,000	ft
	DP outer diameter	OD_2	5 ½	in
	DP inner diameter	ID_2	4.778	in
	DP polar moment of inertia	J_2	38.7	in^4
Steel Properties	Modulus of rigidity (shear)	G	$11.2 \cdot 10^6$	psi
	Acoustic velocity of shear wave	c_s	10,400[13]	ft/s
	Torsional damping factor of DC	γ_1	5	$lb\ ft^2/s\ rad$
	Torsional damping factor of DP	γ_2	0.5	$lb\ ft^2/s\ rad$
Surface	Rig mass moment of inertia	M_θ	$1.55 \cdot 10^8$	$lb\ ft\ s^2$
	Rig torsional spring constant	k_θ	250,000	$lb\ ft/rad$
Other	Weight on bit	WOB	0	lbf
	Excitations per bit rotation	f_e	0.25	

6.2.1 Angular Displacement vs Depth

6.2.1.1 Effect of Torsional Damping Factor

Figure 26 shows how the torsional vibration amplitude varies with depth, for the string described in Table 8. The graphs show two scenarios with different damping coefficients. The blue line depicts an undamped drill string $(\gamma_1 = \gamma_2 = 0)$ and the orange line depicts a damped drill string $(\gamma_1 = 5, \gamma_2 = 0.5)$. As expected, the undamped string experiences significantly larger displacement amplitudes than the damped string. The evaluated drill string has a normal frequency mode at 128 RPM which explains the large amplitudes. Evaluating the charts from left to right, the maximum normalized amplitude seems to increase exponentially. The RPM-values are deliberately chosen close to a resonant mode, to illustrate the concept of a natural

[13] $c_{s-wave} = 10{,}400\, ft/s \approx 2/3\, c_{p-wave}$. Source: (Ultrasonics, 2020).

frequency and emphasize the effect of friction. The effect would be less at other frequencies. More on this in the next section.

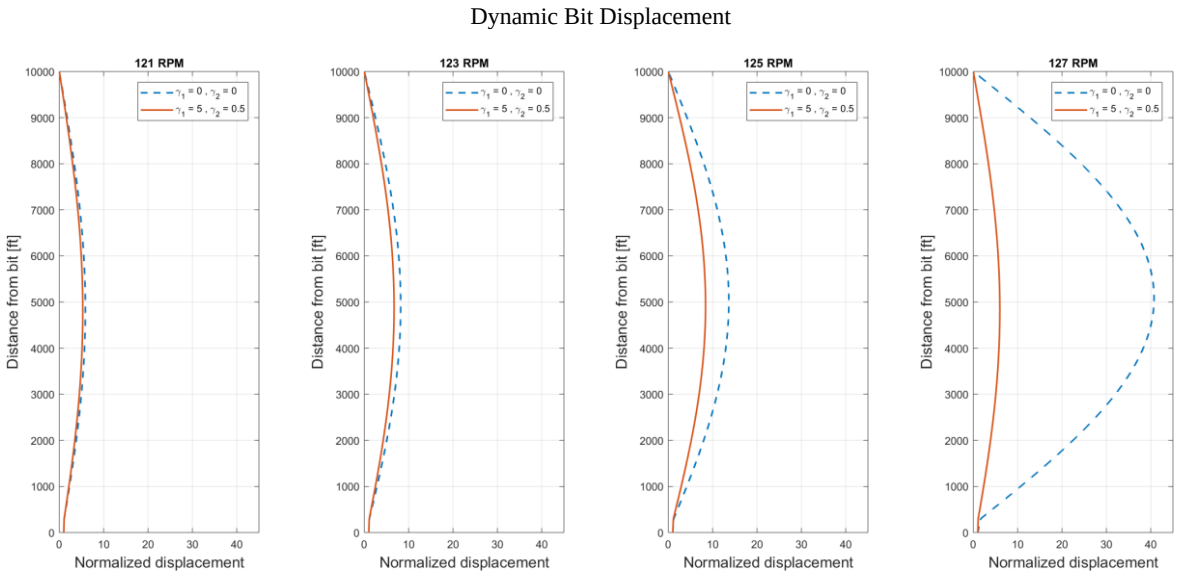

Figure 26: Normalized amplitude of angular drill string vibrations for a damped drill string and an undamped drill string. Frequency response for 121, 123, 125 and 127 RPM. The system has a resonant frequency at 128 RPM. Drill string data in Table 8.

6.2.1.2 Effect of RPM

What happens if the rotational velocity changes? To illustrate this, the excitation frequency is set to once every rotation $(f_e = 1)$, although this is too high to represent torsional stick-slip. When plotting the angular displacement for three different velocities (see Figure 27), it becomes evident that the oscillations are out of phase and that they are dependent on the stick-slip frequency (i.e. RPM). Due to friction in the system, the same element will experience phase differences when the velocity changes.

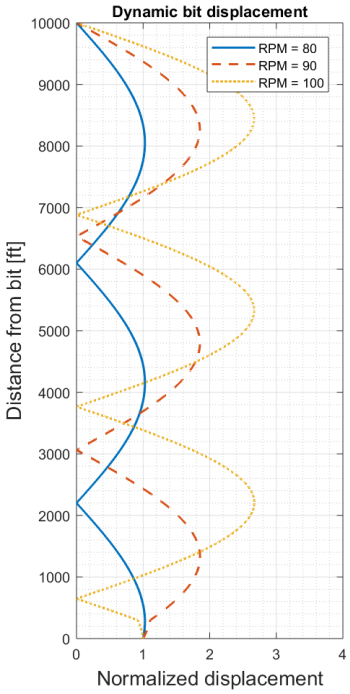

Figure 27: Normalized amplitude of angular drill string vibrations at three different rotational velocities. The excitation frequency is increased to $f_e = 1$ to illustrate the effect of RPM

6.2.2 Natural Frequencies

The effect of frequency on drill string response is shown in Figure 28. The ordinate in this plot represents the ratio of maximum angular displacement in the string to the bit angular displacement amplitude. The abscissa shows the applied RPM, meaning that the actual stick-slip frequency (f_{ss}) is equal to the number of excitations per rotation (e.g. $f_e = 0.25$) times the number of rotations per minute (e.g. $N = 120$), divided by 60 seconds per minute.

$$f_{ss} = \frac{f_e \cdot RPM}{60\ s/min} = \frac{0.25 \cdot 120}{60} = 0.5\ Hz \tag{6.62}$$

The three different curves correspond to different magnitudes of damping. Clearly, some bit displacement frequencies yield a larger drill string response than others. These are the natural frequencies of the system. The curves showcase the response in the entire string, i.e. the combined effect of both DP and DC. The pipe section is more sensitive to changes in frequency due to a longer length and a smaller cross-section. The left plot in Figure 28 shows the response in a string with length 10,000 ft where the first natural frequency modes of the DP can be seen at

$$m_{DP,1} = 128\ RPM\ \wedge\ m_{DP,2} = 256\ RPM$$

With the excitation frequency of once every fourth rotation ($f_e = 0.25$), equation (6.62) yields a stick-slip frequency of

$$f_{ss,1} = 0.53\ Hz\ \wedge\ f_{ss,2} = 1.06\ Hz$$

The short length and thick cross-section of the DC section will push the natural frequencies to higher values, and its first mode is not seen in this frame[14]. The right plot shows the response of a string with a total length of 18,000 ft. As the length of the DC section is unchanged, only the DP modes are shifted. The DC response is not affected by changes in DP length, and is still outside the frame. The new string will have natural frequency modes for the DP at 70, 141, 211 and 281 RPM. Appendix C shows how a change in different parameters will affect the frequency response.

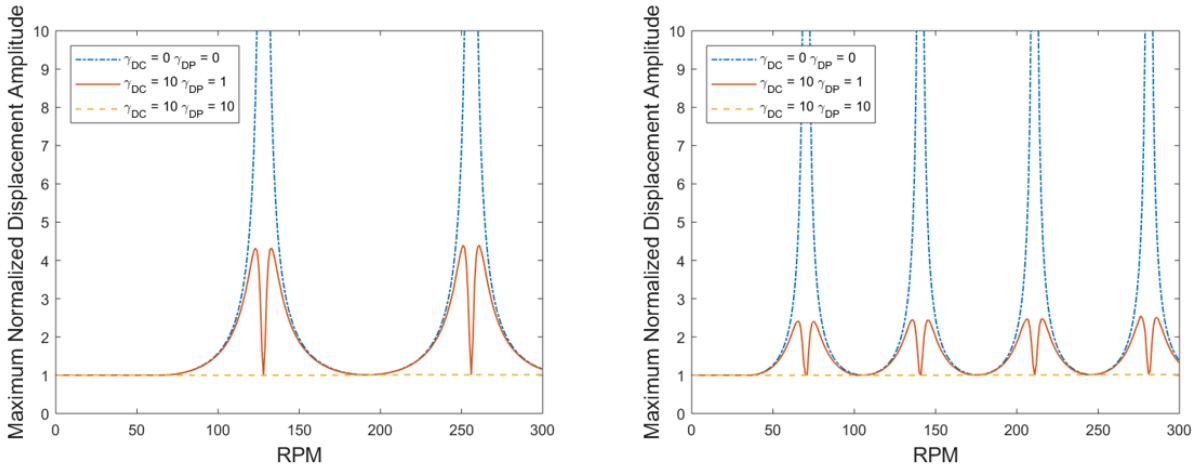

Figure 28: Frequency response of the drill string illustrated in Figure 24 with a total string length of 10,000 ft (left) and 18,000 ft (right). Data is listed in Table 8.

Note that the behavior of the solid line ($\gamma_{DC} = 10, \gamma_{DP} = 1$) does not make sense physically and might be a cause of concern. The reason for this behavior is not yet understood and is likely to be caused by an error in the code. It does not seem to shift the frequencies along the abscissa, so the obtained RPM values should still be sound. The model is run for string lengths between 6-34,000 ft in 4,000 ft increments. As the total string length increases, the natural frequencies

[14] Increase either the RPM or the excitation frequency (f_e) to experience DC resonance.

are shifted towards lower frequencies. The natural frequency modes in the different string lengths are plotted in Figure 30 as a solid line with markers.

Increasing the excitation frequency from 0.25 counts per rotation to 2 counts per rotation will reveal the first DC mode around 260 RPM. However, these frequencies are way too high to represent torsional stick slip, and will not be used. Based on the usual range of DC length (100-300 ft)[15] and the given frequency response, the occurrence of DC resonance during torsional stick-slip is deemed highly unlikely.

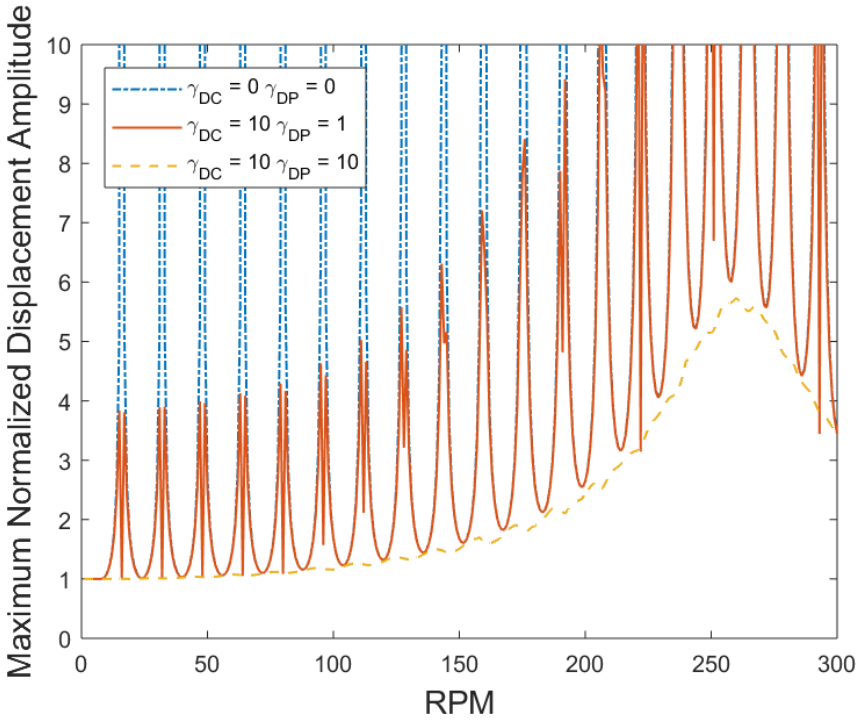

Figure 29: Frequency response of the drill string in Figure 24. The excitation frequency is increased to 2 counts per rotation to see the first DC mode around 260 RPM. Total string length is 10,000 ft.

With the data given in Table 8, the approximation described by equation (6.61) results in the dashed lines plotted in Figure 30. That the values are close gives some assurance that the results are sound. Notice that the resonant frequencies are lower for the approximated case (dashed) than for the simulated case (solid). This makes sense as the approximation replaces the heavy DC section with a lighter DP section. To validate the results, the numerical model was run with DP dimensions assigned to the DC section. With the whole string being uniform[16], the two approaches yielded the exact same result and the two graphs overlapped perfectly. This argues that the results can be trusted.

[15] Approximately 30-90 meters
[16] OD = 5.5 in, ID = 4.778 in

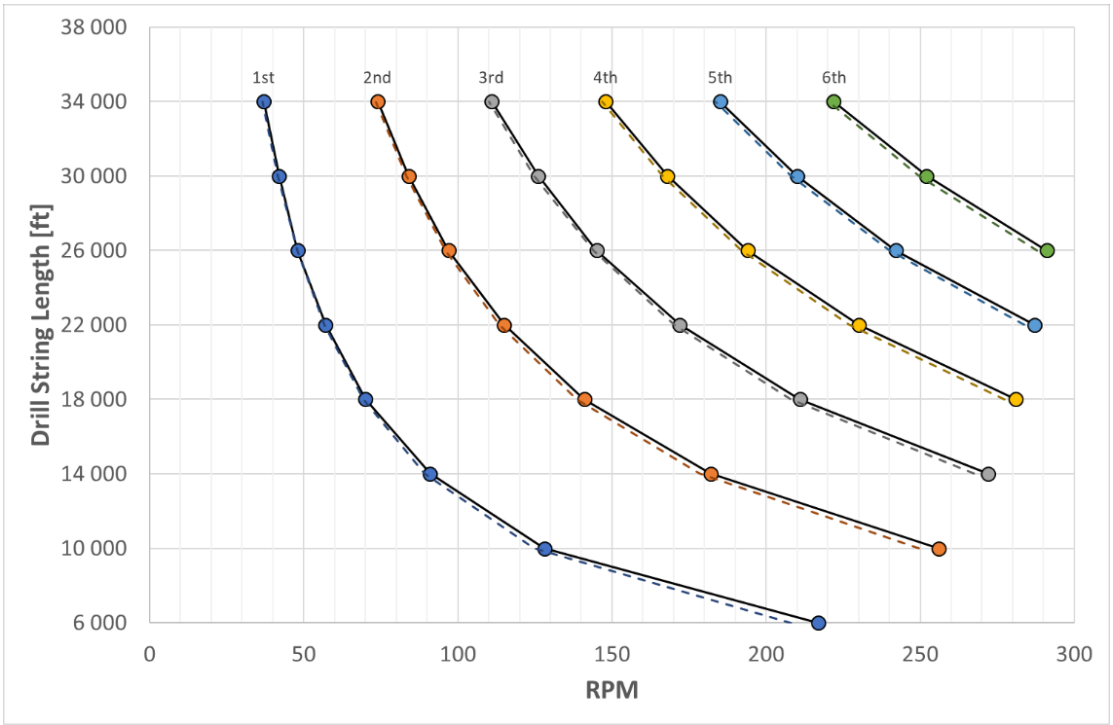

Figure 30: The first natural frequency modes for different string lengths. The solid line is based on numerical calculations while the dashed line is the approximation from equation (6.61).

According to Figure 30, a longer drill string will have more natural frequencies than a shorter drill string. The modes of vibration get more compact, and the risk of drill string resonance increases. At the same time, it is less likely for a rotational velocity to be sustained long enough for a mode to be established, given the increased wellbore friction and bit angular displacement.

With the bit at depth 14,000 ft the frequency of the 1st mode of resonance is 22.75 Hz which corresponds to a rotary speed of 91 RPM. The string has a total of 3 resonant frequencies below 300 RPM. Likewise, with the bit at depth 26,000 ft the frequency of the 1st mode is 12 Hz which corresponds to a rotary speed of 48 RPM, and the string has a total of 6 resonant frequencies below 300 RPM. The first five modes for two string lengths are listed in Table 9.

Table 9: The first five modes of resonance for two string lengths.

	$L_2 = 22,000\ ft$		$L_2 = 30,000\ ft$	
Mode	**Frequency (cps)**	**Rotary speed (RPM)**	**Frequency (cps)**	**Rotary speed (RPM)**
1	0.24	57	0.18	42
2	0.48	115	0.35	84
3	0.72	172	0.53	126
4	0.96	230	0.70	168
5	1.20	287	0.88	210

6.3 Discussion

6.3.1 Frequency Response

Syntax error: Evaluating Figure 26 from left to right, notice that the amplitude of the damped dill string increases over the first three charts, while it suddenly drops slightly in the last. This becomes very clear at 128 RPM, i.e. the first natural frequency. Here, the damped string is close to zero while the undamped string skyrocket. This is contradictory, and not consistent with drill string physics. Hence, it is caused by an error in the code. This error is clearly visible when evaluating the solid line in Figure 28 and Figure 29 ($\gamma_{DC} = 10, \gamma_{DP} = 1$). One would expect the displacement to see its maximum at the natural frequencies, but instead the curve takes a dip, often back to the overdamped case. However, note that this problem is only affecting the ordinate value over the peaks, and does not seem to shift the natural frequencies along the abscissa. Thus, the solution can be accepted for the purpose of determining the natural frequencies. Comparing with the values from the approximation, it further argues that the answers are sound.

Nodal points: It can be shown that the pipe sections that experience the smallest displacements, experience the largest dynamic forces. As the sections with large displacement are shifted far away from their equilibrium positions, this will induce high values of strain in the stationary node elements. When $\gamma_1 = \gamma_2 = 0$, the local stress in the string is proportional to the slope of the displacement curve. Therefore, the maximum dynamic stresses occur at points of zero displacement, called nodal points.

Effect of damping factor on node depth: A question arises whether the depth of a node is dependent on both damping factors, so that altering one of the damping factors will shift the node up or down the string. For example, it was discovered that the DC response changed despite only altering γ_2. This behavior is supported by the equations, and seems to be correct. Referring to equation (6.51), it is evident that

$$\theta_1(x,t) = f(B_1, b_1, \eta_1)$$

where both

$$B_1, b_1 = f(\eta_2)$$

and

$$\eta_1 = f(\gamma_1)$$
$$\eta_2 = f(\gamma_2)$$

This means that the DC angular displacement (θ_1) is a function of both damping factors (i.e. γ_1 and γ_2). The same is true for the DP response in equation (6.52) where

$$\theta_2(x,t) = f(B_2)$$

and

$$B_2 = f(\eta_1, \eta_2)$$

meaning that

$$\theta_2(x,t) = f(\gamma_1, \gamma_2)$$

Resonant Mode Interval: Not surprisingly, the second resonant frequency is double the first resonant frequency. Likewise, the third resonant frequency is three times the first resonant frequency. This is in line with the theory on harmonic modes, presented in section 6.1.4. For instance, in Figure 30, the first six natural frequencies are found at 37, 74, 111, 148, 185 and 222 RPM. Thus, the first line of natural frequencies will also determine the distance between each mode.

String Design: If a planned operation interferes with a natural frequency mode, this problem can be circumvented in two ways; 1) avoid drilling with the specific frequency or 2) remove the problem by design, i.e. adjust DC length or dimensions so that there are no resonant frequencies in the desired interval.

6.3.2 Boundary Conditions

Bit boundary conditions: In reality, the stick-slip behavior can be inflicted on any part of the drill string. For simplicity, this model assumes that the periodic disturbance is felt only at the bit.

Rig boundary conditions: The boundary conditions at the rig is dependent on M and k for axial vibrations. M describes the joint mass moment of inertia of the kelly, swivel and travelling block, while k describes the spring constant of the cables and derrick. Compared to the original paper, the evaluated string is no longer suspended from the top drive, but is rather hanging in slips on the drill floor. This introduces a new set of boundary conditions. M and k are now replaced by M_θ and k_θ. Assigning reasonable values to these parameters is challenging as they describe the mass moment of inertia of the entire MODU and the rotational stiffness of the drill floor, respectively. For all practical purposes, M_θ can be assumed to be extremely high as a rig might weigh 40-50 000 tons. To get a rough estimate of M_θ, the rig is considered as a solid rectangular box with height (h), width (w) and length (l). The mass (m) is evenly distributed throughout this rectangular box, and the box is rotating about a vertical axis through the center. The rig mass moment of inertia is then described by

$$I_d = \frac{1}{12} m(h^2 + w^2) \tag{6.63}$$

and is estimated to be around 50 million kg m^2. Notice that there is no angular displacement at the surface, neither in Figure 26 nor Figure 27, and the string is practically fixed on the drill floor. As for k_θ, this can be disregarded, assuming that the first infinitesimal element below the drill floor has the same rotational stiffness as the rest of the string.

6.3.3 Other Topics

Gravity-term: The axial model includes a gravity term that has no equivalent in the torsional model. For the axial case, this term basically represents the buoyed weight of the submerged string, which ensures that the string is never free of stresses. Without this term, a stationary situation with no axial vibrations would be modelled as if in vacuum, which is obviously incorrect. Although mass forces do not act on the string, it is still under the load of its own weight. This causes static tension and axial displacement, but it is not part of the dynamic response. In the torsional model there is no gravity term, and the rotation is always perpendicular to the longitudinal direction of the drill string. Normal forces in the deviated

sections will obviously induce tangential stresses in the drill string cross-section, but these stresses are not causing any angular displacements and are therefore irrelevant.

Damping constant: In vertical wells, viscous damping and material damping will dominate the friction term. Another factor is the Basset forces which occur when a submerged body accelerates in fluid (Hovda, 2018). The Basset forces describe the acceleration of mud, but are mostly relevant for vertical wells and can arguably be neglected in deviated wells as the damping term will be largely dominated by normal Coulomb friction. Since friction affects the overall behavior of the string, the accuracy of the predictions depends heavily on the knowledge of friction along the string and the choice of damping factor for the collar and pipe sections. Ideally, this should be determined experimentally. Double integration of the accelerations caused by transient torsional vibrations, both downhole and on the surface, should be used to estimate a damping factor, as done by (Dareing & Livesay, 1968). Unfortunately, this requires a downhole recorder and special surface equipment, and is well outside the scope of this paper. Thus, two reasonable damping factors are suggested for the BHA and DP respectively. On a side note; swabbing is shown to have a positive damping effect on torsional vibrations, while surging has a negative impact on torsional oscillation damping (Cayeux et al., 2020).

Wellbore inclination: The original model is meant for vertical wells only. When used on deviated wells, the equations should ideally be modified to make the damping term proportional with the cosine of inclination. Alternatively, a specific damping constant could be assigned to each separate element, but this is a tedious and ineffective approach. The damping constant includes all of material, viscous and contact friction forces where the latter depends heavily on wellbore inclination. The build section, but also the tangent section, will experience much more contact friction that the vertical section. Thus, it will be erroneous to assign the same friction factor to all drill pipe elements. Local hole conditions also play a major role.

Periodic disturbance: The model assumes that the behavior of stick-slip can be described as a periodic pattern. The actual stick-slip movement is erratic, although close to periodic. The assumption of periodic bit disturbance is a good approximation, but it is only valid for a short time. In stick-slip, there is no constant excitation frequency as there are too many factors affecting the transfer of torque between surface and bit. The damping term $[\gamma_\theta \theta_t(x,t)]$ is continuously changing due to well geometry, cuttings distribution, flowing conditions, etc. This leads to small, randomized phase shifts that break up the longer intervals of periodic excitation.

Nevertheless, there is still an imminent danger of destructive drill string resonance, so the RPM should be controlled to avoid operating in the vicinity of the natural frequencies. For a vibration mode to develop in the string, a periodic disturbance of the bit must be sustained for a while. The time it takes for the mode to be established, reflects the amount of energy that is put into the system.

Other vibrations: A real drill string is subjected to a combination of axial, lateral and angular vibrations. Since the theory used in this model assumes that each type of vibration along the string is independent of the other two, this implies that any heave movement must be neglected. Since the model does not account for a combined axial and angular movement, the floating rig must be treated as a fixed installation.

Reference RPM: The model only evaluates the dynamic response, i.e. vibrations caused by changes in the rotational velocity. In reality, the top of drill string is being rotated with a constant velocity and the harmonic disturbance is a result of the bit occasionally sticking to the surface. With the powerful tool of superposition, the static response can be disregarded, and the string behavior can instead be modelled as a stationary string with periodic torsional disturbances exerted on the bit.

Tool joints: (Bradbury & Wilhoit, 1962) show that the effect of tool joints on longitudinal and angular vibrations are negligible. Thus, the drill pipe section is assumed to be a continuous cylinder with uniform cross-sectional area. The same goes for the collar section, only with different dimensions.

7 Tool Proposal

This chapter presents and discusses three different solutions for mitigation of the axial stick-slip problem. The proposed solutions are 1) a downhole PDM tool, 2) a swivel sub and 3) a rotating Iron Rough Neck (IRN). Each tool is presented through rough sketches and tool descriptions before the three solutions are compared across a number of selected criteria. The tools are then given a numerical score in each category before the authors recommendation is given in the end.

7.1 Downhole PDM Tool

The first proposed solution is to install a positive displacement motor (PDM) tool below the drill floor (see Figure 31). The tool will have several PDMs in parallel in a planetary gear configuration. A sketch of the downhole PDM tool characteristics is found in section 7.1.3. With the use of continuous circulation technology, drill string rotation can be maintained during drill pipe connections. The solution is discussed thoroughly in the initial specialization project report (Skrettingland, 2019). This section provides a short summary of the findings and a sketch of the tool characteristics (Figure 32). See Appendix E for detailed charts and tables of motor and pump characteristics.

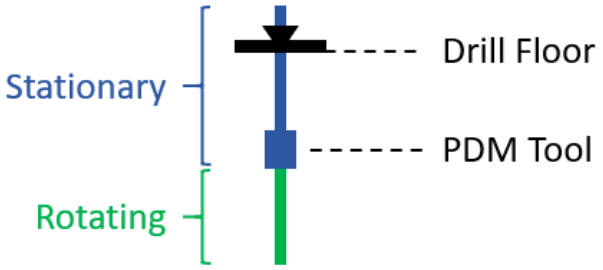

Figure 31: Conceptual illustration of drill string with PDM tool.

7.1.1 Summary

- The torque from one PDM is proportional with the differential pressure across the motor, and independent of the flow rate through the motor.
- The speed of a PDM is proportional with the flow rate through the motor, and independent of the differential pressure across the motor.

- PDMs in parallel: The differential pressure across the tool is independent of the number of motors, while the flow rate necessary to maintain speed is proportional with the number of motors.
- PDMs in series: The differential pressure across the tool is proportional with the number of motors, while the flow rate necessary to maintain speed is independent of the number of motors.
- The gear ratio of planet/sun gear in the transmission will determine the torque boost from each PDM, and the reduction in output RPM.

For a single PDM, higher torque yields lower speed and vice versa. Implementing the transmission as well, there is a high number of possible configurations. Further work is required to determine the optimal choice of motor with respect to torque and speed.

Example[17]*:* Choosing PDM and pump configuration

- Using the strongest 4 ¾ inch PDM in the Navi-Drill handbook (BakerHughes, 2016, p. 108), the Ultra XL/VS with the DuraMax[18] elastomer. The operational limit of this PDM is defined by:
  - Differential pressure[19]: 545 psi
  - Torque: 5,400 Nm
  - Speed: 78 rpm
  - Flow rate: 285 gpm

- Three PDMs in parallel provide sufficient torque when implementing a 4:1 transmission on the output shaft. Unfortunately, the transmission also reduces the output speed to a quarter of the PDM speed, which is most likely too low.

[17] The example is for an extended reach drilling (ERD) well with 8 km tangent at 70 degrees inclination, yielding very high torque values at surface (47,000 Nm). In light of the findings in section 3.2.1, the choice of motor should be reconsidered to offer more speed at the expense of torque output.
[18] The DuraMax elastomer delivers 50% more torque and power, while maintaining the durability and reliability. (BakerHughes, 2016)
[19] Differential pressure is the difference in Standpipe Pressure (SPP) between off-bottom and on-bottom motor operation (i.e. with and without wellbore friction in this case).

- The required flow rate of 855 gpm can be met by two 12-P-160 Triplex mud pumps from National Oilwell Varco (NOV) with the pumps working at 80 strokes per minute. Pump operational limit is defined by:
    - Maximum pressure available in fluid end: 5,000 psi
    - Maximum discharge pressure: 3,690 psi
    - Liner size: 6 ¾ in
    - Flow rate: 669 gpm
    - Pump speed: 120 spm

7.1.2 Important Notes:

- CCS is required to operate the tool during drill pipe connections.
- Available standpipe pressure (SPP) is a limiting factor, and increasing the flow rate will yield issues related to hydraulic friction losses, excessive formation damage and increased need of rig space.
- Directional drilling will require a rotary steerable system (RSS). Slide drilling will not be possible when the PDM tool is installed. Not using a PDM for directional drilling purposes will boost the available standpipe pressure, which is beneficial.
- Installation depth should be shallow and in the vertical section as most of the friction loss happens in the tangent and build-section.
- The tool should arguably be installed in the riser section[20] to circumvent the problem of a decreasing cross-sectional area when a new casing is suspended in the subsea wellhead. Installing the tool in the riser limits the length of one run to the in situ water depth.
- Bypassing of the tool could be solved using a rupture disk, a retrievable plug or by dropping a ball.
- The breakout torque (BOT) above the tool should be high enough to prevent connection break out. According to (Brock, Muradov, Youngson, Brooks, & Payne, 2011), the BOT required for single-start rotary-shouldered connections (RSC) is approximately 80-90 % of the makeup torque (MUT). A drill pipe with nominal diameter 5 ½ inches, a

[20] Typical ID of a riser is 18 ¾ inches.

weight of 24.70 lb/ft and Class I tool joints has a recommended MUT of 59,090 Nm, i.e. 5.9 ton-m[21] (Gabolde & Nguyen, 1991, p. 72).

- The effect might be better for wells that require less torque and can allow PDMs with higher speed.

[21] The calculations of recommended makeup torque imply the use of thread grease containing 40-60 weight % of fine-powdered zinc, totally applied to all the threads and shoulders and not containing more than 0.3% sulfur. The calculation basis account for a tensile stress of 50% for the minimum tensile yield strength for Class I tool joints.

7.1.3 Sketches of the Downhole PDM Tool Characteristics

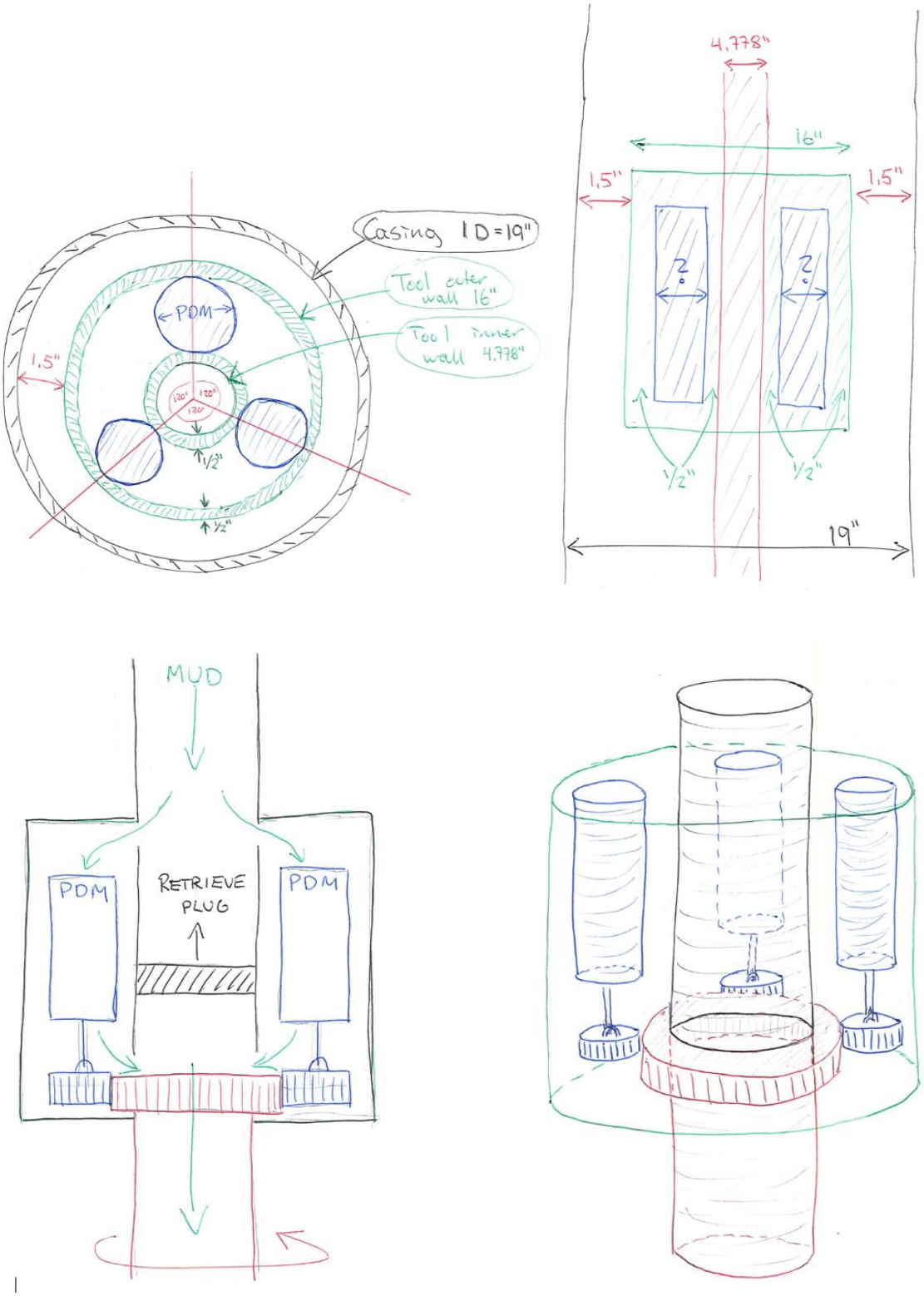

Figure 32: Conceptual sketch of the PDM tool with three motors in parallel. Upper left: cross-sectional area from above. Upper right: cross-sectional area from the side. Bottom left: mud flow. Bottom right: planetary gear configuration.

7.2 Swivel Sub

The second proposed solution is to install a swivel sub on top of each stand. During drill pipe connections, the swivel between the two uppermost stands (i.e. on rig floor level) are activated so that everything below the swivel is being rotated with constant RPM while everything above the swivel is free to move otherwise. The swivel sub will disconnect the rotation of the uppermost stand from that of the rest of the string. Prior to this, there will be a seamless transition from top drive rotation to rotary kelly bushing (RKB) rotation. Thus, applying the swivel sub requires the installation of an RKB system, which is an old fashioned technology that should be accessible on most drilling rigs. With RKB taking over the rotation during drill pipe connections, this enables the use of a normal connection procedure on the stationary part. After the connection, there is a seamless transition from RKB rotation back to top drive rotation. The string is hoisted/lowered another stand and this process is repeated without any major variations in downhole RPM. A sketch of the swivel sub characteristics is shown in Figure 33.

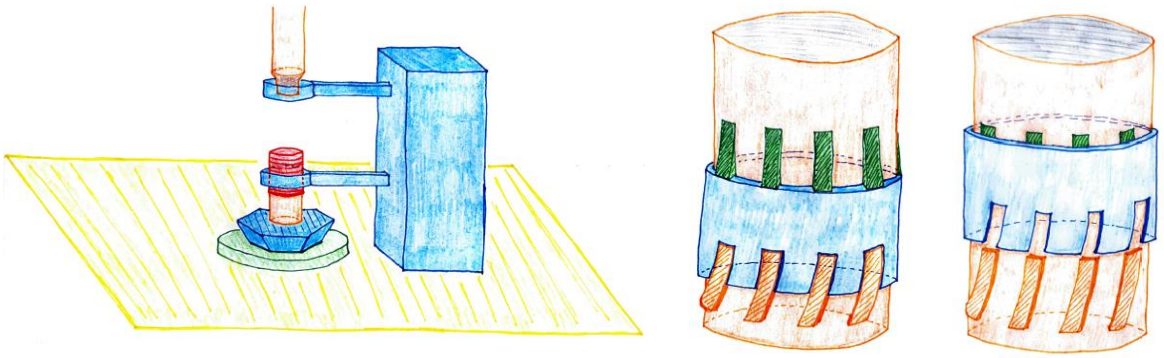

Figure 33: Conceptual sketch of the swivel sub. Left: connection on drill floor with sub in red. Middle: sub in locked position, swivel deactivated. Right: sub in open position, swivel activated.

Note that:

- Each swivel sub is only activated when entering/exiting the hole.
- The locking pins (green) are mounted on springs.
- This solution requires the use of RKB-driven rotation during each connection.
- It requires a seamless transition between top drive rotation and RKB rotation.
- The swivel must be activated/deactivated in a matter of seconds.
- Including the swivel sub is only necessary in the interval where axial stick slip is a problem. The length of this interval is discussed in Chapter 5.

- A brief stop in rotation is most likely necessary to enable proper activation/deactivation without breaking the sub. However, timing this with the heave equilibrium point (i.e. the MSL), the effects of a stop might be minimal. As the string will move with maximum axial velocity, it is not in danger of sticking, and by the time the axial velocity is reduced, the rotation will be re-established. This assumes that the BHA is not stationary during heave. Neither way, achieving constant rotation, bar a short stop, is still an improvement to the current situation.
- Different kinds of bearing assemblies can be used to control the relative motion across the swivel. Ball bearings are used in regular tricone bits and is a viable option, but these will build more than a regular plain bearing, and cross-sectional area might be a constraining factor.
- Proper sealing is important due to very fine particles in the mud. Maintenance is essential to avoid leaking and failure.

7.3 Rotating IRN

The third proposed solution is an IRN that is combined with the RKB and the slips to superimpose the movement of the rotating drill string and break out the pipe during constant rotation. Basically, the slips have the form of a barrel and is hexagonal at the bottom so that it fits the kelly bushing. The barrel is high enough to cover the first half of the tool joint. On top of the barrel sits a hydraulic torque tong that is locked to the rotation of the slips. This tong is used to break out or make up the connections during constant rotation. To unscrew the stand, one could either reduce the top drive speed slightly or apply a spinning device that consists of three wheels, positioned at 120 degrees from each other and driven by a hydraulic motor. After a seamless transition from top drive rotation to RKB rotation, the string will continue to rotate despite the top drive being disconnected. The whole connection process (when tripping out) will look something like:

- Top drive rotation (e.g. 80 RPM)
- Spin up RKB with barrel to match the top drive rotation (80 RPM). Establish no relative movement between the string and slips.
- Set slips and decrease hook load. The entire axial weight is now supported by the slips which also transfers the momentum from RKB to the string.
- Break out upper stand with torque tong attached to the rotating IRN.

- Reduce top drive RPM slightly to unscrew the upper stand (60 RPM).
- Place the disconnected stand in the finger board and get back in position with the top drive.
- Spin up top drive to match the RKB rotation (80 RPM).
- Increase top drive RPM slightly to connect with the tool joint (100 RPM).
- Restore matching rotation (80 RPM) and make up connection with torque tong attached to the rotating IRN.
- Increase hook load and pull slips.

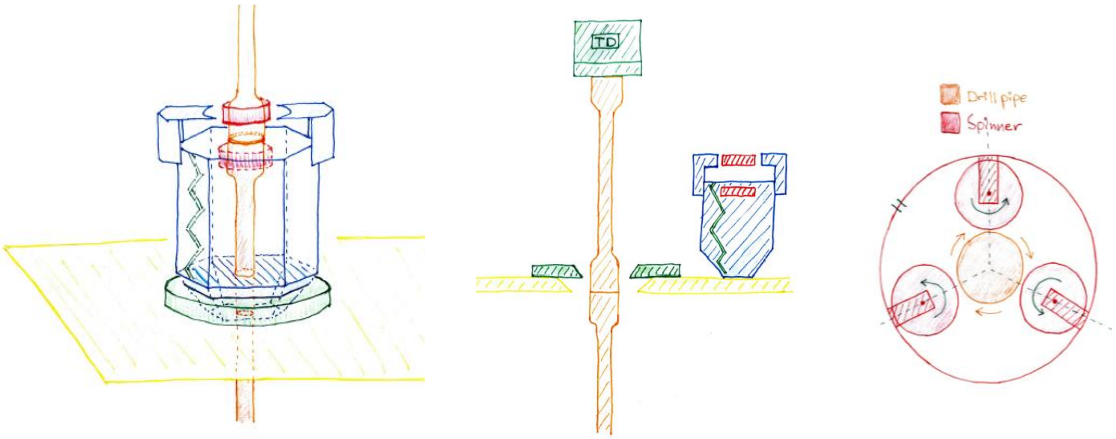

Figure 34: Conceptual sketch of the rotating IRN. Left: IRN in working mode. Middle: IRN in standby mode. Right: spinning device.

7.4 Comparison

Three solutions are described in the previous sections. Key differences between these solutions include:

- For the PDM tool, only the string below the motor is rotating, while for the swivel sub and the rotating IRN, the string is rotated from the rig floor and down.
- The PDM tool requires CCS technology.
- Seamless transition to and from top drive rotation is required in all three solutions, but the PDM tool does not require RKB.
- The swivel sub will probably require a short stop to ensure proper activation/deactivation of the sub, while this is not necessary for the PDM tool or the rotating IRN.

To better compare these, they are evaluated in a table format, based on key properties as cost, feasibility, etc. Table 10 contains short comments in each category for the three proposed solutions. Table 11 puts these comments into a numeric rating for all categories. The tools are rated on a scale from 0 (catastrophic) to 10 (optimal) in accordance with Figure 35. The middle point 5 represents a neutral impact on the decision making. Although the scale ranges from 0-10, the extreme values are not used, and the scale has an effective range between 3-9. All values are simply subjective guesstimates and should not be referred to. The table is only intended for comparison of the three solutions.

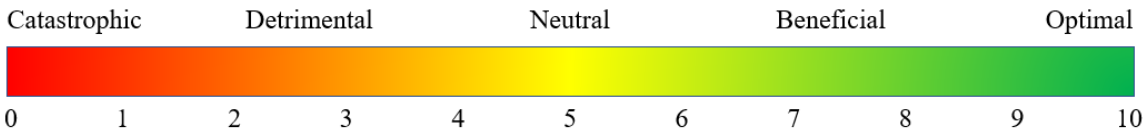

Figure 35: Scale used for numerical comparison in Table 11.

Table 10: Comparison of the three proposed solutions for a number of key factors. Table 11 is a numerical form of the same table.

Example Category	1. *PDM Tool* 2. *Swivel Sub* 3. *Rotating IRN*
Cost	1. Lots of testing. Development of communication & surveillance systems. 2. Relatively simple device. Need many. 3. Requires advanced software.
Simplicity	1. Rotor/stator configuration. Planetary gears. Must allow bypass of tool. Continuous circulation required. 2. On/off with mechanical switch. 3. Superimposing rotation.
Maintenance	1. Elastomers, gears, rotor/stator, wear rings, threads. Between runs. 2. Bearings, switch, threads. Inspect between runs. 3. Hydraulics, power supply, software. Regularly during NPT events.
Consequence of Failure	1. Failure will have larger consequences due to downhole. Possible flow stopper. Tripping required. 2. Failure will have large consequences. Pipe below broken sub will not rotate. Tripping without rotation is required. 3. Failure will have moderate consequences. Maintenance on rig floor. No tripping required.
Safety	1. Downhole, away from personnel. No rotation on rig floor. 2. Risk when switching on/off. Relatively compact device. 3. Moving parts on drill floor. Rotating at significant speed.
Power Supply	1. Differential pressure across PDM. Available SPP is a potential issue. 2. Mechanical switch. 3. Battery or electrical grid.
Innovative	1. Applying PDM technology in a new way. 2. Old concept, new application. 3. Future minded. Reducing the need for human rig personnel.
Feasibility	1. Good knowledge of PDMs. Available SPP is a potential issue.

	2. Easy to implement into old fashioned systems. 3. Continuous Motion Rig[22] utilizes the same principle.
Robustness	1. One device. More moving parts. Subject to vibrations and string forces. 2. Many devices. Less moving parts. Simple construction. 3. Complex installation with hydraulics, electricity, etc. Rotating on drill floor. Many moving parts.
Stability	1. Possibly subject to large vibrations. 2. Possibly subject to large vibrations. Robust device. 3. No downhole vibrations.
Installation Process	1. Extra rig logistics. Make up string and test the tool (10 min each run). 2. Extra rig logistics during operation. Attach to all relevant joints. 3. Install on drill floor (4 hours). Coordinate with rig maintenance for less impact.
Added Connection-Time	1. Seamless transition (5 sec each stand). 2. Attached to stand prior to make up (no extra time). Activate/deactivate sub (10 sec each stand). Seamless transition (5 sec each stand). 3. MUT (10 sec each stand) Seamless transition (5 sec each stand)
Rig Space Occupation	1. Communication and surveillance systems only. Spare parts. 2. Storing subs while not in use. 3. Installed on rig floor. Spare parts.
Gross Weight	1. Downhole motor (200 kg) 2. Many subs of 30 kg 3. IRN (1000 kg)

[22] (WestGroup, 2020)

Table 11: Comparison of the three proposed solutions. Each tool is given a numerical score between 0 and 10 for a number of categories. The score is based on the comments in Table 10.

Category	PDM Tool	Swivel Sub	Rotating IRN
Cost	6	8	5
Simplicity	4	9	4
Maintenance	5	8	6
Consequence of Failure	4	3	8
Safety	7	7	5
Power Supply	5	9	7
Innovative	7	5	8
Feasibility	7	9	7
Robustness	4	9	6
Stability	5	7	8
Installation Process	8	5	3
Added Connection-Time	7	4	4
Rig Space Occupation	8	4	8
Gross Weight	7	3	4
Total Score	**84**	**90**	**83**
Average Score	**6.0**	**6.4**	**5.9**

The total score gives a perspective on the overall versatility of the tool. However, it is better to evaluate one category at a time, as different categories are unequally weighted and will have different impact on the decision making (e.g. cost is arguably more important than gross weight).

7.5 Recommendation

The optimal solution should preferably have a low number of movable parts to minimize the risk of failure. Also, it should be easy to implement into an industry that, in certain areas, has stood still in terms of innovation during the past 50 years. Based on the above comparison, the swivel sub is chosen as the recommended solution to the axial stick-slip problem. The main reasons for this are:

- Easy to implement into an old fashioned industry.
- Mechanically robust and relatively simple.

- Less need for maintenance.
- No need for power supply.

However, it should be stressed that a rotating IRN would promote a change towards an automized drilling process, which is an integral part of the future of petroleum industry.

7.6 Alternative Measures to Mitigate Axial Drag

- Self-Oscillating Rotary Percussion Tool: (SORP, 2019) utilizes a self-oscillating sub to generate high-frequency (600-700 Hz), low-amplitude hydraulic pulses that reduce the axial friction and thereby mitigate weight stacking (i.e. axial stick-slip) and help transmit WOB. The tool requires the installation of CCS.
- Axial Oscillations: (Mills, Menand, & Grissom, 2017) show a beneficial effect from using an axial oscillation tool (AOT) in combination with a mixed aluminum string. (Mahjoub, Dao, & Menand, 2019) found that the impact of the AOT increases with the excitation force amplitude and decreases with higher values of ROP (heave in this case). The tool requires the installation of CCS.
- Torsional Oscillations: This is backed by (Wang, Chen, Rui, & Jin, 2017) who studied the effects of torque rocking motion[23] on the drill string axial drag. They found that the axial friction increases with increasing ROP (i.e. heave) and that the axial drag will decrease with an increasing torsional vibration amplitude. There was also indicated an optimal torsional vibration frequency that minimized axial friction. See Appendix D for more information.
- Roller Centralizer: Essentially a centralizer with wheels. Substitutes the wellbore friction with the internal wheel friction which is far lower.
- Lubricants: Add lubricants to the mud to lower the friction coefficient.
- Hole Cleaning: Proper circulation is key to a clean well. Consider implementing CCS or a bypass valve to increase local flowrate.
- Well Trajectory: The straighter, the better. Drill pipe bending stiffness will cause increased normal forces in a well with complex trajectory.

[23] Torque rocking is a technique where the drill string is rotated right and left by an amount that avoids interference with the bit orientation. The technique is described by (Maidla & Haci, 2004) which discusses how to circumvent axial drag when slide drilling directional wells.

8 The Connection Procedure

Tripping is seemingly a simple operation, but there is a lot of cost-saving potential in optimizing this process. When pulling for example 18,000 ft of drill string, the pipe is racked back in 30 ft stands, meaning that 600 connections are made. Saving 15 seconds each connection will yield a 2.5 hour reduction in tripping time. With a daily rig rate of 500,000 USD per day, this amounts to roughly 50,000 USD. A practical example of a time saving measure is the elimination of axial stick-slip during connections on a floating vessel. This mitigates the downhole pressure fluctuation and prevents lost time events. Table 12 lists the basic activities during a tripping operation.

Table 12: Activities during tripping, listed chronologically.

Tripping out:	**Tripping in:**
• Latch elevator to pipe	• Latch elevator to the top of a free stand
• Remove slips	• Move stand into center line position
• Hoist drill string	• Make up connection
• Set slips	• Remove slips
• Break out connection	• Lower drill string
• Rack back free stand to fingerboard	• Set slips
• Unlatch free stand	• Unlatch elevator
• Lower elevator	• Raise elevator
• Latch the elevator to a new stand.	• Latch elevator to a new free stand

General rules when tripping:

- Keep rotation to avoid stuck pipe, mechanically or differentially.
- Running or pulling speed must be controlled to avoid surge or swab.
- All connections must be made up with the correct torque.
- Gauge[24] stabilizers and check for any damage.
- Apply dope to threads.
- Gently connect box/pin to avoid damage
- Close blind/shear ram when above this height.

[24] Measure the outer diameter. During operations, stabilizers can wear and become under-gauge. If the stabilizers become 3/16" under-gauge, they have to be replaced to operate effectively.

Table 13 below is a reconstruction of data from OSHA (Occupational Safety and Health Administration) at the United States Department of Labor and applies to onshore drilling rigs with an RKB-driven rotation. When using a rig crew during connections, the following table is useful to map the different activities and HSE concerns. Note that for new drilling rigs, the need for human personnel on the rig floor is greatly reduced or even eliminated.

Table 13: Activities and HSE concerns when tripping out of hole.

Activity	Potential Hazards	Possible Solutions
Setting slips	Pinching fingers or other body parts between slips, slip handles or rotary table.	Be aware of hand placement.
	Experience muscle strain from improper lifting technique.	Use proper stance and lifting technique. Slips have three handles. It should be lifted by more than one person.
Breaking out and setting back the kelly	Mud spills may lead to skin contact, loss of footing, etc.	Mud pumps must be shut down. Close the mud saver valve on the kelly (if present). Apply a mud bucket to divert spills.
	Being struck by slip handles in case of RKB rotation.	Stand clear of the rotary table. Use a top drive or other technologies.
	Being struck by kelly while moving it into rathole.	Ensure safe distance to pullback line and rathole.
Attaching elevators to the elevators link	Getting pinched by the elevator links, or between links and hook.	Be aware of hand placement.
	Being struck by elevator.	Keep a safe distance.
	Muscular strains or other damage.	Use lifting equipment. Minimize manual lifting.
Latching elevators to pipe	Pinching fingers or hand.	Be aware of hand placement. Provide instruction for proper latching procedure.

Activity	Potential Hazards	Possible Solutions
	Getting struck by elevator.	Frequent inspection and maintenance of the equipment.
Breaking out pipe	Being struck by swinging tongs, rotating slip handles, reverse backlash of tongs.	Only a minimum of personnel handles the tong. Keep away from the hazardous area at the end of the tong. Good communication. Train personnel in hand placement and positioning.
	Being struck by an unlatched tong or a tong falling because of a broken snub line.	Frequently inspect the equipment and attend to maintenance issues.
Maneuvering pipe to racking area	Pinching hands or fingers between two stands. Crushing toes or feet under a stand.	Avoid hands between two stands. Keep feet away from the bottom of the stand.
	Slips, trips and falls. Muscular strains.	Slip-resistant material and coating. Apply hard hat, gloves and protective footwear. Use proper technique.
Derrickman on the monkey board unlatches the elevators and guide the stand into the fingerboard. Elevator is lowered again to fetch a new stand.	Climbing accident.	Use full body harness and safety lines.
	Falling from monkey board or finger board. Being caught between pipe and object. Muscular strains.	Use full body harness and safety lines. Practice positioning and hand placement. Use pullback ropes.
	Slips, trips, falls.	Slip-resistant material and coating. Apply hard hat, gloves and protective footwear.
	Falling during an emergency descent.	Train personnel. Practice the procedures and the use of emergency equipment.
	Falling objects.	Fasten (tie off) all tools. Do not carry tools in the ladder. Raise tools with a hoisting line.

9 Conclusions

Critical Displacement Length & Minimum RPM

- The critical displacement length is only dependent on string dimensions and wellbore properties, not on heave conditions.
- A stationary BHA can occur when the critical displacement exceeds the heave amplitude, and will occur when it is more than twice the heave amplitude.
- The minimum RPM is dependent on drill string length, accumulated surface torque, angular deflection in the drill string and the rig's heaving motion.
- Increasing the drill string length tends to reduce the required RPM, while the effect of an increasing wave height increases with drill string length.

Angular Drill String Vibrations with Damping

- The damping coefficient greatly affects the drill string response at the resonant frequencies. The amplitude is dependent on damping, while the phase is not.
- The rotational velocity affects both the phase and the amplitude of the drill string response.
- The occurrence of DP resonance during torsional stick-slip is a threat and must be monitored, while DC resonance is deemed highly unlikely.
- The maximum dynamic stresses occur at points of zero displacement, called nodal points

Tool Proposal:

- Considering the three proposed solutions, they must all be combined with the Automated Downhole Choke by (M. Kvernland et al., 2018) to provide a cost-efficient alternative to the Continuous Motion Rig by (WestGroup, 2020).
- Out of the three, the swivel sub is recommended as the cheaper alternative, partly because it is easy to implement, mechanically robust and less prone to failure than the other two. However, it should be stressed that a rotating IRN would promote a change towards an automized drilling process, which is an integral part of the petroleum industry in the future.

10 Further Work

- Apply the approach to real data and compare results to other methods.
- Work on detailed design of tools to discover weaknesses and flaws. Close in on a prototype.
- Initiate dialogue with the industry to discuss the criteria for an alternative tool and the feasibility of the proposed solutions.
- Research possibilities of controlling the timing of a torsional sticking interval.
- A higher wellbore friction coefficient is likely to increase both the amplitude of the angular vibrations and the magnitude of the damping constant. More research should be done on the effects of an increasing friction coefficient.
- Implement Stribeck friction and viscous friction in the model.

11 References

ASM. (1990). *Properties and Selection: Irons, Steels, and High-Performance Alloys* (Vol. 1).

Badran, M., Gooneratne, C., Ahsalan, M., & Shaarawi, A. (2019). *A Rotating Continuous Circulation Tool RCCT for Increasing Drilling Efficiency and Optimizing Borehole Cleaning*.

Bailey, J. J., & Finnie, I. (1960). An Analytical Study of Drill-String Vibration *Journal of Engineering for Industry, Vol. 82*.

BakerHughes. (2016). *Navi-Drill Motor Handbook*: Baker Hughes Incorporated.

Berntsen, M. (2019). *Drillstring Vibrations: A Theoretical Foundation*. Petroleum Technology, Spesialization Project. Department of Geoscience and Petroleum. NTNU.

Bradbury, R. E., & Wilhoit, J. C. (1962). *Effect of Tool Joints on Passages of Plane Longitudinal and Torsional Waves Along a Drill Pipe*. Paper presented at the ASME meeting in Dallas, Texas, September 23-26, 1962.

Brock, J. N., Muradov, A., Youngson, S. S., Brooks, C., & Payne, M. L. (2011). *High Breakout Torque: Hypothesis, Investigation, and Evaluation*. Paper presented at the SPE/IADC Drilling Conference and Exhibition, Amsterdam, The Netherlands. https://doi.org/10.2118/139826-MS

Cayeux, E., Ambrus, A., Øy, L., Helleland, A., Brundtland, S. T., & Nevøy, H. (2020). *Analysis of Torsional Stick-Slip Situations Observed with Downhole High-Frequency Magnetometer Data*. Paper presented at the IADC/SPE International Drilling Conference and Exhibition, Galveston, Texas, USA. https://doi.org/10.2118/199678-MS

Daireaux, B., Dvergsnes, E., Cayeux, E., Bergerud, R., & Kjøsnes, I. (2019). *Automatic Control of Mud Pumps, Draw-Works and Top-Drive on a Floater*. Paper presented at the SPE/IADC International Drilling Conference and Exhibition, The Hague, The Netherlands. https://doi.org/10.2118/194123-MS

Dareing, D. W., & Livesay, B. J. (1968). Longitudinal and Angular Drill-String VIbrations With Damping. *Journal of Engineering for Industry*.

Den Hartog, J. P. (1956). *Mechanical Vibration* (4th ed.). New York: McGraw-Hill.

Faltinsen. (1991). Sea Loads on Ships and Offshore Structures. 24.

Gabolde, G., & Nguyen, J.-P. (1991). *Drilling Data Handbook*: Editions Technip, Institut Francais du Pétrole.

Hovda, S. (2018). Semi-analytical model of the axial movements of an oil-well drillstring in deviated wellbores. *Journal of Sound and Vibration, 433*, 287-298. doi:https://doi.org/10.1016/j.jsv.2018.07.016

Kvernland, M., Christensen, M. Ø., Borgen, H., Godhavn, J. M., Aamo, O. M., & Sangesland, S. (2018). *Attenuating Heave-Induced Pressure Oscillations using Automated Down-hole Choking*. Paper presented at the IADC/SPE Drilling Conference and Exhibition, Fort Worth, Texas, USA. https://doi.org/10.2118/189657-MS

Kvernland, M., Gorski, D., Ana, M. S., Godhavn, J.-M., Aamo, O. M., & Sangesland, S. (2019). Verification of Downhole Choke Technology in a Simulator Using Data from a North Sea Well. *SPE Drilling & Completion, 34*(04), 441-449. doi:10.2118/194143-PA

Mahjoub, M., Dao, N.-H., & Menand, S. (2019). *Modeling the Effect of Axial Oscillation Tools in Torque and Drag Computations*. Paper presented at the SPE/IADC International Drilling Conference and Exhibition, The Hague, The Netherlands. https://doi.org/10.2118/194133-MS

Maidla, E., & Haci, M. (2004). *Understanding Torque: The Key to Slide-Drilling Directional Wells*. Paper presented at the IADC/SPE Drilling Conference, Dallas, Texas. https://doi.org/10.2118/87162-MS

Mills, K., Menand, S., & Grissom, R. (2017). *Using Aluminum Drill Pipe with Axial Oscillation Tools to Significantly Improve Drilling Performance*. Paper presented at the Abu Dhabi International Petroleum Exhibition & Conference, Abu Dhabi, UAE. https://doi.org/10.2118/188865-MS

Noreng, O. (2016). *The Oil Industry and Government Strategy in the North Sea*: Taylor & Francis.

NOV. 12-P-160 Triplex Mud Pump Brochure. Retrieved from https://www.rotatingright.com/pdf/12P-160%20Mud%20Pump%20Brochure.pdf

Paslay, P. R., & Bogy, D. B. (1963). Drill String Vibrations Due to Intermittent Contact of Bit Teeth. *Journal of Engineering for Industry, Vol. 85*(2), 187-194. doi:10.1115/1.3667632

Skrettingland, K. (2019). *Mitigating Axial Stick-Slip During Connections On a Floating Vessel*. Petroleum Technology, Spesialization Project. Department of Geoscience and Petroleum. NTNU.

SORP. (2019). Self-Oscillating Rotary Percussion Drilling Technology for ROP Boost. *Presentation*.

Ultrasonics, D. (2020). Appendix A Velocity Table. Retrieved from https://dakotaultrasonics.com/reference/

Wang, X., Chen, P., Rui, Z., & Jin, F. (2017). Modeling Friction Performance of Drill String Torsional Oscillation Using Dynamic Friction Model. Retrieved from https://doi.org/10.1155/2017/4051541

WestGroup. (2020). Continuous Motion Rig. Retrieved from http://westgroup.no/products/continuous-motion-rig

Wijning, D. (2019). Huisman HCF. Retrieved from https://www.drillingcontractor.org/multifunctional-semisubmersible-designed-with-heave-compensated-drill-floor-and-large-flat-deckspace-53358

APPENDIX

A. Automated Downhole Choke

(M. Kvernland et al., 2018) studied the effects of automated down-hole choking on heave-induced pressure oscillations, and obtained the following results:

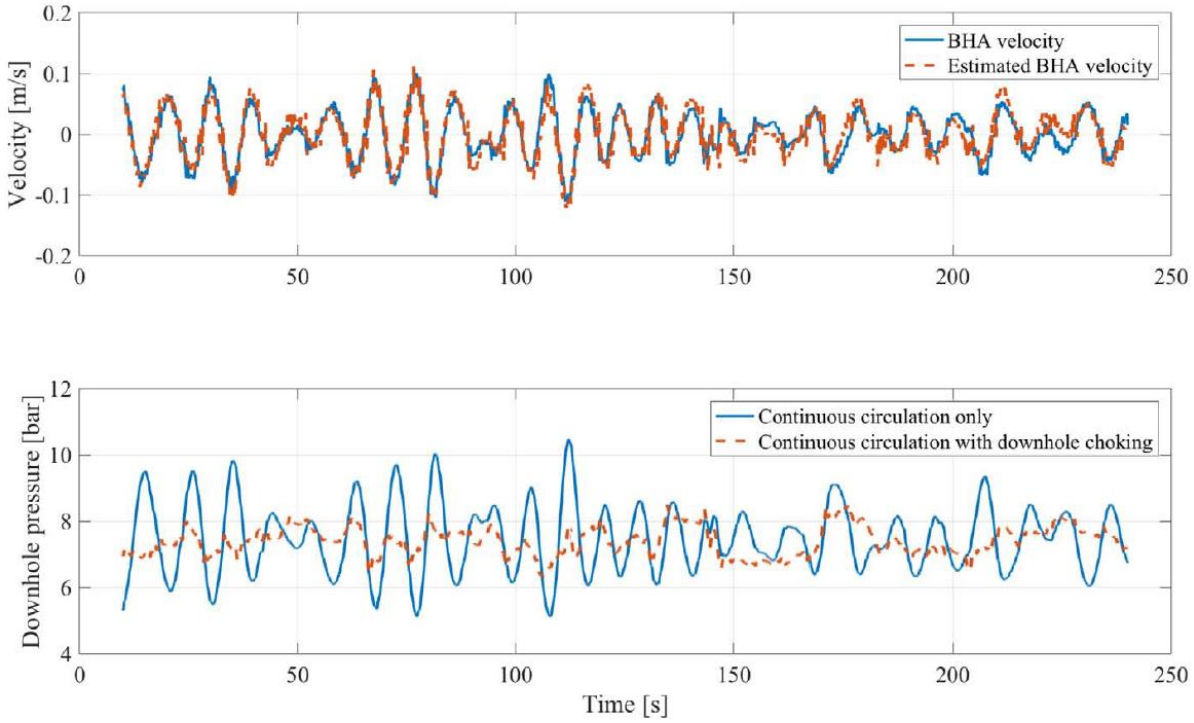

Lab-results showing the effect of downhole choking. The upper plot shows the actual BHA velocity, and the estimate based on acceleration measurements. The bottom plot shows the variation in downhole pressure with and without the utilization of the proposed choke.

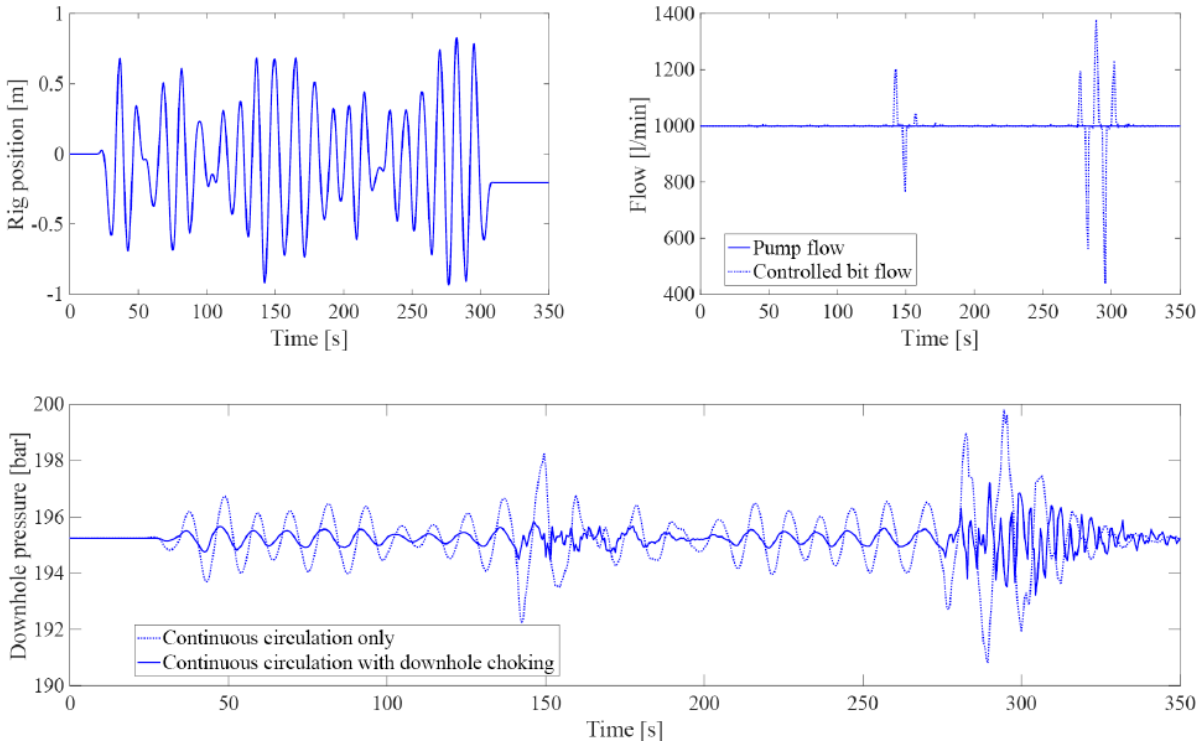

Drill string connection at 5,100 meters in a horizontal well. Notice the complicated rig movement in the upper left. In the upper right, notice the spikes at t ≈ 150 seconds and t ≈ 300 seconds. This is the result of sudden weight release as the axial forces overcome the static friction in the well. A quick response of the downhole choke reduces the pressure peaks (bottom graph), but it is evident that the system is susceptible to unpredictable pressure fluctuations and axial stick-slip.

B. Vibration Sampling Rate

Torsional Vibrations Sampling Rate

A high sampling rate is key to obtain an accurate measurement of torsional vibrations and stick-slip as shown by (Cayeux et al., 2020). In a typical stick-slip situation, the rotational speed may reach 300-400 RPM in a fraction of a second, and data could easily get lost with too low a sampling frequency, leading to misinterpretation of the string behavior. At for example 300 RPM, the BHA rotates 5 times per second. The figure below illustrates how a sampling rate of 10 Hz means that there is 180 degrees between each sample, while 100 Hz will decrease the increments to 18 degrees. Twice the sampling frequency means half the rotational displacement between one measurement and the next. Put into perspective, traditional vibration sensors often record samples at 0.1 - 0.2 Hz, which at 300 RPM corresponds to 25-50 rotations between each measurement. This greatly limits the possibility to understand downhole drill string dynamics. Note that with a sample rate of 5 Hz the string would appear to be stationary while it is in fact rotating one round between each measurement. Thus, the highest possible sample rate should be utilized to fully understand downhole vibrations, and further increasing the frequency to 200 Hz is recommended.

Caption: Measuring drill string rotation at different sample rates.

Transient Parameters

Changing the mud pump flow rate before keeping it constant will result in a long transient period before steady state is reached. Yet, the lateral and rotational drill string movement may still cause substantial downhole pressure fluctuations after this. The continuously changing physical parameters, as for instance the hydraulic and mechanical friction factors, make it really hard to provide accurate results. A good approach can be to continuously monitor and calibrate the input parameters frequently, but this requires advanced technology.

C. Effect of Changing Parameters on the Frequency Response

Drill Pipe Length

Increasing the drill pipe length will shift all natural frequencies to the left, decreasing the interval from one mode to the next. Below is four plots showing the same string, all with the same C length, but a varying DP length. The total string lengths are 10,000 ft (top left), 18,000 ft (top right), 26,000 ft (bottom left) an 34,000 ft (bottom right). Notice the constant distance between two adjacent modes. Changing the DP length will affect the DP modes, but not the DC mode which is not visible here.

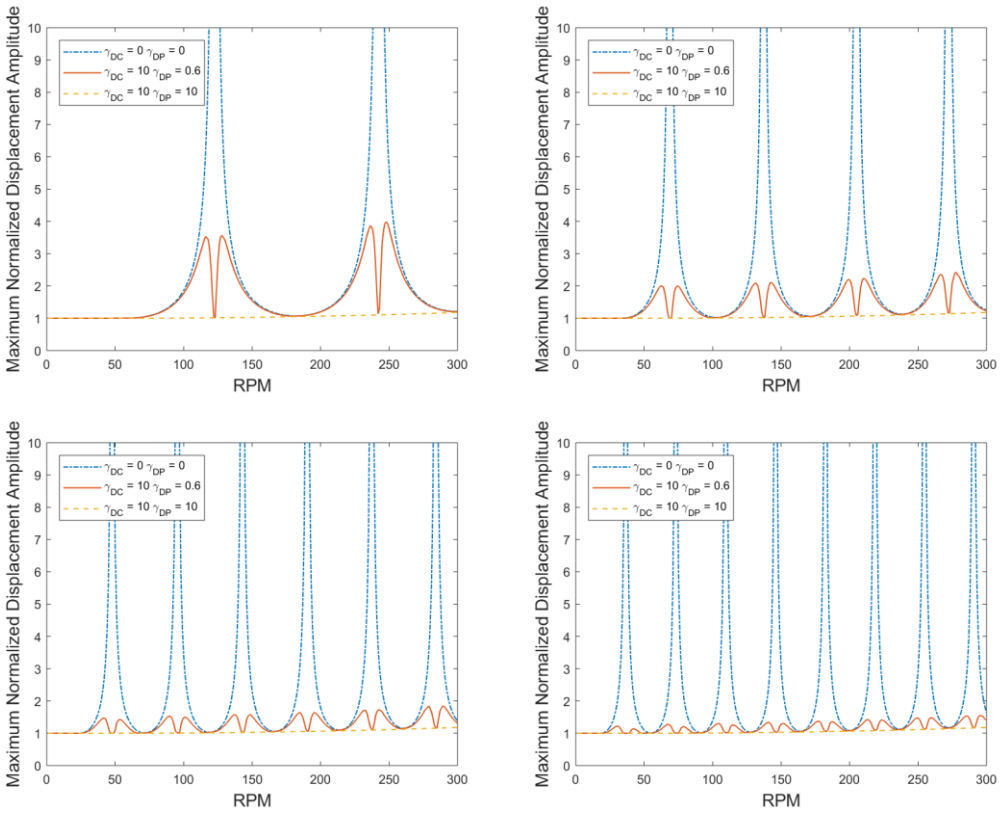

Drill Collar Length

Increasing the DC length will shift the the natural frequencies of the collars to the left, i.e. towards lower frequencies. The two plots below show the effect of increasing the collar length from 800 ft (left) to 1,600 ft (right).

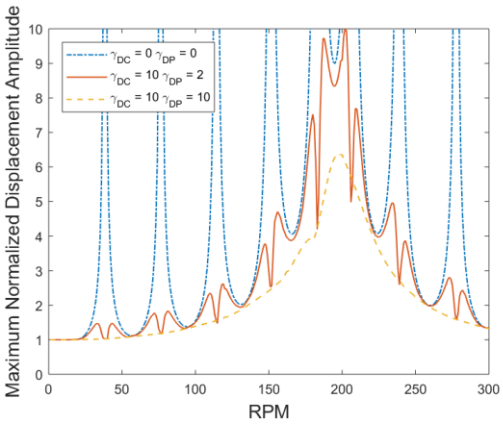

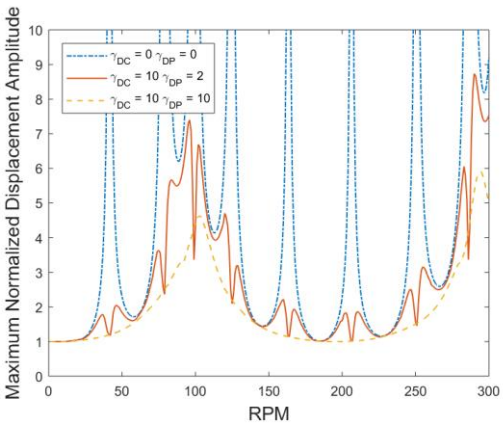

Rig Mass Moment of Inertia (M_θ):

Increasing M from 20,000 (left) to 50,000 (right) lb-ft-sec^2 will also shift the modes slightly to the left.

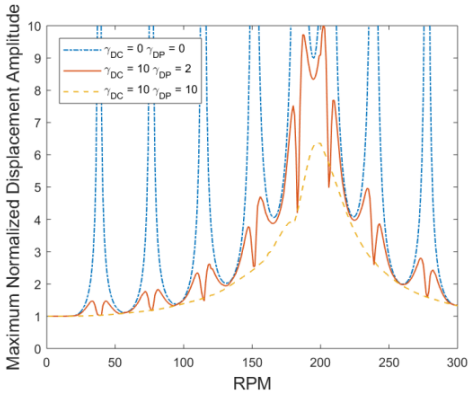

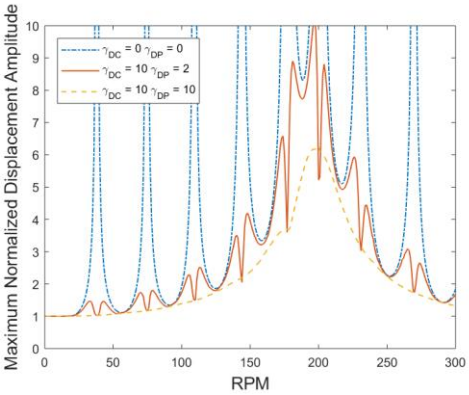

Due to the rig's enormous mass moment of inertia, the string is practically fixed on the surface. This is illustrated by the figure below, showing the normalized displacement of the first four harmonics along the drill string. Here the excitation frequency is set to $f_e = 1$.

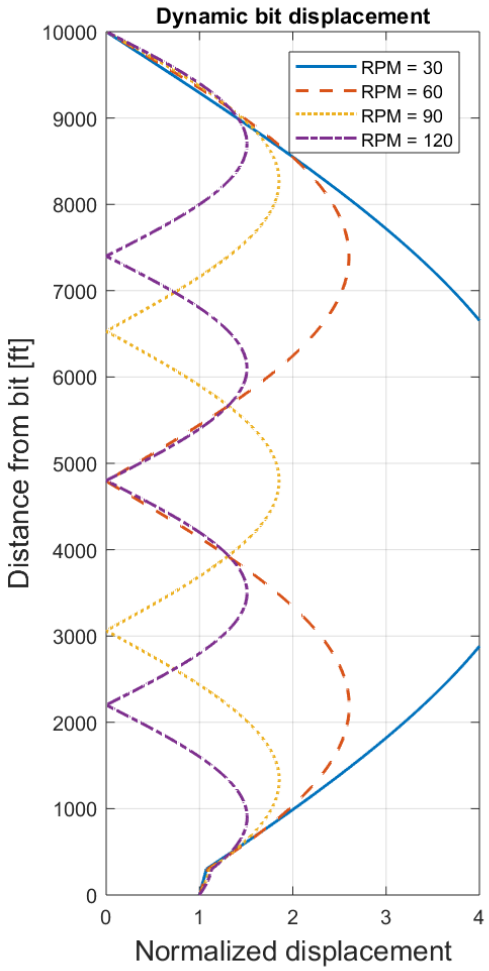
Dynamic bit displacement
RPM = 30
RPM = 60
RPM = 90
RPM = 120
Distance from bit [ft]
Normalized displacement
10000
9000
8000
7000
6000
5000
4000
3000
2000
1000
0
0
1
2
3
4

D. Torsional Oscillations

(Wang, Chen, Rui, & Jin, 2017) studied the effects of torque rocking motion on the drill string axial drag and obtained the following results:

Axial drag vs vibration amplitude (left plot): Influence of torsional oscillation amplitude on the axial friction. F_C is the Coulomb friction force (N), F_{fx} is the axial component of the dynamic friction force (N), v_d is the ROP and Ω_a is the torsional vibration amplitude (RPM). The frequency of torsional vibrations was constant and equal to 5 Hz and the amplitude varied from 10-30 RPM with 2 RPM step. The axial friction increases with increasing ROP, and the axial drag decreases with increasing amplitude.

Axial drag vs vibration frequency (right plot): Influence of torsional oscillation frequency on the axial friction. F_c is the Coulomb friction force (N), F_{fx} is the axial component of the dynamic friction force (N) and Ω_a is the torsional vibration amplitude (RPM). The axial friction decreases from 0.1–1 Hz and increases from 1-10 Hz, suggesting an optimal frequency of 1 Hz. The axial drag is reduced with increasing amplitude.

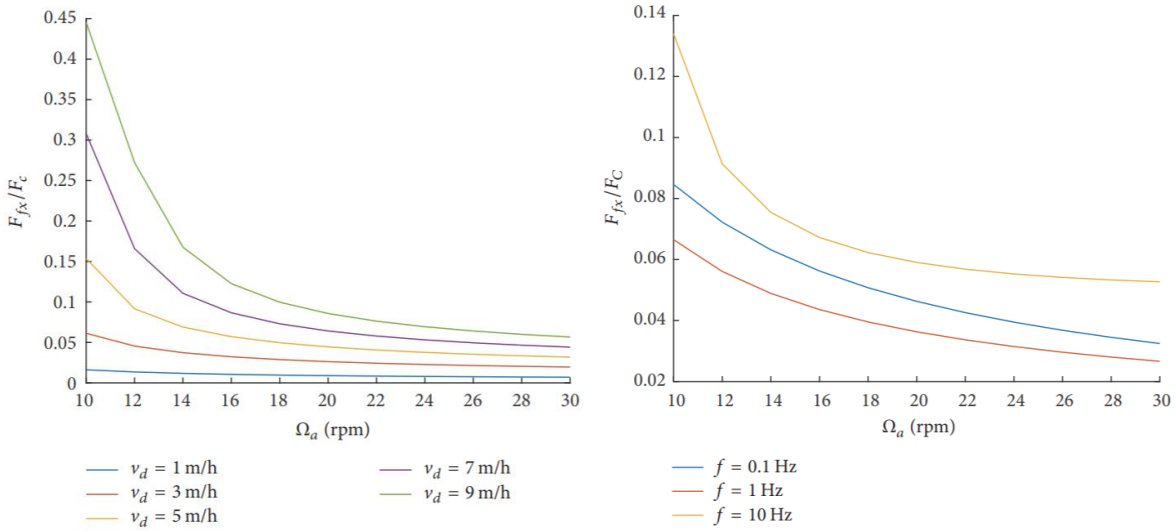

E. PDM Tool Characteristics

4 ¾ in. Ultra XL/VS

5/6 – 2.5 stages

MMTR Compatible

	US Units	SI Units
Flow Rate	105-315 gpm	400-1,200 l/min
Speed	30-85 rpm	
Speed to Flow Ratio	0.27 rev/gal	0.07 rev/l
No Load Pressure Drop	305 psi	21 bar
Standard or High Temperature elastomer		
Operational Limits (Maximum Operational for MMTR)		
Differential Pressure	365 psi	25 bar
Torque	2,650 ft-lbs	3,600 Nm
Power Output	42 hp	32 kW
Maximum Operational		
Differential Pressure	580 psi	40 bar
Torque	4,250 ft-lbs	5,750 Nm
DuraMax elastomer		
Operational Limits (Maximum Operational for MMTR)		
Differential Pressure	545 psi	38 bar
Torque	3,950 ft-lbs	5,400 Nm
Power Output	63 hp	47 kW
Maximum Operational		
Differential Pressure	725 psi	50 bar
Torque	5,300 ft-lbs	7,150 Nm

Performance data for the 4 3/4 in. Ultra XL/VS mud motor. (BakerHughes, 2016, p. 108)

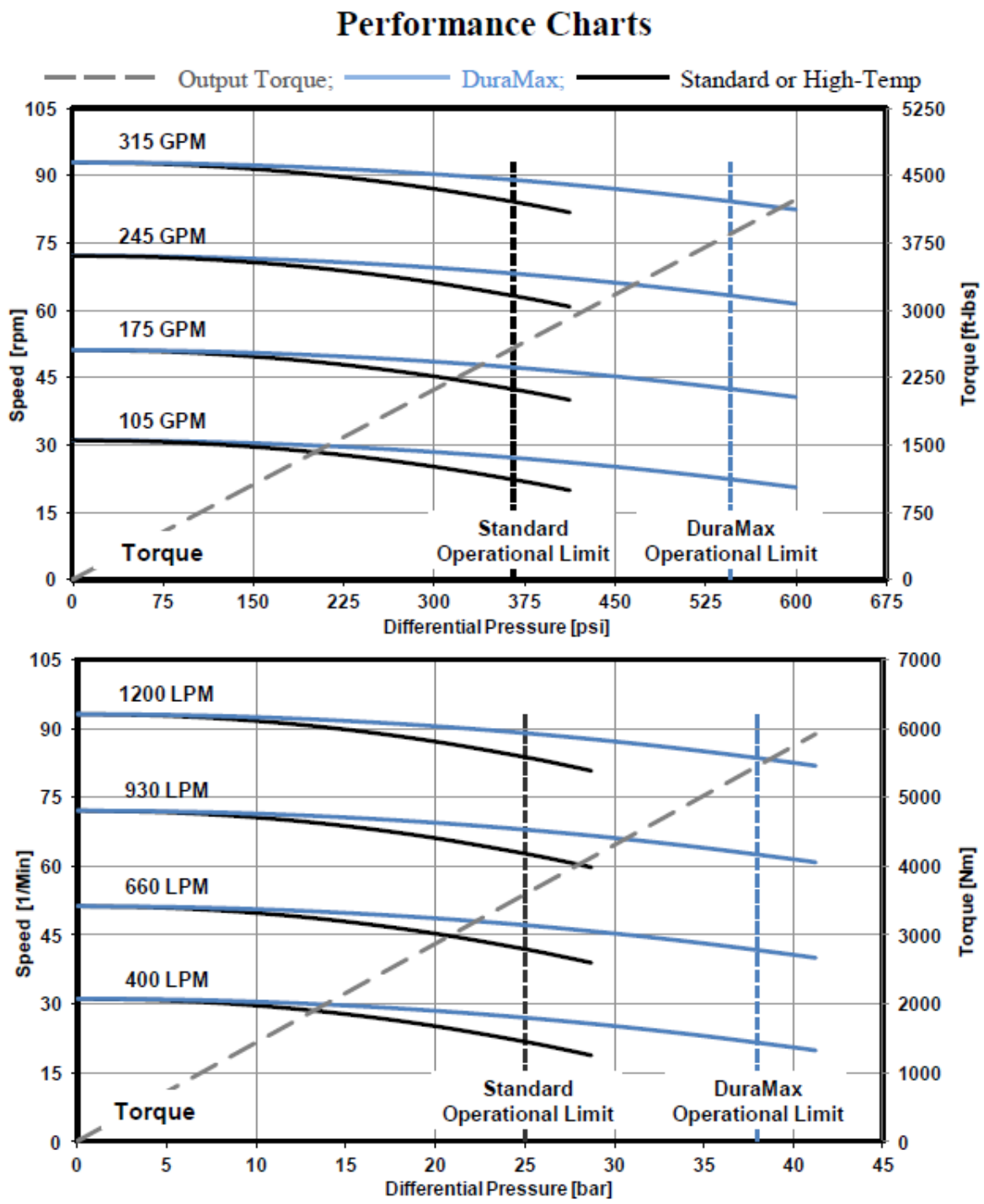

Performance chart for the 4 3/4 in. Ultra XL/VS mud motor. Upper chart has oil field units, lower chart has SI units. (BakerHughes, 2016, p. 108)

PERFORMANCE DATA

Liner size, inches (mm)			7 ¼" (184.2)	7" (177.8)	6 ¾" (171.5)	6 ½" (165.1)	6 ¼" (158.8)	6" (152.4)	5 ¾" (146.1)	5 ½" (139.7)	5" (127)	4 ½" (114.3)
Max. Discharge Pressure, psi (kg/cm^2) with high pressure Fluid End†			3200 (225)	3430 (241.1)	3690 (259.4)	3980 (279.8)	4305 (302.7)	4670 (328.3)	5085 (357.5)	5555 (390.5)	6720 (472.4)	7500 (527.2)
Pump Speed spm	**Input HP, HP (kW)**	**Hyd.** HP, HP (kW)**	**GPM** (LPM**)**	**GPM** (LPM**)**	**GPM** (LPM**)**	**GPM** (LPM**)**	**GPM** (LPM**)**	**GPM** (LPM**)**	**GPM** (LPM**)**	**GPM** (LPM**)**	**GPM** (LPM**)**	**GPM** (LPM**)**
120*	1600* (1193*)	1440 (1074)	***	***	669 (2533)	621 (2349)	574 (2172)	529 (2002)	486 (1840)	444 (1682)	367 (1389)	297 (1124)
100	1333 (994)	1200 (895)	643 (2435)	600 (2270)	558 (2111)	517 (1958)	478 (1810)	441 (1668)	405 (1533)	370 (1401)	306 (1158)	248 (938)
80	1067 (796)	960 (716)	515 (1948)	480 (1816)	446 (1689)	414 (1566)	383 (1448)	353 (1334)	324 (1226)	296 (1121)	245 (927)	198 (750)
60	800 (597)	720 (537)	388 (1461)	360 (1362)	335 (1267)	310 (1175)	287 (1086)	264 (1001)	243 (920)	222 (841)	184 (697)	149 (564)
40	533 (397)	480 (358)	257 (974)	240 (908)	223 (844)	207 (783)	191 (724)	176 (667)	162 (613.1)	148 (561)	122 (462)	99 (375)
Volume/Stroke, gal. (Liters)			6.433 (24.35)	5.997 (22.70)	5.576 (21.11)	5.171 (19.58)	4.781 (18.10)	4.406 (16.68)	4.046 (15.32)	3.702 (14.02)	3.060 (11.58)	2.478 (9.38)

*Rated maximum input horsepower and speed
**Based on 90% mechanical efficiency and 100% volumetric efficiency
***Operation over 675 gpm could result in reduced valve life
†5,000 PSI Fluid End configuration available

Pump performance data for the 12-P-160 Triplex Mud Pump. (NOV)

	PDM in Vertical Section (parallel configuration)	PDM in BHA Section (single configuration)
Cross-sectional area	Dependent on last casing. A bigger cross-sectional area will allow PDMs in parallel and increased output torque.	Dependent on hole size. Likely to be smaller than in the vertical section. However, this may be sufficient if using a single PDM.
Distance to surface	Close to surface. Easy retrieval.	Far from surface. Pull entire DP to retrieve.
Rotation length	From tool down. Most of the drill string is rotated	From tool down. Only BHA is rotated.
Pressure loss	Dependent on motor choice. Differential pressure across the tool is independent of number of motors. However, the frictional pressure loss increases with the flow rate which is proportional with the number of motors.	The decreased cross-sectional area and a lower required torque might vouch for a single and more powerful motor. Therefore bigger differential pressure across the motor. Reduced flow rate gives lower frictional pressure loss
Flow rate	Large. Proportional with number of motors.	Small. No issue.
Continuous flow	Required	Required
Equipment wear	Most of the string rotates during connections.	Only BHA rotates during connection.
Average drag resistance per meter	Low. Dominated by drill pipe.	High. Dominated by BHA.
Impact on total torque	Huge	Minor

Comparing the installation of a PDM based tool in the vertical section to the installation of a PDM based tool in the BHA section. A more elaborative discussion can be found in (Skrettingland, 2019).

F. MATLAB #1 – Input Parameters

Reading Parameters File:

For use in "Methods of mitigating axial stick-slip during connections".

This script produces a struct with all relevant well data. The script will be used as input in other functions.

Well data:

DP and BHA data:

```
Well.Name = 'WellData';
Well.BHA_length = 300*0.3048;                %[m]
Well.BHA_weight = 174.11;                    %[kg/m]
Well.BHA_OD = 7*0.0254;                      %[m]
Well.BHA_ID = 2.25*0.0254;                   %[m]
Well.DP_weight = 32.59;                      %[kg/m]
Well.DP_OD = 5.5*0.0254;                     %[m]
Well.DP_ID = 4.778*0.0254;                   %[m]
Well.DP_TJOD = 7*0.0254;                     %[m]
Well.Steel_E = 200e9;                        %[Pa]
Well.Steel_G = 79.3e9;                       %[Pa]
```

Wellbore trajectory data:

```
Well.VerticalSection = 1000;                 %[m]
Well.ROC = 860;                              %[m]
Well.BUR = (2/360*2*pi)/30;                  %[rad/m] = 2 deg per 30 m
Well.SailAngle = 80/360*2*pi;                %[rad] = 80 deg
Well.TD = 18000*0.3048;                      %[m]
Well.TangentLength = Well.TD-Well.ROC*Well.SailAngle-Well.VerticalSection; %[m]
Well.IntLength = 1;                          %[m]
Well.k = Well.Steel_E*pi/4*(Well.DP_OD^2-Well.DP_ID^2)/Well.TD; %[N/m]
```

Other well data:

```
Well.HoleSize = 8.5*0.0254;                  %[m]
Well.Friction = 0.18;                        %[-]
Well.rho = 1400;                             %[kg/m3]
Well.B = 0.82;                               %[-]
Well.g = 9.81;                               %[m/s2]
Well.WOB = 0;                                %[N]
Well.TOB = 0;                                %[Nm]
```

Drill string motion data:

```
Motion.WaveHeight = 3;                       %[m]
Motion.WaveAmplitude = Motion.WaveHeight/2; %[m]
Motion.WavePeriod = 12;                      %[s]

Motion.RPM_0 = 80;                           %[rpm]
Motion.RPM_int = 10;                         %[rpm]
```

```
Motion.Trip_0 = 0;                          %[m/s]
Motion.Trip_int = 0;                        %[m/s]
```

Wave plot details:

```
Interval = 0.05;                             %[s]
MaxTime = 30;                               %[s]
PhaseShift = 0.00;                          %[rad]
```

RPM plot:

```
RPMs = (0:10:200);                          % to plot effect of rotation
```

G. MATLAB #2 – Well Discretization

Discretized Wellbore: Tension, Normal Force and Torque

Introduction:

This script reads the "Parameters.mlx" and plots tension, normal force and torque along the drill string as a function of measured depth.

```
clear
close all
clc
run ('Parameters.mlx')
```

Defining depths:

```
MD_KOP = Well.VerticalSection;
MD_EOB = MD_KOP + Well.ROC*Well.SailAngle;
MD_TopBHA = MD_EOB + max((Well.TangentLength-Well.BHA_length),0);
MD_BIT = MD_EOB + Well.TangentLength;
```

Constructing the output vectors:

```
MDs = fliplr(MD_BIT:-Well.IntLength:0);
NormalForce = ones(1,length(MDs));
Tension = ones(1,length(MDs));
Torque = ones(1,length(MDs));
Inclination = ones(1,length(MDs))*Well.SailAngle;

% Initial Conditions @ BIT
NormalForce(length(MDs)) = (Well.IntLength*Well.BHA_weight*Well.g*Well.B)*sin(Well.SailAngle);
Tension(length(MDs)) = -Well.WOB;
Torque (length(MDs)) = -Well.TOB;

for i = (length(MDs)-1):-1:1
    if MDs(i) >= MD_TopBHA && MDs(i) < MD_BIT          % TANGENT BHA
        NormalForce(i) = (Well.IntLength*Well.BHA_weight*Well.g*Well.B)*sin(Well.SailAngle);
        Tension(i) = Tension(i+1) + (Well.IntLength*Well.BHA_weight*Well.g*Well.B)*(cos(Well.Sa
        Torque(i) = Torque(i+1) + Well.Friction*Well.BHA_OD/2*abs(NormalForce(i));

    elseif MDs(i) < MD_TopBHA && MDs(i) >= MD_EOB      % TANGENT DP
        NormalForce(i) = (Well.IntLength*Well.DP_weight*Well.g*Well.B)*sin(Well.SailAngle);
        Tension(i) = Tension(i+1) + (Well.IntLength*Well.DP_weight*Well.g*Well.B)*(cos(Well.Sai
        Torque(i) = Torque(i+1) + Well.Friction*Well.DP_TJOD/2*abs(NormalForce(i));

    elseif MDs(i) < MD_EOB && MDs(i) >= MD_KOP         % BUILD
        Inclination(i) = Inclination (i+1) - Well.BUR*Well.IntLength; % [rad/m]*[10m]
        NormalForce(i) = (Well.IntLength*Well.DP_weight*Well.g*Well.B)*sin((Inclination(i)+Incl
        Tension(i) = Tension(i+1) + (Well.IntLength*Well.DP_weight*Well.g*Well.B)*cos((Inclinat
        Torque(i) = Torque(i+1) + Well.Friction*Well.DP_TJOD/2*abs(NormalForce(i));

    elseif MDs(i) < MD_KOP                             % VERTICAL
        Inclination(i) = 0;
        NormalForce(i) = 0;
        Tension(i) = Tension(i+1) + (Well.IntLength*Well.DP_weight*Well.g*Well.B);
        Torque(i) = Torque(i+1) + Well.Friction*Well.DP_TJOD/2*abs(NormalForce(i));
```

```
    else
        disp('Error')
    end
end
```

Plotting:

```
figure('name','Discretized')

subplot(3,1,1);
plot(MDs,Tension,'k','LineWidth',1)
hold on
grid on
plot([MD_KOP MD_KOP],[0 10e5],'--b',[MD_EOB MD_EOB],[0 10e5],'--b',[MD_TopBHA MD_TopBHA],[0 10e
ylabel('Axial Tension [N]')
title('Properties along the string')

subplot(3,1,2);
plot(MDs,Torque,'k','LineWidth',1)
hold on
grid on
plot([MD_KOP MD_KOP],[0 3e4],'--b',[MD_EOB MD_EOB],[0 3e4],'--b',[MD_TopBHA MD_TopBHA],[0 3e4],
ylabel('Torque [Nm]')

subplot(3,1,3);
plot(MDs,NormalForce,'k','LineWidth',1)
hold on
grid on
plot([MD_KOP MD_KOP],[-1e3 2e3],'--b',[MD_EOB MD_EOB],[-1e3 2e3],'--b',[MD_TopBHA MD_TopBHA],[-
xlabel('Measured Depth [m]')
ylabel('Normal Force / meter [N]')
plot3props = gca;
plot3props.YAxis.Exponent = 3;      % Plotting as 10^3
```

Adjusting graph height

```
x0 = 0.1300;
y0 = 0.1577;
width= 800;
height= 1000;
set(gcf,'Position',[x0,y0,width,height])
```

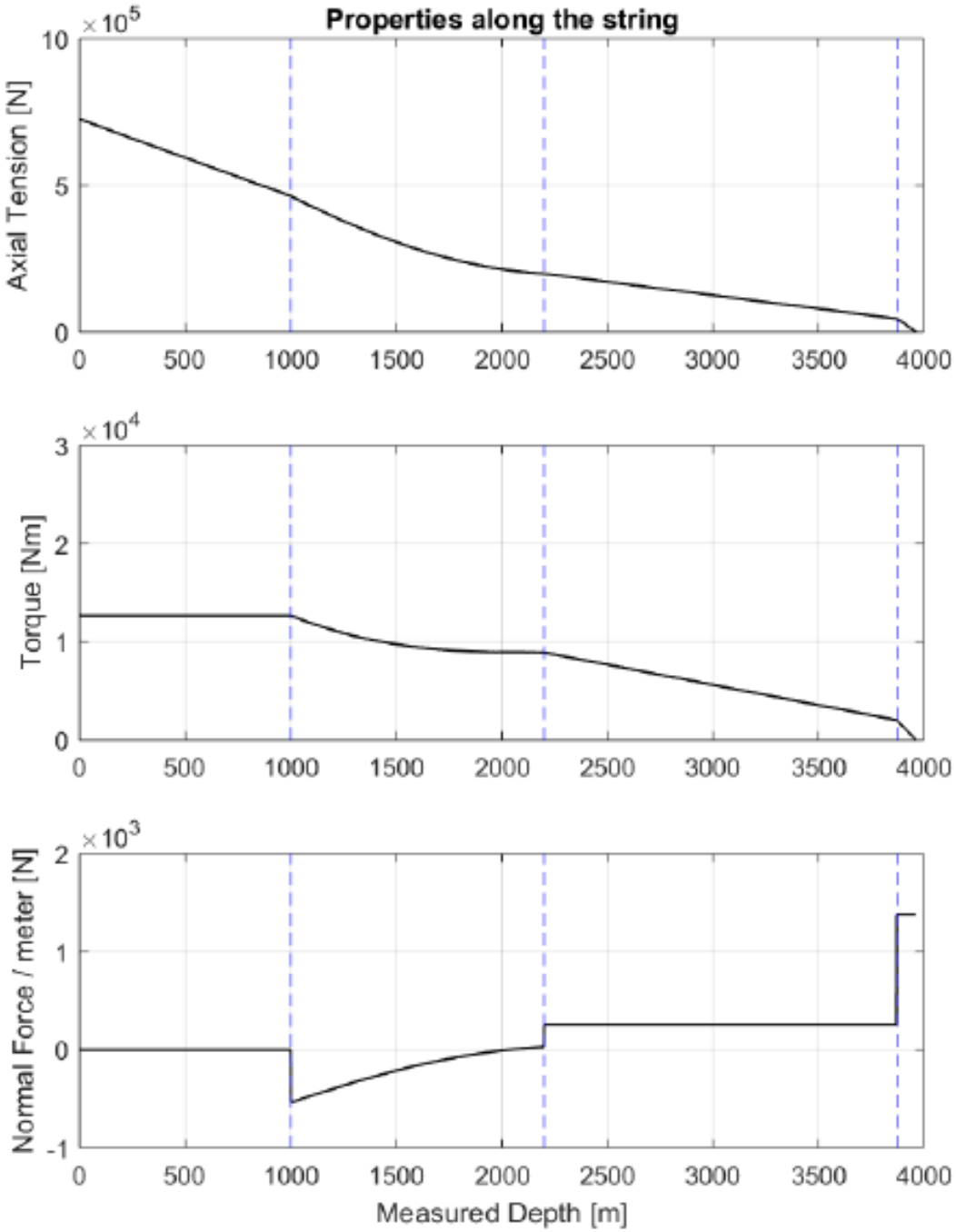
Properties along the string
Axial Tension [N]
×10^5
10
5
0
Torque [Nm]
×10^4
3
2
1
0
Normal Force / meter [N]
×10^3
2
1
0
-1
0
500
1000
1500
2000
2500
3000
3500
4000
Measured Depth [m]

H. MATLAB #3 – Heave Motion

Heave Motion

Introduction:

1. This script will use the data from "Parameters.mlx" to plot the oscillating behavior of the rig floor (top of drill string).
2. It finds the critical displacement and plots it over the heave motion to determine the time intervals of axial sticking.
3. Further, it looks at the effect of drill string rotation on axial drag. Is it possible to "rotate out" some of the axial drag? The script plots the reduction in axial drag for a range of RPM values.

```
clear
close all
clc
run('Parameters.mlx')
```

Allocating data:

```
% Select time span
TimeSpan = (0:Interval:MaxTime);
w = 2*pi/Motion.WavePeriod;

h_vector = Motion.WaveAmplitude*sin(w.*TimeSpan+PhaseShift);        % displacement
v_vector = Motion.WaveAmplitude*w*cos(w.*TimeSpan+PhaseShift);      % velocity
a_vector = -Motion.WaveAmplitude*w^2*sin(w.*TimeSpan+PhaseShift);   % acceleration
```

Plotting data:

```
figure('name','HeaveMotion');
plot(TimeSpan,h_vector,TimeSpan,v_vector,'--',TimeSpan,a_vector,':','LineWidth',1.5)
grid on
legend('Displacement [m]','Velocity [m/s]','Acceleration [m/s2]',...
    'Location','southoutside')
xlabel('Time [s]')
title('Rig Floor Heave Motion')
```

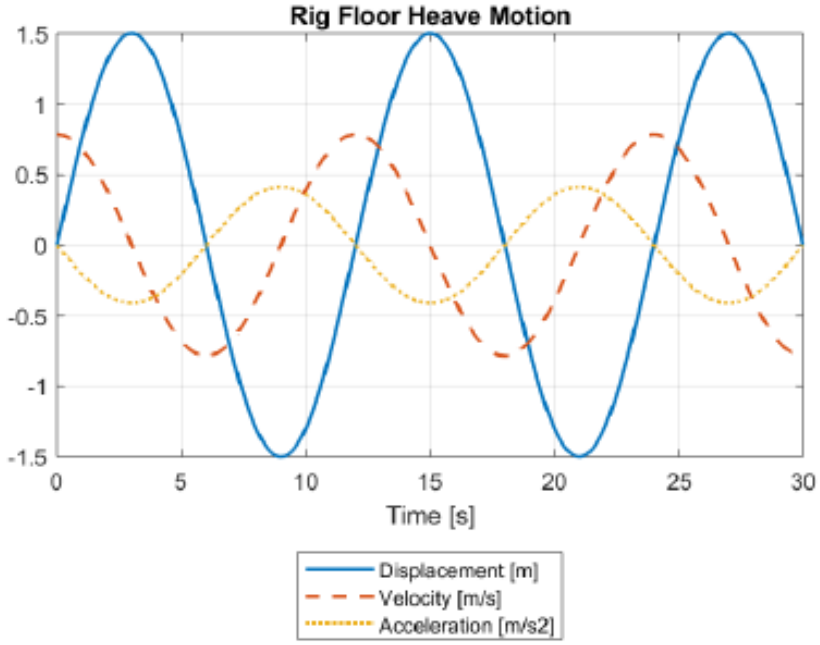

Axial Stick-Slip

This section evaluates the axial drag forces along the wellbore. What length (ΔL) must the drill string be compressed to generate a restoring force that is large enough to overcome the sum of axial drag forces? In other words; when does the string slip in the axial direction?

By finding the compressed length, the given wave properties are used to determine the amount of time that can pass by before a shock is initiated ("best situation" at crest or through and "worst situation" at the MSL). What RPM must be maintained to ensure that the torsional sticking time is shorter than the axial sticking time?

```
WellData = ForceCalc;
```

Welldata (i.e. the output of "ForceCalc.m") is a matrix on the form [Measured Depths; Tension values; Normal Force values; Torque values], i.e.

```
% [     MD1 MD2 MD3     ...     MDn-1   MDn
%       F1  F2  F3      ...     Fn-1    Fn
%       N1  N2  N3      ...     Nn-1    Nn
%       T1  T2  T3      ...     Tn-1    Tn      ]
```

To get the total drag force (ΣR), simply multiply the normal force with the friction coefficient, to find the drag force on each element, and sum up all drag contributions.

```
DragForce = Well.Friction*abs(WellData(3,:));  % Drag vector
TotalDrag = sum(DragForce);
```

The restoring force is determined by $F = k\,\Delta L$, where k is steel stiffness and ΔL is displacement. The string slips when the restoring force equals the drag force above.

$$k = \frac{EA}{L} = \frac{E * \pi \frac{(OD^2 - ID^2)}{4}}{L} \qquad \text{and} \qquad \Delta L = \frac{\Sigma R}{k}$$

```
k = Well.Steel_E*pi*(Well.DP_OD^2-Well.DP_ID^2)/4/Well.TD;  %[N/m]
dL = TotalDrag/k;                                           %[m]
```

The string will slip once it is compressed by more than a length of ΔL. How long time does that correspond to with the heave behavior plotted above? Determine the longest and shortest time interval for the rig floor to heave more than ΔL.

```
figure('name','Axial Stick-Slip')
hold on
plot(TimeSpan,h_vector,'Linewidth',1)
plot([0 MaxTime],[0 0],'Linestyle','--','Color',[0, 0.4470, 0.7410])
%plot(TimeSpan,abs(v_vector),'k:')
%grid on
ylabel('Axial Displacement [m]','fontweight','bold','fontsize',12)
xlabel('Time [s]','fontweight','bold','fontsize',12)
title('Top of Drill String Movement','fontsize',12)
axis([0 MaxTime -2 2])

% Rectangle 1 - worst situation
TimeList = TimeSpan(find(abs(dL/2-h_vector) < 0.1));
int = find(TimeList>0.25*Motion.WavePeriod,1);
x1 = TimeList(int);
y1 = -dL/2;
TimeList = TimeSpan(find(abs(dL/2+h_vector) < 0.1));
int = find(TimeList>0.5*Motion.WavePeriod,1);
w1 = TimeList(int)-x1;
h1 = dL;
rectangle('Position',[x1 y1 w1 h1],'LineStyle','--','LineWidth',2,'EdgeColor',1/255*[243 27 41])

% Rectangle 2 - best situation
TimeList = TimeSpan(find(abs(max(h_vector)-dL-h_vector) < 0.05));
int = find(TimeList>0.75*Motion.WavePeriod,1);
x2 = TimeList(int);
y2 = max(h_vector)-2*dL;
Further = TimeSpan(find(abs(max(h_vector)-2*dL-h_vector) < 0.05));
int = find(Further>1.25*Motion.WavePeriod,1);
w2 = Further(int)-x2;
h2 = 2*dL;
if dL<Motion.WaveAmplitude
    rectangle('Position',[x2 y2 w2 h2],'LineStyle','--','LineWidth',2,'EdgeColor',1/255*[243 27
    plot([x2 x2+w2],[y2+dL y2+dL],'LineStyle','--','LineWidth',1,'Color',1/255*[243 27 41])
    fprintf(['The critical heave distance is \t dL = %4.2f meters. \n' ...
        'The shortest reaction time is \t T1 = %4.2f seconds. \n' ...
        'The longest reaction time is \t T2 = %4.2f seconds.'],dL,w1,w2)
elseif (dL>=Motion.WaveAmplitude && dL<Motion.WaveHeight)
    rectangle('Position',[Motion.WavePeriod -dL Motion.WavePeriod 2*dL],'LineStyle','--','LineWi
    plot([Motion.WavePeriod 2*Motion.WavePeriod],[0 0],'LineStyle','--','LineWidth',1,'Color',1/
    fprintf(['The critical heave distance is \t dL = %4.2f meters. \n' ...
        'The shortest reaction time is \t T1 = %4.2f seconds. \n' ...
```

```
        'The longest reaction time is \t T2 = no upper limit.'],dL,w1)
elseif dL>=Motion.WaveHeight
    rectangle('Position',[Motion.WavePeriod -dL Motion.WavePeriod 2*dL],'LineStyle','--','Linel
    plot([Motion.WavePeriod 2*Motion.WavePeriod],[0 0],'LineStyle','--','LineWidth',1,'Color',
    fprintf(['The critical heave distance is \t dL = %4.2f meters. \n' ...
        'The shortest reaction time is \t T1 = no upper limit. \n' ...
        'The longest reaction time is \t T2 = no upper limit.'],dL,w1)
end
```

```
The critical heave distance is   dL = 1.84 meters.
The shortest reaction time is   T1 = 2.55 seconds.
The longest reaction time is   T2 = no upper limit.
```

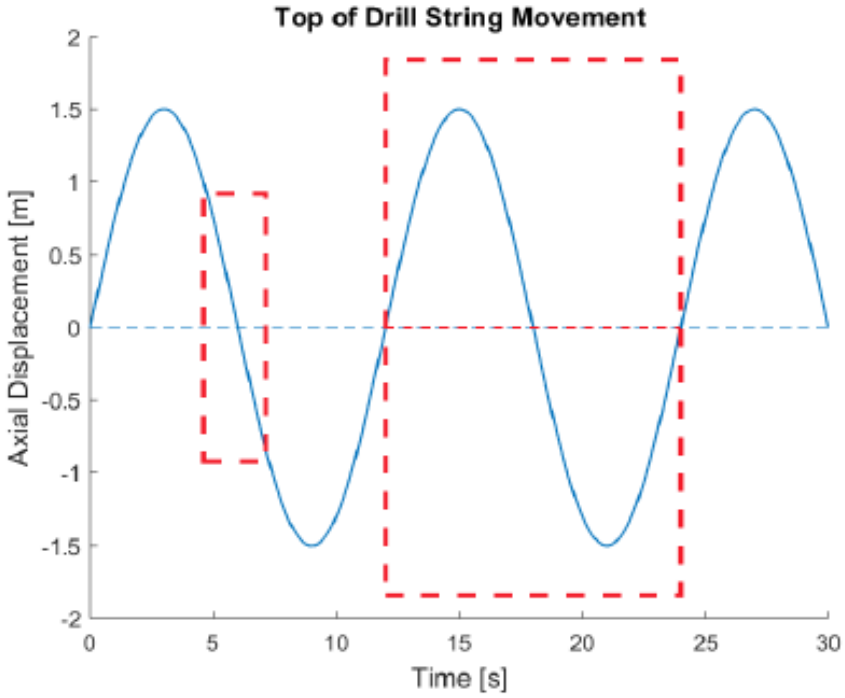

Effect of Rotation on Axial Drag

This section evaluates the relationship between axial (heaving) and tangential (rotating) velocity. By exerting rotation on the drill string, it is possible to "rotate out" some of the axial drag, but how big is the effect of increasing RPM?

Drag with no rotation:

Locating the top of BHA to calculate the summed drag forces along the DP and BHA respectively

```
MD_TopBHA = Well.VerticalSection + Well.ROC*Well.SailAngle ...
    + max((Well.TangentLength-Well.BHA_length),0);
index = find(WellData(1,:) > MD_TopBHA,1);

% The drag is then
DP_Drag = sum(DragForce(1:(index-1)));
```

```
BHA_Drag = sum(DragForce(index:length(DragForce)));
InitialDrag = DP_Drag + BHA_Drag;
```

Drag with different RPMs:

Important to separate between BHA, resting on the BHA_OD and DP resting on the DP_TJOD. As the BHA_OD is higher than the DP_TJOD, it will give increased tangential velocities along the BHA, and more reduction in axial drag forces. The large weight of the BHA also enhances any effects of a change in total velocity.

```
RPM_vector = RPMs;                          % List of RPMs for x-axis
v_axial = max(v_vector);                    % maximum heave velocity
v_DP_tan = ones(1,length(RPM_vector));      % tangential velocity DP
v_DP_tot = ones(1,length(RPM_vector));      % total velocity DP
v_BHA_tan = ones(1,length(RPM_vector));     % tangential velocity BHA
v_BHA_tot = ones(1,length(RPM_vector));     % total velocity BHA
Reduction = ones(1,length(RPM_vector));
Comparison = ones(1,length(RPM_vector));

for i = 1:length(RPM_vector)
    v_DP_tan(i) = pi*Well.DP_TJOD*RPM_vector(i)/60;     % using TJOD for DP
    v_DP_tot(i) = sqrt(v_axial^2 + v_DP_tan(i)^2);
    v_BHA_tan(i) = pi*Well.BHA_OD*RPM_vector(i)/60;     % Using OD for BHA
    v_BHA_tot(i) = sqrt(v_axial^2 + v_BHA_tan(i)^2);

    NewDrag = DP_Drag*v_axial/v_DP_tot(i) + BHA_Drag*v_axial/v_BHA_tot(i);
    Reduction(i) = 100 - NewDrag/InitialDrag*100;

    % Comparing to see effect of different BHA tangential velocity
    OnlyTJOD = DP_Drag*v_axial/v_DP_tot(i) + BHA_Drag*v_axial/v_DP_tot(i);
    Comparison(i) = 100 - OnlyTJOD/InitialDrag*100;
end


figure('name','RPM')
plot(RPM_vector,Reduction,'b',RPM_vector,Comparison,'--b','LineWidth',1)
grid on
%legend('BHA and DP','Only DP','Location','southeast')
xlabel('RPM','fontweight','bold','fontsize',14)
ylabel('% Reduction','fontweight','bold','fontsize',14)
title('RPM Effect on Axial Drag','fontweight','bold','fontsize',14)
```

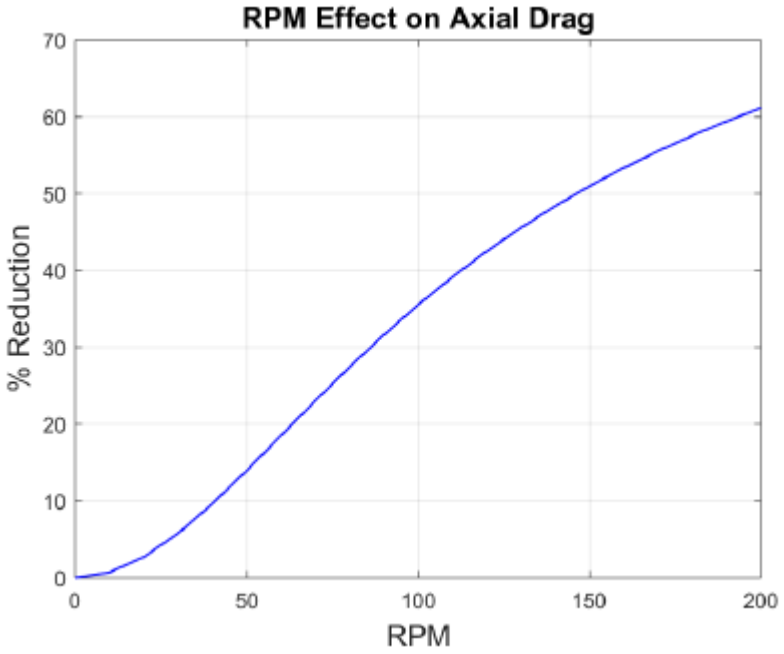

I. MATLAB #4 – BHA Angular Displacement

BHA and Top Joint Angular Displacement

Introduction:

This script is sketching the assumed relationship between top joint rotation and BHA rotation.

```
clear
close all
clc
```

Angular displacement

```
Top = (0:1:18);
Bit = [0 0 0 0 0 0 0 5 5 5 5 5 10 10 10 10 10 15 15];
Diff = Top-Bit;

subplot(2,1,1)
plot(Top,Top,'--',Top,Bit,'LineWidth',1)
grid on
legend('Top Joint','BHA','Location','southeast')
ylabel('Rotations','fontweight','bold','fontsize',12)
title('Angular Displacement')

subplot(2,1,2)
plot(Top,Diff,'Color',[0.9290, 0.6940, 0.1250],'LineWidth',1)
grid on
legend('Difference','Location','southeast')
ylabel('Rotations','fontweight','bold','fontsize',12)
xlabel('Top Joint Rotations','fontweight','bold','fontsize',12)
```

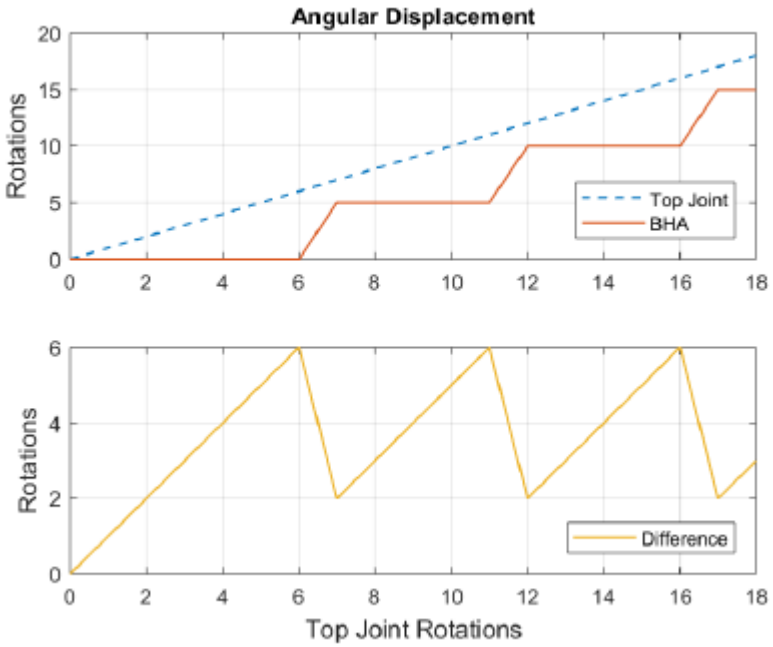

J. MATLAB #5 – Critical Time Intervals

Sticking Time vs Drill String Length

Introduction:

This script is plotting the time intervals of axial sticking as a function of drill string length. The time values (T1 and T2) are obained by running "HeaveMotion.mlx" for each string length (L).

```
clear
close all
clc
```

Time Intervals:

```
L = 1000*(8:2:22);
x = [0.19 0.37 0.60 0.93 1.35 1.84 2.41 3.04];
T1 = [0.30 0.50 0.80 1.20 1.80 2.55 3.60 5.35];
T2 = [2.45 3.35 4.45 5.70 7.55 NaN NaN NaN];

figure
plot(L,x,L,T1,L,T2,'--','LineWidth',1)
hold on
plot([7000 23000],[1.5 1.5],'Linestyle','--','Color',[0, 0.4470, 0.7410])
plot([7000 23000],[3 3],'Linestyle','--','Color',[0, 0.4470, 0.7410])

grid on
legend('x_{crit} [m]','T1 [s]','T2 [s]','Location','northwest')
xlabel('Drill string length [ft]','fontweight','bold','fontsize',12)
title('Time to build up restoring force')
axis([L(1)-1000 L(end)+1000 0 7])
plotprops = gca;
plotprops.XAxis.Exponent = 3;      % Plotting as 10^3
```

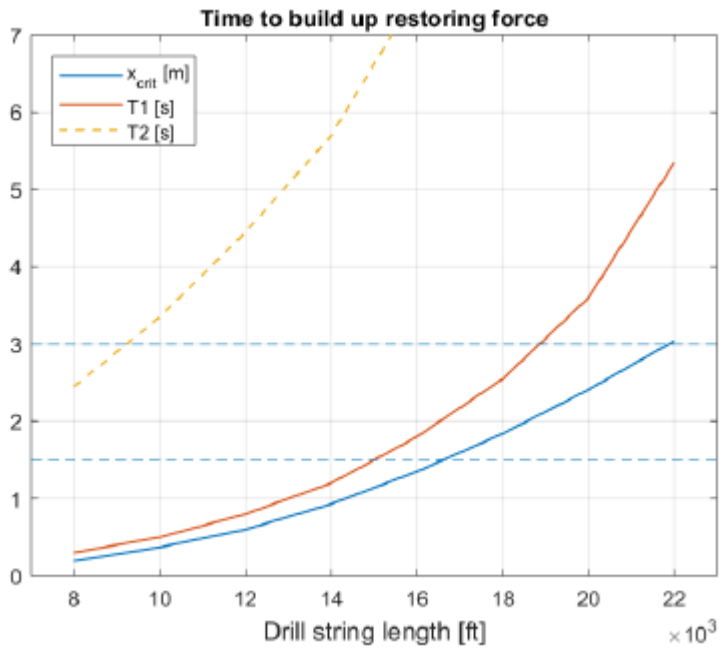

Dual axis:

```
figure
yyaxis left
plot(L,T2,':',L,T1,'LineWidth',1)
ylabel('Sticking time [s]')
xlabel('Drill string length [ft]','fontweight','bold','fontsize',12)
title('Time to build up restoring force')

yyaxis right
plot(L,x,'LineWidth',1)
hold on
plot([7000 23000],[1.5 1.5],'--',[7000 23000],[3 3],'--')
ylabel('Critical displacement [m]')

legend ('T_2','T_1','x_{crit}','Location','northwest')
grid on
axis([L(1)-1000 L(end)+1000 0 8])
plotprops = gca;
plotprops.XAxis.Exponent = 3;      % Plotting as 10^3
```

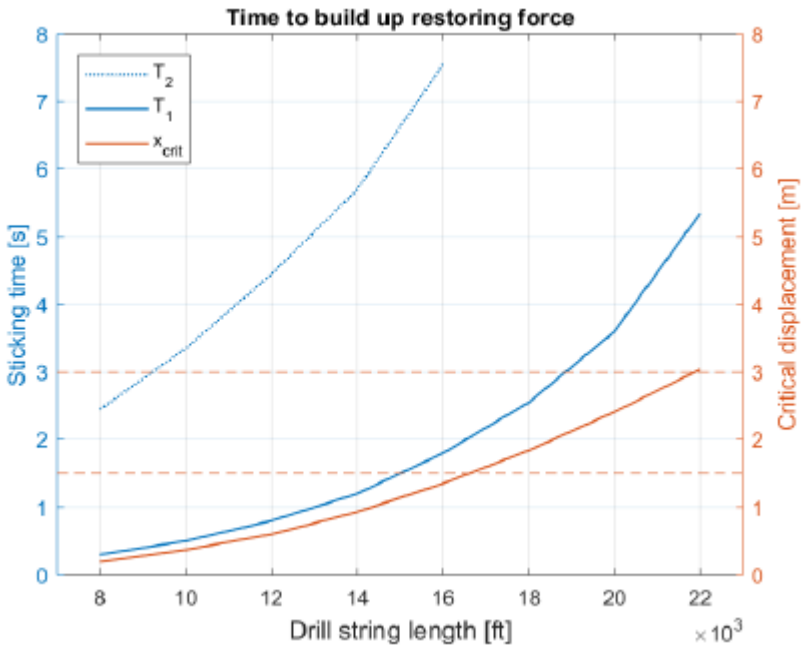

K. MATLAB #6 – Minimum RPM

Minimum RPM vs Drill String Length

Introduction:

This script calculates the minimum RPM required on the top joint to ensure that torsional slipping occurs before axial slipping on the BHA. The minimum RPM is calculated for a range of drill string lengths (L) with time intervals (T1 and T2) obtained with "HeaveMotion.mlx".

```
clear
close all
clc
run('Parameters.mlx')
```

Preallocating vectors:

```
L = 0.3048*1000*(8:2:22);                   %[m]
G = Well.Steel_G;                           %[Pa]
Twist = zeros(1,length(L));         % summed angular displacement
%A = pi/4*(Well.DP_OD^2-Well.DP_ID^2);       %[m2] csa of DP
%E = Well.Steel_E;                           %[Pa]
%x = zeros(1,length(L));             % critical (axial) displacement
```

The modified version of the function "ForceCalc" at the bottom of this script is used to calculate the drill string forces for all drill string lengths (L) and the angular displacement in each element. The output of the function is a matrix on the form [Measured Depths; Tension values; Normal Force values; Torque values; Twist], i.e.

```
% [     MD1 MD2 MD3     ...     MDn-1   MDn
%       F1  F2  F3      ...     Fn-1    Fn
%       N1  N2  N3      ...     Nn-1    Nn
%       T1  T2  T3      ...     Tn-1    Tn
%       Ø1  Ø2  Ø3      ...     Øn-1    Øn  ]
```

The angular displacement (θ) is found in each differential element along the string. It is given by the formula $\theta_i = \frac{LT}{JG} = \frac{\Delta L * T_i}{J_k * G}$ where ΔL is the interval length, T_i is the torque in a given element, J_k is the polar moment of inertia where k=(1, 2) for BHA and DP respectively, and G is the shear modulus of steel.

```
for i = 1:length(L)
    % Anglular Displacement
    WellData = ForceCalc(L(i));
    Twist(i) = sum(WellData(5,:));                  %[rad]

    % Critical Displacement (assuming only DP)
    %DragForce = Well.Friction*abs(WellData(3,:));   % Drag vector
    %k = E*A/L(i);                                   %[N/m]
    %x(i) = sum(DragForce)/k;                        %[m]
end

Twist                                               %[rad]
```

```
Twist =
    7.9705   14.0761   21.8214   31.5731   43.1200   55.8950   69.8716   85.0267
```

```
T1 = [0.30 0.50 0.80 1.20 1.80 2.55 3.60 5.35];     %[s]
T2 = [2.45 3.35 4.45 5.70 7.55 NaN NaN NaN];        %[s]
RPM1 = 2/3.*Twist/2/pi*60./T1
```

```
RPM1 =
  169.1396  179.2229  173.6489  167.5004  152.5058  139.5446  123.5601  101.1769
```

```
RPM2 = 2/3.*Twist/2/pi*60./T2
```

```
RPM2 =
   20.7110   26.7497   31.2178   35.2632   36.3590       NaN       NaN       NaN
```

Plotting:

```
figure
yyaxis left
plot(L,RPM1,L,RPM2,':','LineWidth',1)
ylim([0 1.05*max(RPM1)])
grid on
title('Minimum RPM vs Drill String Length','fontweight','bold','fontsize',14)
ylabel('Minimum RPM','fontweight','bold','fontsize',12)
xlabel('Drill String Length [m]','fontweight','bold','fontsize',12)

yyaxis right
plot(L,Twist/2/pi)
ylabel('Rotations @ Surface Torque')
legend('Mean Sea Level (T_1)','Crest/Trough (T_2)','Angle of Twist','Location','southeast')
```

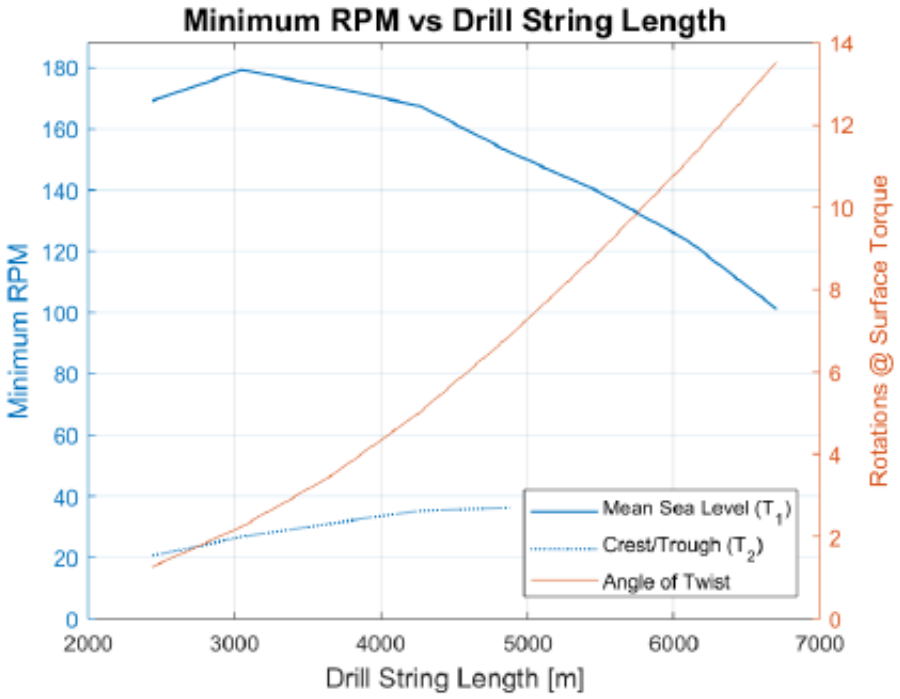

```
function [output] = ForceCalc (L)
%% Introduction:
% This script plots tension, normal force and torque along the
% drill string as a function of measured depth. It also finds
% the angular displacement in each element.

run('Parameters.mlx')
Well.TD = L;
Well.TangentLength = Well.TD-Well.ROC*Well.SailAngle-Well.VerticalSection; %[m]
J1 = pi/32*(Well.BHA_OD^4-Well.BHA_ID^4);   %[m4] BHA polar moment
J2 = pi/32*(Well.DP_OD^4-Well.DP_ID^4);     %[m4] DP polar moment

%% Defining depths:
MD_KOP = Well.VerticalSection;
MD_EOB = MD_KOP + Well.ROC*Well.SailAngle;
MD_TopBHA = MD_EOB + max((Well.TangentLength-Well.BHA_length),0);
MD_BIT = MD_EOB + Well.TangentLength;

%% Preallocating the output vectors:
MDs = fliplr(MD_BIT:-Well.IntLength:0);
NormalForce = ones(1,length(MDs));
Tension = ones(1,length(MDs));
Torque = ones(1,length(MDs));
Twist = zeros(1,length(MDs));
Inclination = ones(1,length(MDs))*Well.SailAngle;

% Initial Conditions @ BIT
NormalForce(length(MDs)) = (Well.IntLength*Well.BHA_weight*Well.g*Well.B)*sin(Well.SailAngle);
Tension(length(MDs)) = -Well.WOB;
Torque (length(MDs)) = -Well.TOB;

for i = (length(MDs)-1):-1:1
    if MDs(i) >= MD_TopBHA && MDs(i) < MD_BIT           % TANGENT BHA
        NormalForce(i) = (Well.IntLength*Well.BHA_weight*Well.g*Well.B)*sin(Well.SailAngle);
        Tension(i) = Tension(i+1) + (Well.IntLength*Well.BHA_weight*Well.g*Well.B)*(cos(Well.Sai
        Torque(i) = Torque(i+1) + Well.Friction*Well.BHA_OD/2*abs(NormalForce(i));
        Twist(i) = Well.IntLength*Torque(i)/J1/Well.Steel_G;          %[rad]

    elseif MDs(i) < MD_TopBHA && MDs(i) >= MD_EOB       % TANGENT DP
        NormalForce(i) = (Well.IntLength*Well.DP_weight*Well.g*Well.B)*sin(Well.SailAngle);
        Tension(i) = Tension(i+1) + (Well.IntLength*Well.DP_weight*Well.g*Well.B)*(cos(Well.Sail
        Torque(i) = Torque(i+1) + Well.Friction*Well.DP_TJOD/2*abs(NormalForce(i));
        Twist(i) = Well.IntLength*Torque(i)/J2/Well.Steel_G;          %[rad]

    elseif MDs(i) < MD_EOB && MDs(i) >= MD_KOP          % BUILD
        Inclination(i) = Inclination (i+1) - Well.BUR*Well.IntLength; % [rad/m]*[10m]
        NormalForce(i) = (Well.IntLength*Well.DP_weight*Well.g*Well.B)*sin((Inclination(i)+Incli
        Tension(i) = Tension(i+1) + (Well.IntLength*Well.DP_weight*Well.g*Well.B)*cos((Inclinati
        Torque(i) = Torque(i+1) + Well.Friction*Well.DP_TJOD/2*abs(NormalForce(i));
        Twist(i) = Well.IntLength*Torque(i)/J2/Well.Steel_G;          %[rad]

    elseif MDs(i) < MD_KOP                              % VERTICAL
        Inclination(i) = 0;
        NormalForce(i) = 0;
```

```
        Tension(i) = Tension(i+1) + (Well.IntLength*Well.DP_weight*Well.g*Well.B);
        Torque(i) = Torque(i+1) + Well.Friction*Well.DP_TJOD/2*abs(NormalForce(i));
        Twist(i) = Well.IntLength*Torque(i)/J2/Well.Steel_G;          %[rad]

    else
        disp('Error')
    end
end

output = [MDs;Tension;NormalForce;Torque;Twist];

end
```

L. MATLAB #7 – Angular Displacement vs Depth

Angular Vibrations Normalized Amplitude

This script calculates the maximum normalized displacement along a drill string in the case of torsional vibrations.

The script is based on:

- The paper by Dareing and Livesay, "Longitudinal and Angular Drill-String Vibrations With Damping", Journal of Engineering for Industry, November, 1968
- Previous work done by co-student Mads Berntsen on reproducing the vibration model in the above paper for the case with axial vibrations.

```
clc
clear
close all
```

Well and string dimensions

```
L1 = 300;                   % [ft] Length of drill collars
D2 = 5.5;                   % [in] DP OD
d2 = 4.778;                 % [in] DP ID
J2 = pi*(D2^4-d2^4)/32;     % [in^2] Cross-sectional DP area
D1 = 7;                     % [in] DC OD
d1 = 2.25;                  % [in] DC ID
J1 = pi*(D1^4-d1^4)/32;     % [in^2] Cross-sectional DC area
L2 = 10000;                 % [ft] Drill string length (Well MD)
```

Operating parameters

```
WOB = 0;                    % [lbf] Weight on bit
RPM = [80,90,100];          % [RPM] Rotational rate
f = 1*RPM/60;             % [Hz] Excitations per sec
w = 2*pi*f;                 % [rad/sec] angular velocity
Theta_0 = 2*pi;             % [rad] Amplitude of bit displacement
```

Steel properties

```
G = 11.2*10^6;              % [psi] Modulus of rigidity (shear and torsion) for steel
c = 10400;                  % [ft/sec] Shear velocity in steel
gamma_1 = 5;               % [(lb*ft/rad)/(sec/ft)] torsional damping factor of DC
gamma_2 = 0.5;                % [(lb*ft/rad)/(sec/ft)] torsional damping factor of DP
```

Topside properties

```
k = 250000;                 % [lb-ft/rad] torsional spring constant
M = 5e9/32.1741;            % [lb-ft-sec^2] Mass moment of inertia of rotary drive mechanism
t_2 = 0:0.01:6;             % [sec] vector of time
```

Calculations of unknowns

Setting up the expressions for the four complex numbers determined by the boundary conditions (B1, b1, B2 and b2). These will be used as input to the function at the bottom, when solving the equation.

```
for count = 1:length(RPM)
w_1=w(count);

eta1 = sqrt((w_1^2/c^2)-(1i*gamma_1*w_1)/(J1*G));                % (n1)
eta2 = sqrt((w_1^2/c^2)-(1i*gamma_2*w_1)/(J2*G));                % (n2)
b2 = atan((J2*G*eta2)/(M*w_1^2-k)) - eta2*L2;                    % boundary condition @ top DP
b1 = atan(((J1*G*eta1)/(J2*G*eta2))*tan(eta2*L1+b2)) - eta1*L1;  % boundary condition @ top DC
B2 = -(1i*Theta_0)/(sin(b1)) * (sin(eta1*L1+b1)/sin(eta2*L1+b2)); % boundary condition @ top DC
B1 = -(1i*Theta_0)/sin(b1);                                      % boundary condition @ bit
```

Find Time of Max Bit Displacement

```
bit_displacement = sin(w_1.*t_2);
int = find(bit_displacement==max(bit_displacement),1);
t = t_2(int);
```

Plot the displacement along the drillstring

Solving the equation by running the function at the bottom with the parameters calculated above. This is done for all RPM values. Storing the answer as a column in the matrix U, before plotting the differnet columns in this matrix as lines in the chart.

```
[Theta,x] = AngVib(Theta_0,B1,eta1,b1,L1,B2,eta2,b2,L2,w_1,t);
U = zeros(length(Theta),length(RPM));
U(:,count)= abs(Theta/Theta_0);
%txt = ['Frequency = ',num2str(f(count)),' Hz'];
txt = ['RPM = ',num2str(RPM(count))];
lin={'-','--',':'};

figure(1)
p = plot(U(:,count),x,'Linestyle',lin{count},'Linewidth',1.5,'DisplayName',txt);
hold on
end

grid on
grid minor
legend show
title('Dynamic bit displacement')
ylabel('Distance from bit [ft]','fontweight','bold','fontsize',14)
xlabel('Normalized displacement','fontweight','bold','fontsize',14)
axis([0 4 0 10000])         % For comparison

x0 = 60;
y0 = 60;
width= 350;
height= 700;
set(gcf,'position',[x0,y0,width,height])
```

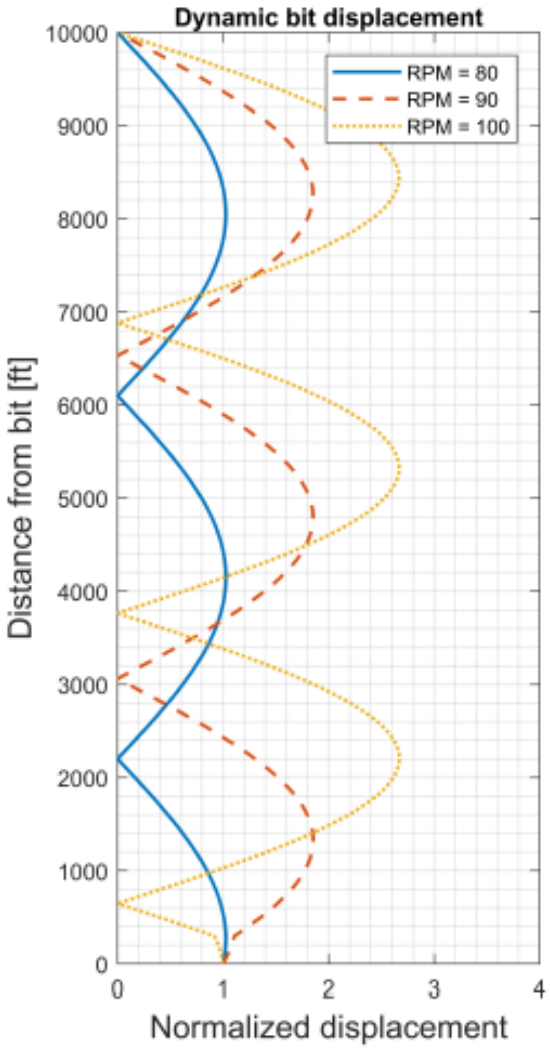


```
function [Theta,x] = AngVib(Theta_0,B1,eta1,b1,L1,B2,eta2,b2,L2,w,t)

dx = L2/1000;
Theta = zeros(1,1000);
x = zeros(1,1000);

Theta(1) = real(-1i*Theta_0*exp(1i*w*t));          % @ bit

for p = 2:1000
    x(p) = x(p-1)+dx;

    if x(p) < L1
```

```
        Theta(p) = real(B1 * sin(eta1*x(p)+b1)*exp(1i*w*t)); % BHA
    else
        Theta(p) = real(B2 * sin(eta2*x(p)+b2)*exp(1i*w*t)); % DP
    end
end

end
```

M. MATLAB #8 – Natural Frequencies

Natural Frequencies

This script is used to determine the natural frequencies of a drill string system. The final plot will show the resonant frequency modes for both the DP section and the DC section.

The script is based on:

- The paper by Dareing and Livesay, "Longitudinal and Angular Drill-String Vibrations With Damping", Journal of Engineering for Industry, November, 1968
- Previous work done by co-student Mads Berntsen on reproducing the vibration model in the above paper for the case with axial vibrations.

```
clc
clear
close all
```

Well and string dimensions

```
L1 = 300;                   % [ft] Length of drill collars
D1 = 7;                     % [in] DC OD
d1 = 2.25;                  % [in] DC ID
J1 = pi*(D1^4-d1^4)/32;     % [in4] DC polar moment of inertia

L2 = 10000;                 % [ft] Drill string length (MD)
D2 = 5.5;                   % [in] DP OD
d2 = 4.778;                 % [in] DP ID
J2 = pi/32*(D2^4-d2^4);     % [in4] DP polar moment of inertia
```

Operating parameters

```
WOB = 0;                    % [lbf] Weight on bit
RPM = (0:1:300);            % [RPM] Rotational rate
f = 2*RPM/60;             % [Hz] Excitations per second
w = 2*pi*f;                 % [rad/sec] angular velocity
Theta_0 = 2*pi;             % [rad] Amplitude of bit displacement
```

Steel properties

```
G = 11.2*10^6;                  % [psi] Shear modulus for stainless steel
c = 10400;                      % [ft/sec] Shear velocity in steel
Gamma_1 = [0, 10, 10];          % [(lb*ft/rad)/(sec/ft)] torsional damping factor of DC
Gamma_2 = [0, 1, 10];           % [(lb*ft/rad)/(sec/ft)] torsional damping factor of DP
```

Topside properties

```
k = 250000;                     % [lb-ft/rad] torsional spring constant
M = 5e9/32.1741;                % [lb-ft-sec^2] Mass moment of inertia of entire rig
t_2 = 0:0.01:6;                 % [sec] vector of time
```

Calculation of unknowns

Setting up the expressions for the four complex numbers determined by the boundary conditions (B1, b1, B2 and b2). These will be used as input to the function at the bottom, when solving the equation.

```
U = zeros(length(RPM),length(Gamma_1));

for count_gamma = 1:1:length(Gamma_1)
    gamma_1 = Gamma_1(count_gamma);
    gamma_2 = Gamma_2(count_gamma);

for count = 1:length(RPM)
    w_1=w(count);

eta1 = sqrt((w_1^2/c^2)-(1i*gamma_1*w_1)/(J1*G));                % (n1)^2
eta2 = sqrt((w_1^2/c^2)-(1i*gamma_2*w_1)/(J2*G));                % (n2)^2
b2 = atan((J2*G*eta2)/(M*w_1^2-k)) - eta2*L2;                    % boundary condition @ top DP
b1 = atan(((J1*G*eta1)/(J2*G*eta2))*tan(eta2*L1+b2)) - eta1*L1;  % boundary condition @ top DC
B2 = -(1i*Theta_0)/(sin(b1)) * (sin(eta1*L1+b1)/sin(eta2*L1+b2)); % boundary condition @ top DC
B1 = -(1i*Theta_0)/sin(b1);                                      % boundary condition @ bit
```

Find Time of Max Bit Displacement

```
bit_displacement = sin(w_1.*t_2);
int = find(bit_displacement==max(bit_displacement),1);
t = t_2(int);
```

Solve Equation

Solving the equation by running the function at the bottom with the parameters calculated above. This is done for all RPM values. Storing the answer as a column in the matrix U.

```
[Theta,x] = AngVib(Theta_0,B1,eta1,b1,L1,B2,eta2,b2,L2,w_1,t);

Theta = abs(Theta/Theta(1));                % Making all values absolute and normalized
U(count,count_gamma) = max(Theta);

end
end
```

Plot results

```
figure(1)
plot(RPM, U(:,1),'-.',RPM, U(:,2),RPM, U(:,3),'--','LineWidth',1);
legend('\gamma_{DC} = 0 \gamma_{DP} = 0','\gamma_{DC} = 10 \gamma_{DP} = 1','\gamma_{DC} = 10 \ga
axis([0 max(RPM) 0 10])
ylabel('Maximum Normalized Displacement Amplitude','fontweight','bold','fontsize',14)
xlabel('RPM','fontweight','bold','fontsize',14)
```

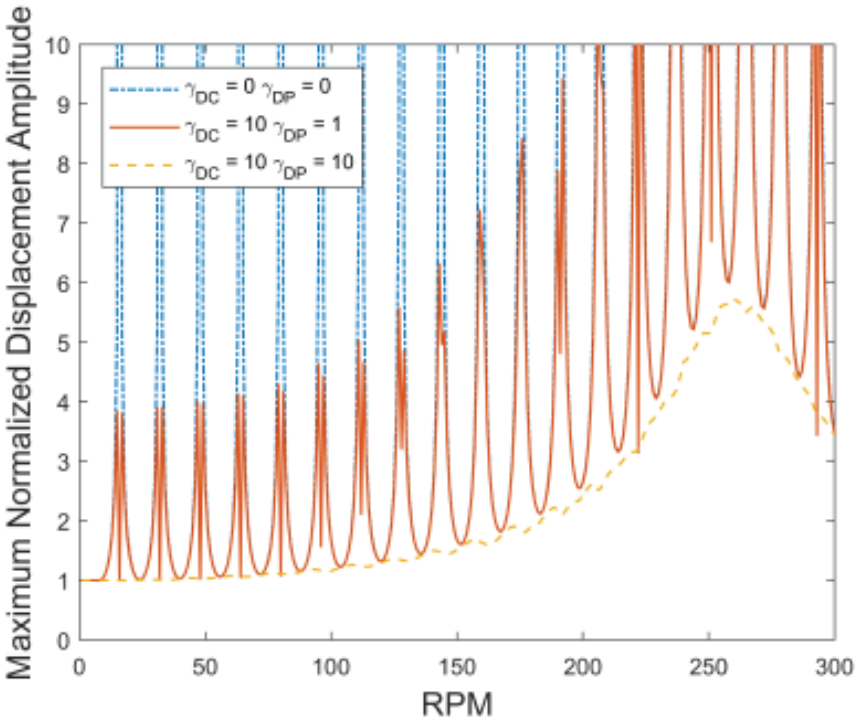

Natural frequencies

Extracting the coordinates of the peaks.

```
[pks,locs] = findpeaks(U(:,1),RPM);
NatFreqListDP = locs'                          % [RPM]
```

```
NatFreqListDP =
    16
    32
    48
    64
    80
    96
   112
   128
   144
   160
    ⋮
```

```
%[pks1,locs1] = findpeaks(U(:,3),RPM);
%NatFreqListDC = locs1'                         % [RPM]
```

```
function [Theta,x] = AngVib(Theta_0,B1,eta1,b1,L1,B2,eta2,b2,L2,w,t)

dx = L2/1000;
Theta = zeros(1,1000);
```

```
x = zeros(1,1000);

Theta(1) = real(B1 * sin(eta1*x(1)+b1)*exp(1i*w*t));         % Bit

for p = 2:1000
    x(p) = x(p-1)+dx;

    if x(p) < L1
        Theta(p) = real(B1 * sin(eta1*x(p)+b1)*exp(1i*w*t)); % BHA
    else
        Theta(p) = real(B2 * sin(eta2*x(p)+b2)*exp(1i*w*t)); % DP
    end
end

end
```

Karsten Skrettingland

Mitigating Axial Stick-Slip During Connections on a Floating Vessel

NTNU
Norwegian University of
Science and Technology